CANADIAN THESES

THÈSES CANADIENNES

NOTICE

The quality of this microfiche is heavily dependent upon the quality of the original thesis submitted for microfilming. Every effort has been made to ensure the highest quality of reproduction possible.

If pages are missing, contact the university which granted the degree.

Some pages may have indistinct print especially if the original pages were typed with a poor typewriter ribbon or if the university sent us an inferior photocopy.

Previously copyrighted materials (journal articles, published tests, etc.) are not filmed.

Reproduction in full or in part of this film is governed by the Canadian Copyright Act, R.S.C. 1970, c. C-30.

AVIS

La qualité de cette microfiche dépend grandement de la qualité de la thèse soumise au microfilmage. Nous avons tout fait pour assurer une qualité supérieure de reproduction.

S'il manque des pages, veuillez communiquer avec l'université qui a conféré le grade.

La qualité d'impression de certaines pages peut laisser à désirer, surtout si les pages originales ont été dactylographiées à l'aide d'un ruban usé ou si l'université nous a fait parvenir une photocopie de qualité inférieure.

Les documents qui font déjà l'objet d'un droit d'auteur (articles de revue, examens publiés, etc.) ne sont pas microfilmés.

La reproduction, même partielle, de ce microfilm est soumise à la Loi canadienne sur le droit d'auteur, SRC 1970, c. C-30.

THIS DISSERTATION
HAS BEEN MICROFILMED
EXACTLY AS RECEIVED

LA THÈSE A ÉTÉ
MICROFILMÉE TELLE QUE
NOUS L'AVONS REÇUE

NL-339 (r.86/06)

Canada

Vibration Isolation Characteristics of a Class of Semi-Active Suspensions

James Alanoly

A Thesis

in

The Department

of

Mechanical Engineering

Presented in Partial Fulfillment of the Requirements
for the Degree of Master of Engineering at
Concordia University
Montréal, Québec, Canada

November 1985

ISBN 0-315-30652-1

ABSTRACT

Vibration Isolation Characteristics of a
Class of Semi-Active Suspensions

James Alanoly

In this thesis, the vibration isolation characteristics of six types of semi-active suspension schemes are presented. All schemes are analysed with a similar set of basic parameters and are compared on the basis of peak and RMS acceleration transmissibilities. The performance of each system is evaluated by comparson with passive and active isolators, and with each other.

The suspension system is modeled as a single degree-of-freedom base excited system. All six semi-active schemes give rise to ordinary differential equations containing discontinuities. Computer simulation is carried out to determine system response. In the case of two of the schemes, a special software package was used for stability analysis. The possible lock-up behaviour in three of the systems which use continuously varying damping is dealt with in a unified manner. The other schemes which are based on On-Off damping are examined for the possibility of unstable switching behaviour which may lead to chatter of the On-Off valve.

Experimental results are also presented for a semi-active control scheme employing On-Off damping. The laboratory prototype

consisted of a modified off-road motorcycle front fork fitted with a solenoid controlled damper orifice. The experimental results showed excellent correlation with theory and demonstrated the effectiveness of semi-active suspension for vibration isolation.

ACKNOWLEDGEMENTS

The author would like to express his appreciation and gratitude to Dr. S. Sankar for his guidance and support during the course of this study.

He is also thankful for the help and encourgement he received from other faculty members, graduate students and laboratory personnel in the Department of Mechanical Engineering at Concordia University.

The financial support provided through Natural Sciences and Engineering Research Council Grant P-8007 is also gratefully acknowledged.

The author also acknowledges with deep gratitude the love, patience and constant encouragement of his wife Lucy, and daughter, Beth, without which this work would not have been possible.

Sincere thanks are also due to Ms. Nancy Nicholson for typing this manuscript.

TABLE OF CONTENTS

Page

LIST OF FIGURES

Page

LIST OF TABLES

Page

LIST OF TABLES

NOMENCLATURE

a	Amplitude of harmonic input displacement
a_s	Amplitude level for which Type-6 semi-active system is tuned
A	Root mean square value of response acceleration
c, c_1, c_2	Damping coefficient
$F(.,.)$	Function describing a set of differential equations
F_d	Damper force
F'_d	Normalized damper force
F_k	Spring force
F'_k	Normalized spring force
F_s	Total suspension force
$F_u(.,.)$	Jacobian matrix of $F(.,.)$ with respect to $\underline{u}$
F_o	Normalized Coulomb friction force
$F_1(.,.)$	Function describing a differential equation for ϕ 0
$F_{1,i}$	Force in the semi-active isolator of Type i for ϕ_i 0
$F_2(.,.)$	Function describing a differential equation for ϕ 0
$F_{2,i}$	Force in the semi-active isolator of Type i for ϕ_i 0
I	Quadratic performance index
k	Spring stiffness
m	Sprung mass
p	Solution component of the nonlinear oscillator
q	Solution component of the nonlinear oscillator
r	Homotype parameter
s	Arclength parameter

t	Time
t_o	An arbitrary instant in time
t^*	Time when the condition function changes sign
T	Transmissibility
$\underline{u}$	Vector of independent variables of a system
v	Absolute velocity of sprung mass
$\underline{v}$	Solution vector of a linearized system
V	Amplitude of relative velocity
$\tilde{V}$	Fundamental solution matrix of a system
V_s	Switching velocity for Type 6 semi-active system
x	Sprung mass displacement
y	Displacement of isolator base
z	Relative displacement between sprung mass and base
α	Gain in Type 3 semi-active system
γ	Weighting factor in quadratic performance index
ζ, ζ_1, ζ_2	Damping ratio
ρ	Period of periodic solution for $\underline{u}$
σ	An arbitrary constant
τ	Period of harmonic input excitation
ϕ	Condition function
ϕ_i	Condition function of Type-i semi-active system
ω	Circular frequency of input excitation
ω_n	Natural frequency of a spring-mass system

CHAPTER 1

INTRODUCTION AND LITERATURE REVIEW

1.1 GENERAL INTRODUCTION

Suspensions are an integral part of any vehicle. They perform the important task of isolating the passenger and cargo from terrain induced shock and vibration. A vehicle suspension unit usually consists of a spring and damper. Normally they are "Passive Units" because they do not require any external power. By using hydraulic or pneumatic power and sophisticated control devices, it is possible to make "Active Suspensions" which could give substantially more improved performance than passive ones. But they are more complex, expensive, and less reliable than passive suspensions.

A compromise between the active and passive types is the "Semi-Active" suspension system. In this system, no external power is required. Desired forces are generated in a passive damper by modulating orifice areas for fluid flow. However, like an active suspension system, this also requires an instrumentation package and control devices. It has been shown that a semi-active suspension can provide a performance superior to that of a passive one without the cost and complexity of a fully active suspension. It is the purpose of this investigation to carry out a comprehensive study of semi-active suspensions.

1.2 STATE OF THE ART AND LITERATURE REVIEW

Conceptual design of a vehicle suspension is usually carried out

using a single-degree-of-freedom model. Although this is a simple model, its characteristrics must be understood before a multi-degree of-freedom model is studied. A single-degree-of-freedom vehicle schematic is shown in Figure 1.1. This model neglects the unsprung mass and the primary suspension, and assumes that the terrain surface is closely followed by the base of the suspension. The suspension is represented as a force generator S which consists of a spring and a damper mounted in parallel. The requirement on the suspension is that it should minimize the force transmitted to the mass while not exceeding its limits of travel (rattle space).

Several passive, active and semi-active suspension concepts have been proposed to achieve this with varying degrees of success. The focus of the present investigation is on the use of semi-active suspension for vibration isolation. Therefore the literature review will emphasize that area. However, a brief review of the vast amount of literature on passive and active suspensions will also be presented. This will help to place the semi-active suspension in its context as being a compromise between active and passive suspensions, and demonstrate its advantages.

1.2.1 PASSIVE SUSPENSION

The essential features of a passive suspension are a resilient load-supporting mechanism (spring) and an energy-dissipating mechanism (damper). In ground vehicle applications coil springs, torsion bars or leaf springs are often used and are generaly assumed to be linear and massless. Damping is usually nonlinear in

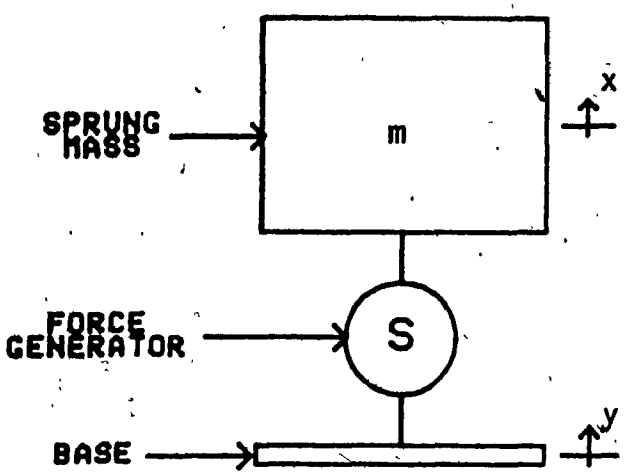

Fig. 1.1: Schematic of a Single-Degree-of-Freedom Vibration Isolator

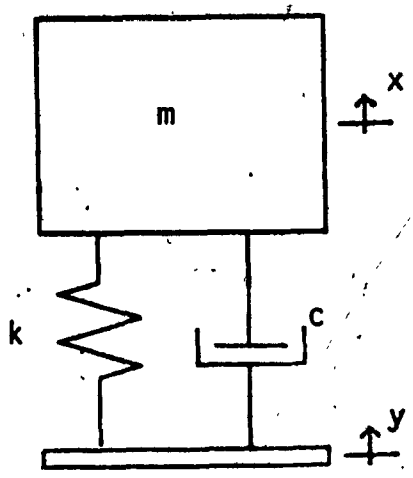

Fig. 1.2: Schematic of a Passive Isolator

character but often assumed to be linear. Thus the simplified form of isolator can be modeled as shown in Figure 1.2. The linear assumptions are reasonable because many suspensions operate much of the time in approximately linear regimes. Further, linear theory gives results that can be generalized and can point out general restrictions on performance.

The equation of motion of a passive single degree of freedom isolator can be written as:

$$m\ddot{x} + c(\dot{x}-\dot{y}) + k(x-y) = 0 \quad \ldots\ldots\ldots\ldots\ldots\ldots (1.1)$$

or

$$\ddot{x} + 2\zeta\omega_n(\dot{x}-\dot{y}) + \omega_n^2(x-y) = 0 \quad \ldots\ldots\ldots\ldots\ldots (1.2)$$

where

$$\omega_n^2 = k/m \quad \text{and} \quad \zeta = c/(2\sqrt{km}) \quad \ldots\ldots\ldots\ldots (1.3)$$

Transmissibility is defined for harmonic input as the ratio of the steady-state response amplitude to the excitation amplitude. For the passive system described above, it is [1]:

$$T = \frac{|X|}{|Y|} = \sqrt{\frac{1 + (2\zeta\frac{\omega}{\omega_n})^2}{[1 - (\frac{\omega}{\omega_n})^2]^2 + [2\zeta\frac{\omega}{\omega_n}]^2}} \quad \ldots\ldots\ldots\ldots (1.4)$$

Figure 1.3 shows this transmissibility plotted for several values of the damping ratio, ζ. This plot illustrates the fundamental performance characteristic of most passive suspensions, linear and

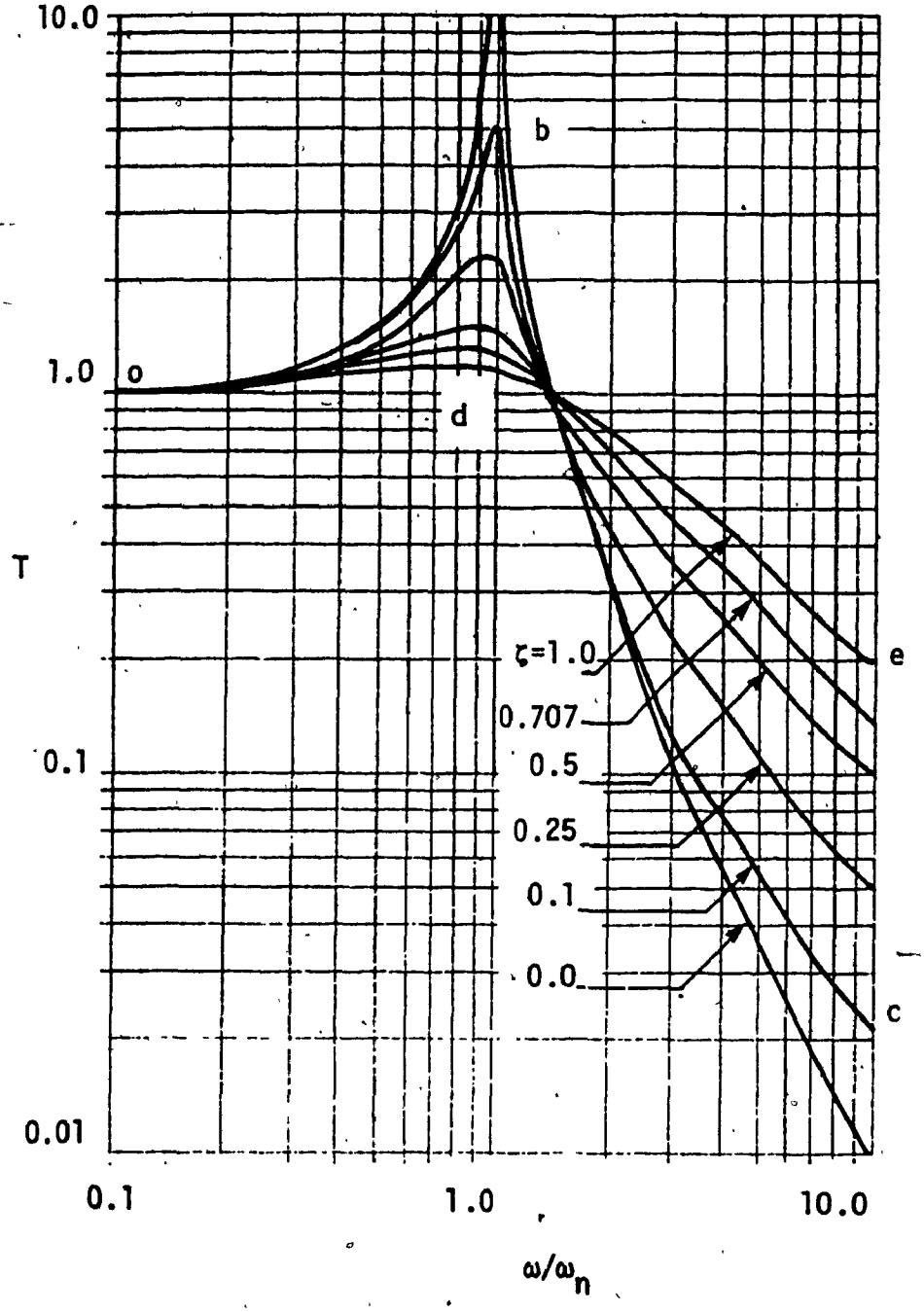

Fig. 1.3: Transmissibility Plot of a Passive Isolator

nonlinear.

Based on this transmissibility plot, it can be seen that there is a need for a trade-off between the performance at low frequencies ($\omega<\sqrt{2}\omega_n$) and that at high frequencies ($\omega>\sqrt{2}\omega_n$). Lower damping gives good isolation at high frequencies and poor resonance characteristics. However, higher damping results in good resonance isolation at the expense of high frequency performance.

As mentioned earlier, damping is seldom perfectly linear. Many researchers have studied isolators with nonlinear damping. Crede and Ruzicka [2] have presented the results of viscous and Coulomb friction dampers connected rigidly or elastically. Once again, resonance can only be avoided at the expense of high frequency isolation. Ruzicka and Derby [3, 4] have studied various nonlinearities including quadratic, Coulomb, velocity n-th power and hysteritic damping. They used equivalent linearization technique [1] to analyze each system. It was reported that for velocity n-th power damping with higher values of the exponent, the high frequency isolation worsens if the resonant response is the same.

In pratical applications, the damping characteristics could be even more complex than the above nonlinear models suggest. Segel and Lang [5] present a very detailed model of an automotive shock absorber. It has 82 different parameters and takes into account fluid compressibility, development of vapor phase at low fluid pressures etc. Computer simulation was used for the analysis.

However, the emphasis in this work is on the modeling of the complex fluid flows inside a damper and not on the overall suspension system performance. van Vliet [6] studied motorcycle suspensions with a highly nonlinear model using computer simulation. The model included nonsymmetrical quadratic fluid damping, Coulomb friction, nonlinear spring due to entrapped air column, etc.

The above studies all point out the same basic problem with passive suspenions, namely the conflicting requirement of achieving low transmissibility at high frequencies and a close to unity transmissibility at low frequencies. Since such a requirement on transmissibility is impossible, practical suspension design is a compromise, depending on application. In general, the minimum natural frequency that can be achieved is about 1 Hz due to the fact that the static deflection varies inversely as the square of the natural frequency [7]. Damping is chosen to limit the resonant peak to an acceptable value.

1.2.2 ACTIVE SUSPENSION

In the case of active suspension, an active force generator is used to control the vehicle mass (Fig. 1.4). The force generator is normally conceived to minimize the transmitted acceleration while staying within its travel limits. Therefore, a commonly used performance criterion in the synthesis of an active force generator is that the index

$$I = \int_0^\infty [(x-y)^2 + \gamma \ddot{x}^2]dt \quad \ldots\ldots\ldots\ldots\ldots (1.5)$$

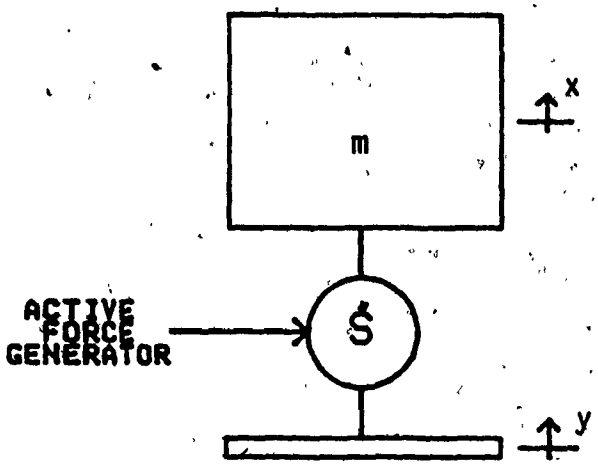

Fig. 1.4: Schematic of an Active Isolator

be minimum (γ is a weighting factor). Using optimal control theory it has been shown [8] that the suspension force is

$$F_s = -c\dot{x} - k(x-y) \quad \ldots\ldots\ldots\ldots\ldots\ldots\ldots\ldots (1.6)$$

so that

$$m\ddot{x} + c\dot{x} + k(x-y) = 0 \quad \ldots\ldots\ldots\ldots\ldots\ldots\ldots\ldots (1.7)$$

or

$$\ddot{x} + 2\zeta\omega_n\dot{x} + \omega_n^2(x-y) = 0 \quad \ldots\ldots\ldots\ldots\ldots\ldots\ldots\ldots (1.8)$$

with ω_n and ζ as defined in equation (1.3). The transmissibility of this system is then given by

$$T = \frac{1}{\sqrt{[1 - (\frac{\omega}{\omega_n})^2]^2 + [2\zeta\frac{\omega}{\omega_n}]^2}} \quad \ldots\ldots\ldots\ldots\ldots\ldots\ldots\ldots (1.9)$$

and is shown plotted in Figure 1.5. Since the damping force is to be proportional to the absolute velocity of the sprung mass, this system is equivalent to the one shown in Figure 1.6, with a passive damper connected between the mass and the inertial frame. Hence this system is called a "Sky-Hook Isolator". Using the performance criterion of Equation (1.5), damping ratio ζ was established to be $1/\sqrt{2}$ [8]. The optimum transmissibility is also shown in Figure 1.5. This has no resonance amplification, and provides high isolation beyond resonance. Comparing it with the passive suspension performance in Figure 1.3, it can be seen that the optimum active suspension performance is much superior to any passive system throughout the frequency range.

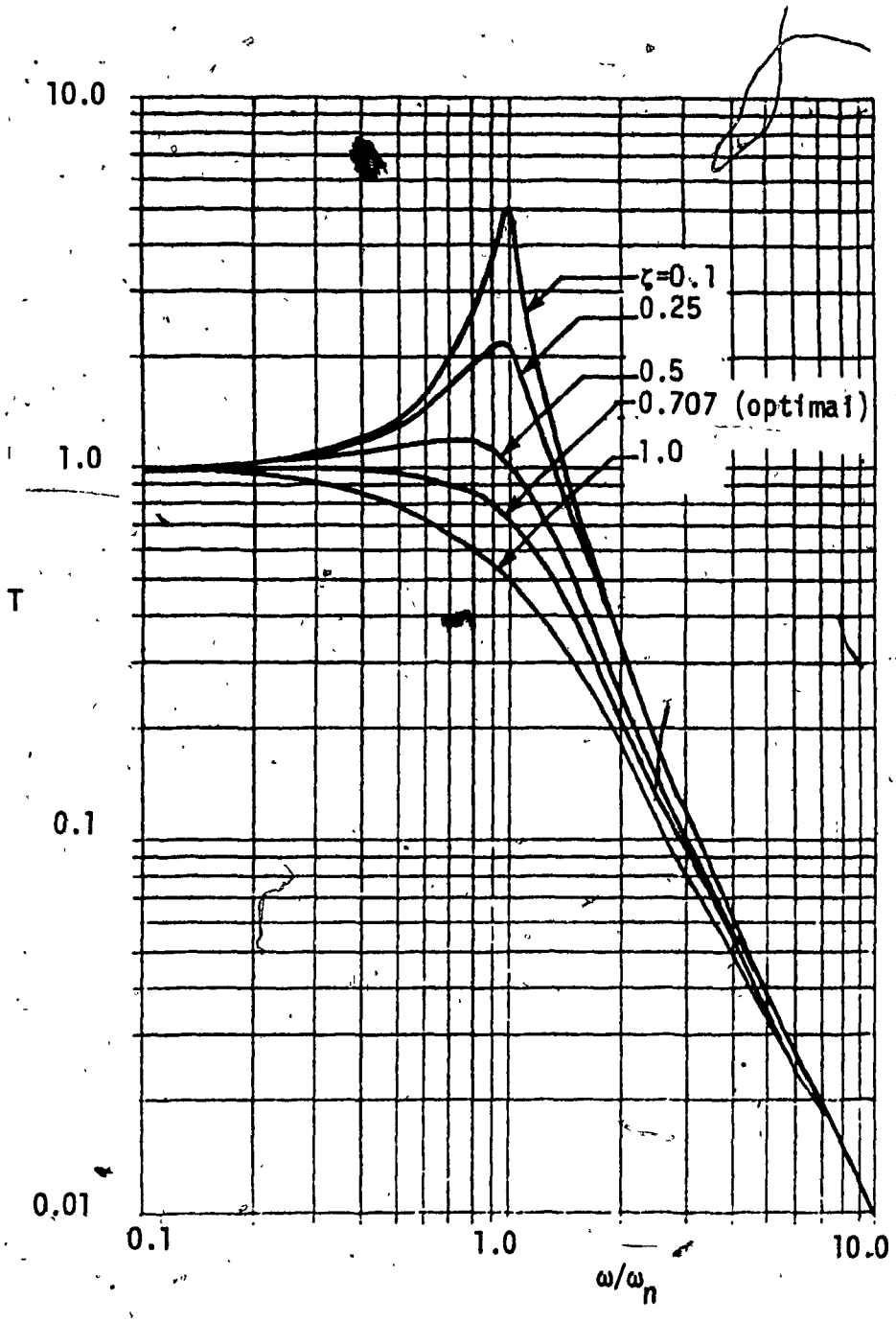

Fig. 1.5: Transmissibility Plot of an Active Isolator

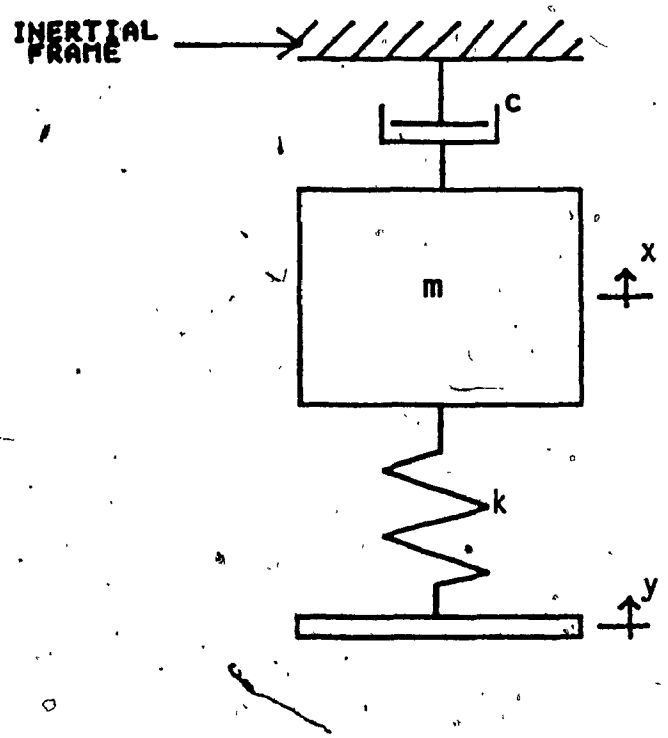

Fig. 1.6: Schematic of a Sky-hook Isolator

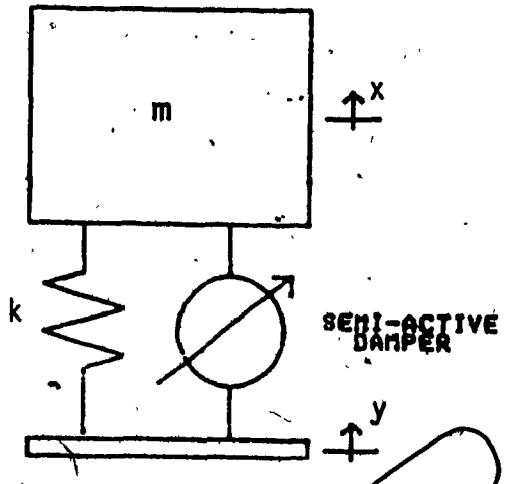

Fig. 1.7: Schematic of a General Semi-Active Isolator

A number of papers [9, 10, 11] discuss active suspensions using this control scheme. However this scheme has a severe limitation because of the need to measure absolute velocity of the sprung mass. It is assumed that this can be achieved by integrating acceleration signal. In vehicle applications, most of the input vibration energy occurs at low frequencies [12]. Hence, integrating low frequency acceleration signals to get accurate velocity values could be a formidable task [13].

Active suspension can also be based on several other control strategies. Cavanaugh [14] used a servo-actuator with integral displacement feedback. Schubert and Ruzicka [15] proposed a weighted feedback of relative displacement, relative velocity and acceleration. This system can have extremely low natural frequency and is insensitive to vehicle loading. Guntur and Sankar [16] examined various active control methods and suggested the use of passive elements in parellel with the active components to ensure fail-safe operation. Bender [8, 17] proposed preview control where the road input is sensed before it reaches the suspension. Sachs [18] proposed continuous monitoring of terrain PSD with the help of an on-board computer and varying suspension parameters periodically.

Despite the wealth of theoretical studies [19], few active suspensions have been realized in practice. In fact the only common type of "active" suspension is a "load leveler" in which the average suspension deflection is maintained at zero through the use of a slow feedback system [10, 14]. The main reason why active suspensions

are not widely adopted is because of their installation and maintenance costs, and their reduced robustness and reliability.

1.2.3 SEMI-ACTIVE SUSPENSION

As was seen from earlier sections, the active suspension can perform better than passive ones. However, the improvement in performance may not justify its cost. The concept of semi-active suspension was first proposed by Crosby and Karnopp [20] in 1973. This scheme does not require hydraulic power. Forces are generated in a damper by modulating its fluid flow orifices. It attempts to emulate a sky-hook active damper for certain parts of a vibration cycle.

Figure 1.7 shows the schematic of a general semi-active isolator. The semi-active damper generates the damper force, F_d according to a certain semi-active control scheme and is nonlinear. The spring force, F_k, is generated by a linear spring and can be mathematically expressed as $F_k = k(x-y)$.

In a semi-active force generator, since no power is supplied, the force generated is such that the power

$$F_d \cdot (\dot{x}-\dot{y}) \geq 0 \quad \ldots\ldots\ldots\ldots\ldots\ldots\ldots\ldots\ldots\ldots \quad (1.10)$$

i.e., the power associated with F_d is always dissipated. In Crosby and Karnopp's scheme,

$$F_d = \begin{cases} c\dot{x} & , \quad \dot{x}(\dot{x}-\dot{y}) > 0 \\ 0 & , \quad \dot{x}(\dot{x}-\dot{y}) < 0 \end{cases} \quad \ldots\ldots\ldots\ldots\ldots\ldots\ldots\ldots \quad (1.11)$$

This scheme was shown to give a response close to that of an active suspension [20, 21]. To implement this control logic, one needs a servovalve with a very large bandwidth as well as the measurement of absolute and relative velocities. As mentioned earlier, the accurate measurement of the absolute velocity of a moving vehicle is a near impossible task. Therefore, this scheme has not been implemented for vehicle suspensions to date. However, several theoretical results have been presented for vehicle applications including air-cushion vehicles, military tanks and agricultural tractors, [22-26, 30, 31]. The concept was also applied to the control of structural vibrations of vehicles and buildings [27-29]. In all these instances it has been claimed that the semi-active isolator is superior to a passive system and that its performance is comparable to that of an active one.

The control scheme in equation (1.11) requires a continuous modulation of damper orifice area. A simpler on-off scheme was proposed and experimental results were presented [22, 30, 31, 33]. In this case, the damper force and the control logic where governed by

$$F_d = \begin{cases} c(\dot{x}-\dot{y}) & , \quad \dot{x}(\dot{x}-\dot{y}) > 0 \\ 0 & , \quad \dot{x}(\dot{x}-\dot{y}) < 0 \end{cases} \qquad \ldots\ldots\ldots\ldots\ldots\ldots \quad (1.12)$$

The difference between Equations (1.11) and (1.12) is that in the latter, the force is proportional to the relative velocity across the damper. Thus this scheme can be implemented using an on-off damper. Experimental results reported indicate that the on-off semi-

active isolator is superior to passive one.

For all the work referenced above in this section, suspension performance was characterized by displacement transmissibility plots. It can be seen from equations 1.11 and 1.12 that the damper force has step discontinuties. Therefore, it will contribute to sudden acceleration changes. Since the system is nonlinear, acceleration transmissibility may not be equal to displacement transmissibility. This point will be detailed in a later section.

The experimental work reported [33-35] were conducted in laboratories and absolute mass velocity was directly measured using linear velocity transducer. However, as noted earlier, this would not have been possible for a vehicle application. Margolis [13] considered the effect of using realistic feedback signals. An acceleration feedback was also provided to compensate for the non-ideal velocity feedback. it was found that the performance was inferior to the ideal feedback, but still better than the passive case. However, this was only an analytical study.

Krasnicki [32] and Boonchanta [35] have presented the experimental results for the continuous semi-active control scheme of Equation 1.11. Boonchanta studied both single-degree-of-freedom and 2-DOF systems. Using displacement transmissibilities, he showed that the experimental results vindicated theoretical predictions. The high frequency performance was somewhat inferior to a lightly damped passive system. But resonance peak was effectively eliminated.

Rakheja [36] proposed an on-off semi-active damper based on another scheme. The control requires the measurement of relative velocity and relative displacement, both of which are directly measurable even in vehicle applications. The scheme is:

$$F_d = \begin{cases} c_1(\dot{x}-\dot{y})|\dot{x}-\dot{y}|, & (\dot{x}-\dot{y})(x-y) < 0 \\ c_2(\dot{x}-\dot{y})|\dot{x}-\dot{y}|, & (\dot{x}-\dot{y})(x-y) > 0 \end{cases} \quad \ldots\ldots\ldots\ldots\ldots (1.13)$$

Vibration isolation characteristics of this type of system will be analysed in detail in the present study.

Another class of isolators which could also be classified as on-off semi-active system are "dual-phase" dampers. Snowdon [37] and Guntur and Sankar [38] have studied the shock isolation characteristies of these suspensions. Hundal [39] has also studied the two stage damper used as an impact absorber.

1.3 SCOPE OF THE PRESENT STUDY

In this study, various semi-active schemes will be evaluated for their vibration isolation. These schemes include the three found in literature [20, 33, 36] and three new ones to be proposed.

Chapter 2 presents the various isolator models and their equations of motion. For this purpose, a generalized computer program is developed to analyse any of these systems. Chapter 3 details the solution procedure and Chapter 4 presents the results for

various schemes. Most of the analysis is carried out using computer simulations. In two cases, the results of the investigation on the stability of the semi-active control schemes are also presented.

Chapter 5 presents the experimental investigation of an on-off semi-active damping suspension unit. The prototype was constructed by modifying a commercial off-road motorcycle front fork. The experimental results validate predictions presented in Chapter 4. Finally, in Chapter 6, general conclusions are drawn and recommendations made for future study.

CHAPTER 2

SEMI-ACTIVE SUSPENSION MODELS

2.1 INTRODUCTION

A single-degree-of-freedom suspension model is used to study the various semi-active schemes. Six types of control strategies are analyzed: The damping force in the suspension unit is generated passively by modulating the fluid flow through the damper orifices. These damper force functions depend on whether a condition function is postive, negative or zero. Based on the nature of these condition functions, the six semi-active control schemes can be divided into three classes. In each class there are two types: in the first type the damper orifice area is continuously modulated (requiring servo-control); the second type is based on on-off control. Table 2.1 summarizes these various types. Type 1 and 2 are Karnopp and Crosby's continuous [20] and on-off [33] schemes. Type 3 in an original concept using continuous control derived from Rakheja's [36] on-off scheme which is Type 4. Type 5 and 6 are based on relative velocity measurement alone.

Referring to Figure 1.7 the equation of motion of the suspended mass can be written as:

$$m\ddot{x} + F_d + F_k = 0 \quad \ldots\ldots\ldots\ldots\ldots\ldots\ldots\ldots \quad (2.1)$$

where

$$F_k = kz \,, \qquad z = x-y$$

or

$$\ddot{x} + F_d' + \omega_n^2 z = 0 \quad \ldots\ldots\ldots\ldots\ldots\ldots\ldots\ldots \quad (2.2)$$

where

$$F_d' = F_d/m \ .$$

F_d' is the force generated in the semi-active damper according to the formulations that follow (Sections 2.2-2.7). These sections only treat the case of the condition function being negative or positive. When the condition function is zero, all the 6 schemes can be treated in a unified manner. This is detailed in Section 2.8.

Table 2.1: The Six Semi-Active Schemes

Type No.	Basis of Control Scheme	Continuous/On-off
1	Abs. vel. and rel. vel.	Continuous
2	Abs. vel. and rel. vel.	On-off
3	Rel. disp. and rel. vel.	Continuous
4	Rel. disp. and rel. vel.	On-off
5	Relative velocity	Continuous
6	Relative velocity	On-off

2.2 TYPE 1 SEMI-ACTIVE SYSTEM

This scheme was described in Chapter I. However, for the sake of completeness, the damper force equations will be repeated here.

$$F_d' = \begin{cases} 2\zeta\omega_n \dot{x} & , \quad \ddot{x}\dot{z} > 0 \\ 0 & , \quad \ddot{x}\dot{z} < 0 \end{cases} \qquad \ldots\ldots\ldots\ldots\ldots\ldots \quad (2.3)$$

2.3 TYPE 2 SEMI-ACTIVE SYSTEM

This uses an on-off control with the damper force defined by:

$$F_d' = \begin{cases} 2\zeta\omega_n \dot{z} & , \quad \ddot{x}\dot{z} > 0 \\ 0 & , \quad \ddot{x}\dot{z} < 0 \end{cases} \qquad \ldots\ldots\ldots\ldots\ldots\ldots \quad (2.4)$$

This scheme was originally proposed by Roley [30, 31]. He presented simulation results for a four-degree-of-freedom tractor cab suspension system with random inputs. He concluded that the Type 2 system gives 20 to 30 percent better vibration attenuation than a passive system. Krasnicki [33] reported experimental results for sinusoidal excitation. Hrovat and Margolis [34] also presented experimental results of a pneumatic on-off isolator employing the same condition function as Equation (2.4). The results from both these investigations show that although the semi-active suspension provided good low frequency isolation, the high frequency performance was compromised. Margolis, et al. [22] also studied pneumatic suspension system based on Type 2 control scheme and presented simulation and experimental results for step inputs.

The vibration isolation characteristics of the basic Type 2 system has not been theoretically studied in detail so far. This task is undertaken here. It will be shown that this system has some inherent drawbacks.

2.4 TYPE 3 SEMI-ACTIVE SYSTEM

Rakheja [36] observed that the damping force in a passive damper tends to increase the acceleration of the sprung mass during part of a vibration cycle. This happens when the spring force and the damper force have the same direction. Therefore it was proposed that an on-off damper be used which gives zero (or a very low) damping during this part of the cycle. When this is not the case, the damper acts like a fixed orifice passive damper. However, when spring force and the damper force are in opposite directions, if it is possible to generate a force in the damper with the same magnitude as the spring force but opposing it, then the net force acting on the mass will be zero. This idea is the basis of Type 3 semi-active scheme.

Thus for Type 3 system,

$$F_d' = \begin{cases} -\alpha\omega_n^2 z, & z.\dot{z} < 0 \\ 0, & z.\dot{z} > 0 \end{cases} \qquad \ldots\ldots\ldots\ldots\ldots\ldots\ldots\ldots (2.5)$$

where α is the gain. In this study the effect of α on the system behaviour will be investigated.

It is possible to implement this scheme using a servo-actuator to control the damper orifice. This would be similar to the

implementation of Type 1 semi-active damper reported by Boonchanta [35]. From the control point of view, the obvious advantage of this system is that it requires only the measurement of relative displacement and relative velocity. These quantities can be measured directly even for a moving vehicle suspension.

2.5 TYPE 4 SEMI-ACTIVE SYSTEM

This scheme corresponds to the one by Rakheja [36], except with a difference in that a damper with linear viscous damping will be used instead of quadratic damping. The damper force is then given by:

$$F_d' = \begin{cases} 2\zeta\omega_n \dot{z} , & z.\dot{z} < 0 \\ 0 , & z.\dot{z} > 0 \end{cases} \quad \ldots\ldots\ldots\ldots\ldots\ldots\ldots\ldots (2.6)$$

It was found that this scheme has inherent stability problems and this will be investigated in detail.

2.6 TYPE 5 SEMI-ACTIVE SYSTEM

This type of system has the damper force

$$F_d' = \begin{cases} F_o , & \dot{z} > 0 \\ -F_o , & \dot{z} < 0 \end{cases} \quad \ldots\ldots\ldots\ldots\ldots\ldots\ldots\ldots (2.7)$$

where F_o is a constant. This damper force can be produced in a semi-active way by a continuous modulation of damper orifices. However, the forces given by Equation (2.7) can also be generated passively by a Coulomb friction device. One distinctive feature of

Coulomb friction is that it causes the suspension to lock-up under certain conditions. A generalized treatment of the lock-up behaviour for all semi-active isolators is dealt with in detail in Section 2.8.

The suggestion that the damper provide a constant force as in Equation (2.7) can be arrived at intuitively. From Figure 1.3, which shows the transmissibility of a passive isolator, one can observe that the highly damped system has good resonance isolation while giving a bad high frequency isolation. This is due to the dependence of damper force on frequency (via velocity). In order to avoid this one can arrive at the concept of a damper which gives a constant magnitude force opposing the relative motion, irrespective of frequency.

From a shock isolation point of view, a spring and Coulomb damper suspension has been identified as an optimum isolator [40, 41]. Its vibration isolation characteristics has been studied by several researchers. Levitan [42] used a Fourier series approximation for the Coulomb friction force. He obtained closed form solutions for the case when continuous motion exists. Schlesinger [43] has presented exact analytical solution for sticking and slipping phases. For system with friction between mass and ground, exact analytical solutions [44, 45], and numerical simulation results [46] are also available.

In the present study, the Coulomb friction damped isolator is presented as Type 5 semi-active system. This has been done primarily

for the sake of completeness. It will be shown that Type 6 semi-active system is an on-off control version of the Type 5 system. Moreover the exact numerical simulation results for the Coulomb damped suspension is not known to have been reported so far. The results presented, although not new, compares well with analytical studies referred to earlier. This demonstrates the accuracy of the simulation methodology; in particular that of a unified treatment of lock-up condition for all semi-active schemes (section 2.8).

2.7 TYPE 6 SEMI-ACTIVE SYSTEM

This scheme operates based on relative velocity, and the damper force is

$$F_d' = \begin{cases} 2\zeta_1\omega_n\dot{z} & , \quad |\dot{z}| < V_s \\ 2\zeta_2\omega_n\dot{z} & , \quad |\dot{z}| > V_s \end{cases} \qquad \ldots\ldots\ldots\ldots\ldots\ldots\ldots (2.8)$$

where $\zeta_2 < \zeta_1$, and V_s is called the switching velocity. This scheme is similar to the dual phase damping proposed for shock mounts by Snowdon [37]. In the present study the scheme is extended for vibration isolation and the criterion for selecting V_s is formulated.

The passive suspension system shown in Figure 1.2 is characterized by the set of equations (1.1) to (1.4). The transmissibility of this system is shown in Figure 1.3, plotted for various values of damping ratio, ζ. Referring to this figure, we denote the response for $\zeta = 0.1$ as "oabc" and that for $\zeta = 1.0$ as "odbe". The aim of Type 6 semi-active system is to try to obtain a

response curve such as "odbc". This corresponds to a passive system with $r = 1.0$ for $\omega < \sqrt{2}\omega_n$ and $r = 0.1$ for $\omega > \sqrt{2}\omega_n$.

From Equation (1.1), the amplitude of the steady state relative velocity can be written as

$$V = \frac{(\frac{\omega}{\omega_n})^2 \, a\omega}{\sqrt{[1 - (\frac{\omega}{\omega_n})^2]^2 - (2\zeta\frac{\omega}{\omega_n})^2}} \quad \ldots\ldots\ldots\ldots\ldots\ldots (2.9)$$

where a is the amplitude of the sinusoidal input. Figure 2.1 shows this plotted for $\zeta = 0.1$ and $\zeta = 1.0$. It can be seen that the curve for $\zeta = 1.0$ increases monotonically with frequency. Thus the value of the amplitude of the relative velocity is a measure of the frequency. This value at $\omega = \sqrt{2}\omega_n$ is denoted as V_s. Then from Equation (2.9),

$$V_s = \frac{2\sqrt{2}}{3} \, a\omega_n \quad \ldots\ldots\ldots\ldots\ldots\ldots (2.10)$$

This is the switching velocity, for the Type 6 on-off semi-active damper described by Equation (2.8).

Damping force of the form in Equation (2.8) can be produced by a relief valve mounted on the damper piston. In fact, such an arrangement can be seen in some off-road motorcycle rear shock-absorbers [47]. Attempts are also made to incorporate them in aircraft landing gear [48]. However these designs are carried out on purely empirical basis. In the present study, a systematic theoretical basis for such suspensions has been presented. Experimental results are also presented for this type of isolator which confirm the theoretical predictions.

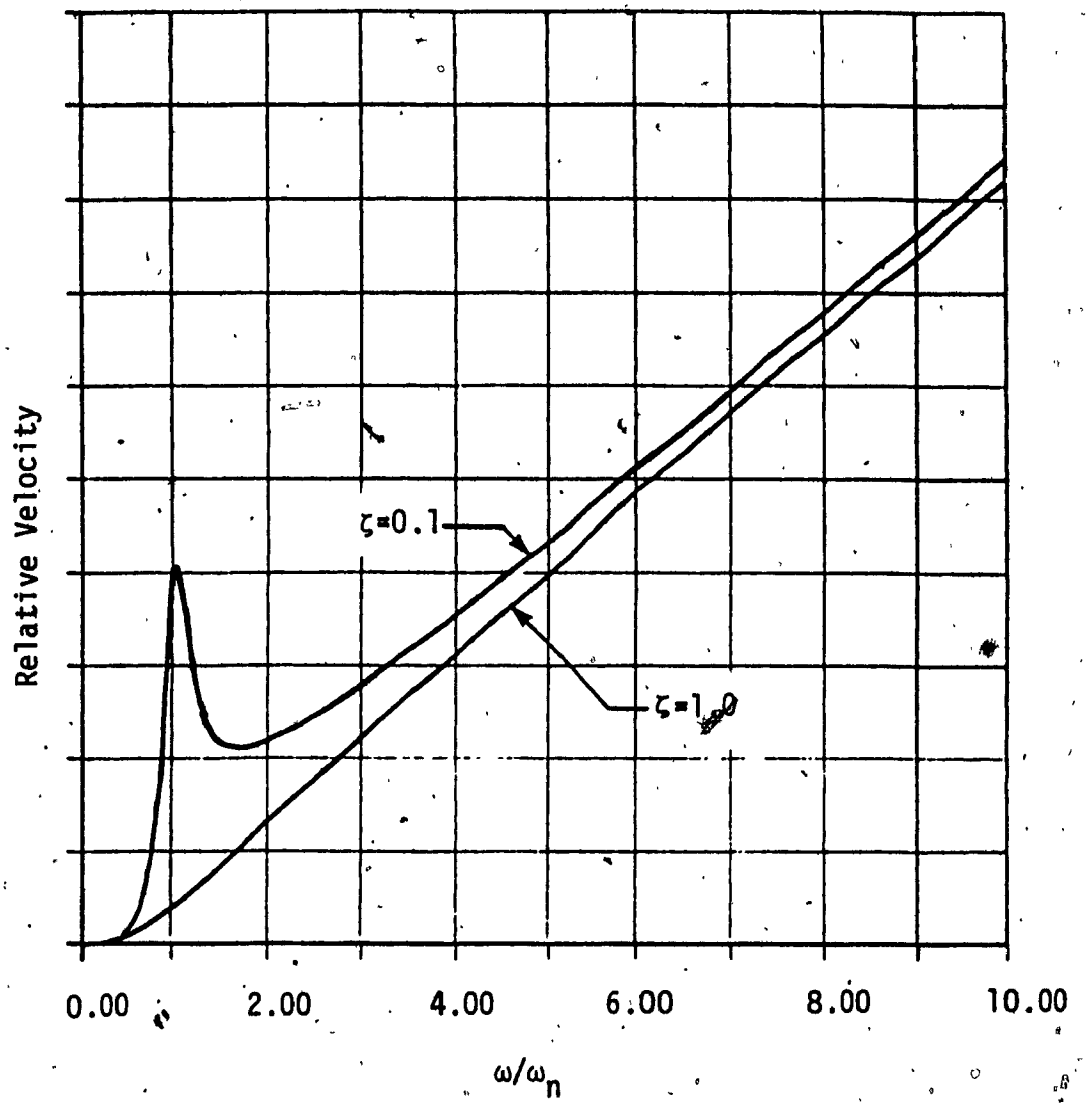

Fig. 2.1: Steady-State Amplitude of Relative Velocity

2.8 SYSTEM EQUATIONS WHEN CONDITION FUNCTION BECOMES ZERO

In the foregoing sections equations of motion for the 6 types of semi-active schemes have been presented. In each of these schemes the damping force was defined for the positive and negative values of the condition function. The situation when the condition function is zero is treated in this section. Only the semi-active schemes employing continuous control (Types 1, 3, and 5) can possibly handle this situation adequately. The on-off control schemes, by their very nature, can only provide two stages of damping forces corresponding to the positive or negative sign of the condition function. Therefore, one must examine the on-off control schemes to see if the switching behaviour is stable.

2.8.1 Continuous Control Semi-Active Schemes

Karnopp, et al. [20, 21] have described the control strategy for the Type 1 system when the condition function is zero. For this system, the condition function is

$$\phi_1 = \dot{x}(\dot{x} - \dot{y})$$

when $\phi_1 = 0$, two special cases exist. In the first case $\dot{x} = 0$, in which case, it is desired to have $F_d' = 0$. The second case is when $\dot{x} \neq 0$ and $(\dot{x} - \dot{y}) = 0$. In this case, the semi-active damper can attempt to apply the force $2\zeta\omega_n\dot{x}$. Depending on subsequent time history of motion, the condition function becomes either negative or positive so that Equation (2.3) applies, or the force $2\zeta\omega_n\dot{x}$ may be large enough to lock-up the system. During lock-up, $\ddot{x} = \ddot{y}$ and the spring force is $F_k' = \omega_n^2 (x - y)$. Then the damper force is

$$F_d' = -\ddot{y} - \alpha\omega_n^2 (x - y) \quad \ldots\ldots\ldots\ldots\ldots\ldots\ldots\ldots (2.11)$$

Thus the Type 1 semi-active system will lock-up when $(\dot{x} - \dot{y}) = 0$ and the desired force $2\zeta\omega_n\dot{x}$ is greater than the expression in Equation (2.11).

Following a similar argument, it is possible to deal with $\phi_3=0$ situation for the Type 3 system. In this situation also two special cases arise. In the first case $(x - y) = 0$, in which case, the damping force $F_d' = 0$. The second case occurs when $(\dot{x} - \dot{y}) = 0$ and $(x - y) \neq 0$. In this case, the system will lock-up if the desired force F_d', $(F_d' = -\alpha\omega_n^2(x - y))$ is greater than the expression in Equation (2.11).

For the Type 5 system, the zero condition function, $\phi_5 = 0$ occurs when $(\dot{x} - \dot{y}) = 0$. In this case, the lock-up persists as long as the lock-up force of Equation (2.11) is less than the friction force, F_0, i.e., lock-up exists for

$$F_0 > |\ddot{y} + \omega_n^2 (x - y)| \quad \ldots\ldots\ldots\ldots\ldots\ldots\ldots (2.12)$$

The above arguments can be unified to provide a succinct, yet general, condition for lock-up situation. This will in fact define the necessary condition for the existence of solutions for differential equations with discontinuities.

Consider a first order differential equation such as

$$\dot{x} = \begin{cases} F_1(x, t) & , \quad \phi > 0 \quad \ldots\ldots\ldots\ldots\ldots\ldots (2.13) \\ F_2(x, t) & , \quad \phi < 0 \quad \ldots\ldots\ldots\ldots\ldots\ldots (2.14) \end{cases}$$

where $\phi = \phi(x, t)$ $\ldots\ldots\ldots\ldots\ldots\ldots\ldots\ldots (2.15)$

$\dot{x}$ is defined by either Equation (2.13) or (2.14) depending on the sign of the condition function, ϕ. Suppose ϕ is initially greater than zero and that it now becomes zero. Consequently we switch from Euation 2.13 to Equation 2.14. Now if ϕ is less than zero, the solution continues in time. However at $\phi = 0$, if the very act of switching to a different equation causes ϕ to revert back to its original sign, then the differential equation ceases to have a solution. Although the situation is illustrated for one variable and one condition function, the principle applies to systems of equations as well.

In the case of Type 1, 3 and 5 semi-active suspensions this situation occurs when the relative velocity is zero. Hence, the damper can cause the system to lock-up until the change in the relevant variable permits it to continue the operation according to the force equations given in earlier sections. Thus the lock-up is caused when the conditon function becomes zero and the consequent sudden change in damper force is likely to cause the condition function to revert to its earlier sign.

2.8.2 On-Off Semi-Active Schemes

The possibility of the system equation ceasing to have solution at points of discontinuity exists in the on-off case as well. By their very nature, the on-off damper cannot cause lock-up in that situation. Therefore, a successful on-off control scheme must ensure that it will not cause the system to be 'stuck', or provide an adequate strategy to deal with that possibility. The three on-off schemes, namely, Type 2, 4 and 6 systems will be examined in this regard.

For Type 2 system, the condition function, $\phi_2 = 0$ when either $(\dot{x} - \dot{y}) = 0$ or $\dot{x} = 0$. When $(\dot{x} - \dot{y})$ passes through zero, the damper force is not discontinuous because it is proportional to the relative velocity (see Equation 2.4). However, when $\dot{x}$ passes through zero, there is a step discontinuity in the damper force. Depending on the relative magnitude of system parameters and variables, the change in this force may be sufficiently large to cause $\dot{x}$ to change direction at $\dot{x} = 0$ and return ϕ_2 to its original sign. Mathematically, the initial value problem gets 'stuck' at that point.

For the Type 4 system, the condition function, $\phi_4 = 0$, when either $(\dot{x} - \dot{y}) = 0$ or $(x - y) = 0$. As in Type 2 system, there will not be a problem at $(\dot{x} - \dot{y}) = 0$ because the damper force is continuous at this point. When $(x - y)$ passes through zero, there will be a step discontiniuity in the damper force. However, since the velocity is continuous, the relative displacement cannot change

direction at $\phi_4 = 0$. Therefore Type 4 on-off scheme switching is stable.

Switching operation in Type 6 system is stable if $\zeta_2 < \zeta_1$. Otherwise the switching may become unstable. This can be proven as follows. Since velocity and displacement are continuous, their values just before and just after switching are the same. Thus, from Equations (2.2) and (2.8), before switching,

$$\ddot{x}^- = -2\zeta^-\omega_n\dot{z} - F_k' \quad \ldots\ldots\ldots\ldots\ldots\ldots\ldots \quad (2.16)$$

After switching,

$$\ddot{x}+ = -2\zeta^+\omega_n\dot{z} - F_k' \quad \ldots\ldots\ldots\ldots\ldots\ldots\ldots \quad (2.17)$$

But $\ddot{z} = \ddot{x} - \ddot{y}$ and $\ddot{y}+ = \ddot{y}^-$

Then $(\ddot{z}+ - \ddot{z}^-) = 2\omega_n\dot{z}\,(\zeta^- - \zeta+) \quad \ldots\ldots\ldots\ldots\ldots \quad (2.18)$

This situation is illustrated in Figure 2.2 for Type 6 system in which $\zeta_2 < \zeta_1$. This figure is based on simulation results (Figure 4.42) with some exaggerations for clarity. The superscript - or + indicates the value of the respective quantity just before and just after switching takes place. It is noted that the change in the absolute value of the relative acceleration is positive at all the four switching instants per period. This means that switching causes the relative velocity to continue in its direction at a faster rate. Therefore the switching is stable. However, if

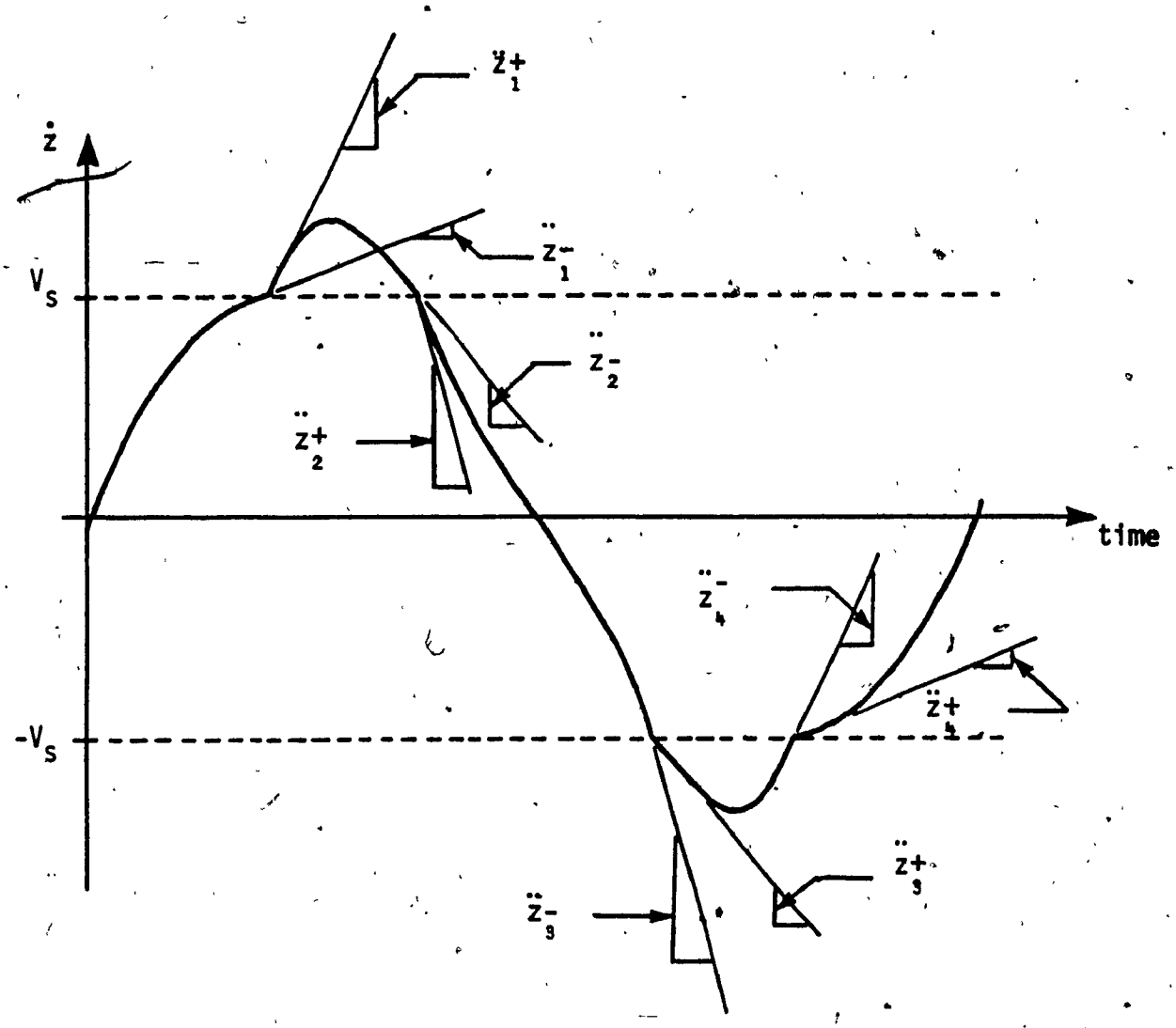

Fig. 2.2: Variation of $\dot{z}$ with Time for Type 6 System

c_2 c_1, there is a possibility that the switching will be unstable. Simulation results have borne out these conclusions.

2.8.3 Conclusion

All the six semi-active schemes presented are characterized by discontinuous differential equations. The behaviour of the various schemes at the point of discontinuity has been examined in the foregoing sections. The control schemes call for lock-up of the damper in Type 1, 3 and 5 systems under certain conditions. However, in physical implementation of the control schemes, true lock-up may be impossible because of time delays in the control loop (except for Type 5 system, if it is configured as a passive Coulomb friction isolator). What will happen is that the damper force will oscillate about the lock-up force with the relative velocity nearly zero [21]. Eventually the system variable change so that the system breaks out of the lock-up situation. The exact nature of lock-up behaviour is obviously dependent on the physical implementation of the control scheme. This aspect of the problem is not investigated in this study.

In the case of the on-off control scheme of Type 2 isolator, it was found that the switching will be 'unstable' under certain conditions. In a physical realization this means that the on-off solenoid will exhibit 'chatter', limited by its time constant. Once again the behaviour depends on the physical parameters of the control set up, and is not studied here. Type 4 and Type 6 on-off control schemes have been shown to have stable switching operation.

2.9 SUMMARY

In this Chapter, the damper force equations were presented for the six types of semi-active suspensions proposed. Three of the schemes require continuous servo-operated damping control and other three, simple on-off valves. All six of the schemes are characterized by ordinary differential equations containing discontinuities. These equations have been defined for positive and negative values of the condition function. The case when condition function becomes zero is dealt with separately. It has been shown that Type 1, 3 and 5 systems may lock-up in this situation. Type 2 system may cease to have further solution (mathematicallly) under certain circumstances.

Figure 2.3 will help to visualize the characteristics of the damper force generated according to the six different schemes. The plots are drawn for a hypothetical case of $\zeta = \alpha = \omega_n = \zeta_1 = F_0 = 1.0$, $\zeta_2 = 0.2$, $V_s = 0.5$, $y = \text{Sin}\ (t)$ and $x = \text{Sin}\ (t + \frac{\pi}{4})$ with $0 < t < 2\pi$.

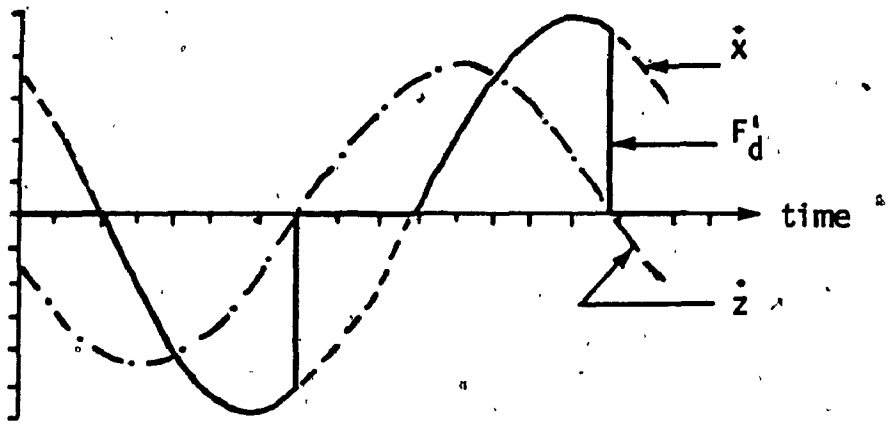

Fig. 2.3 (a): Damper Force in Type 1 System

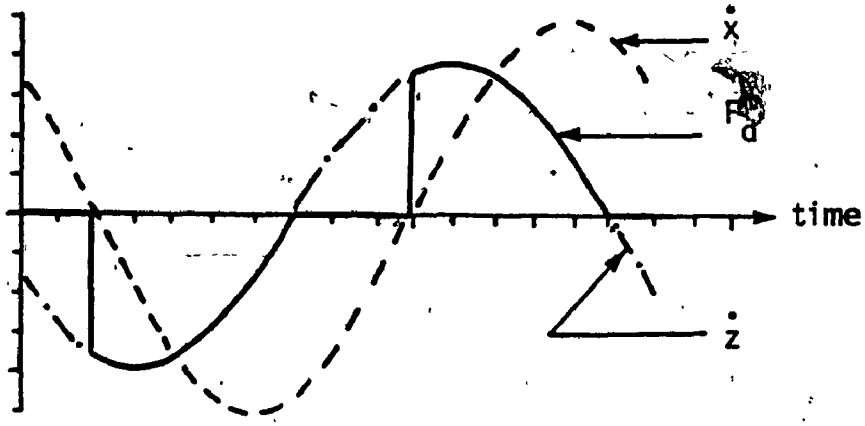

Fig. 2.3 (b): Damper Force in Type 2 System

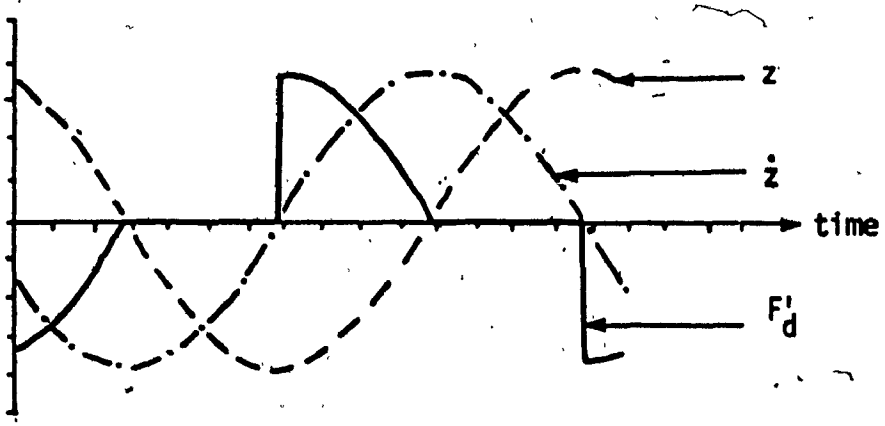

Fig. 2.3 (c): Damper Force in Type 3 System

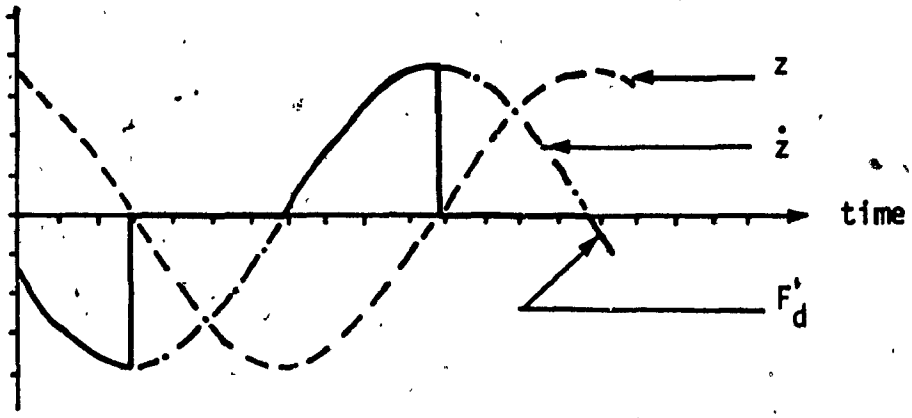

Fig. 2.3 (d): Damper Force in Type 4 System

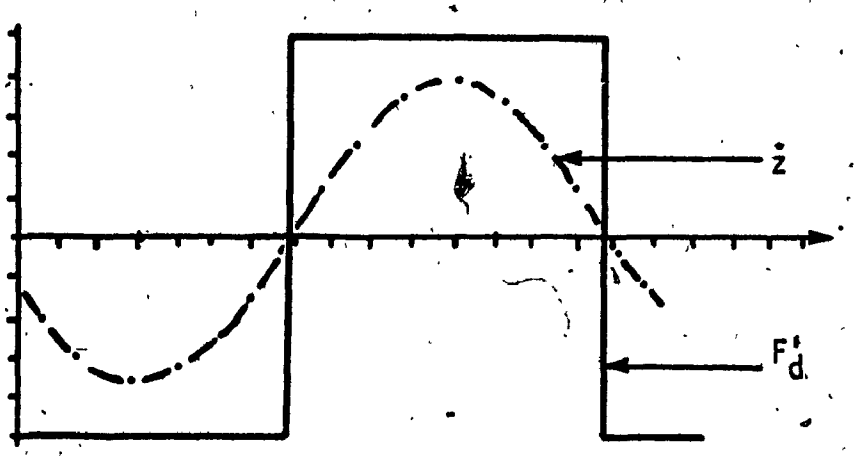

Fig. 2.3 (e): Damper Force in Type 5 System

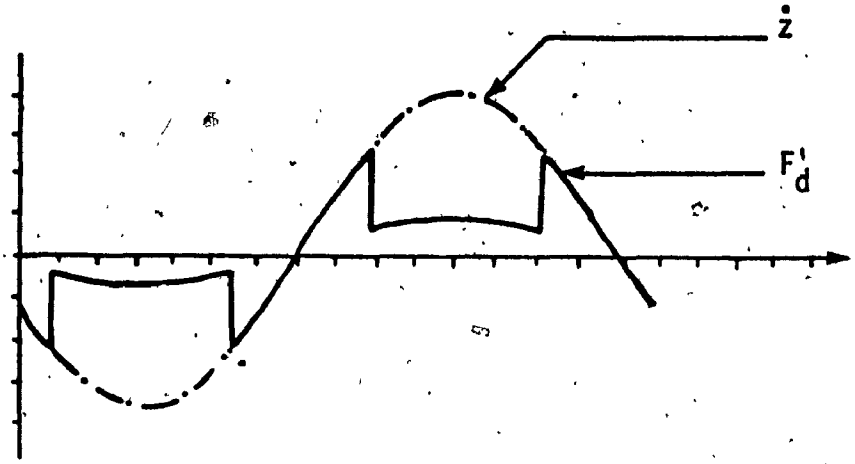

Fig. 2.3 (f): Damper Force in Type 6 System

CHAPTER 3

SOLUTION PROCEDURE

3.1 INTRODUCTION

The equations of motion of the semi-active suspension systems described in Chapter 2 have step discontinuities and hence are nonlinear. Therefore no closed form solution is possible. Equivalent linearization technique may be used to linearize the nonlinear problem. However, the nonlinearities which are dealt with are significant and a linearized model would be highly inaccurate [49, 50]. Furthermore, the very purpose of this study is to see the effect of damping nonlinearities on the system behaviour and hence linearization would be self-defeating.

3.2 COMPUTER SIMULATION

The most direct and fast way of solving the system equations is by computer simulation. This is the approach used by previous investigators [20, 36]. In simulation, the differential equation are solved as an initial value problem for a given set of parameters. When a frequency domain performance is desired (such as transmissibility), the simulation is carried out at each discrete frequency. The simulation proceeds in time until a 'steady-state' is reached. Then the response variables are evaluated and the process is repeated for the next frequency.

The second order differential equation (Eqn. (2.1)) describing the system is rewritten as a pair of first order equations. The

numerical integration is carried out using a 4th order Runge-Kutta algorithm [51]. The discontinuities in the equation require special treatment. Otherwise the integration algorithm will be very inefficient and will cause inaccurate results [52, 53].

The system differential equations can be rewritten as

$$\dot{x} = v$$
$$\dot{v} = -F_d' - \omega_n^2(x - y) \quad \ldots\ldots\ldots\ldots\ldots\ldots\ldots\ldots\ldots\ldots (3.1)$$

where

$$y = a \sin \omega t \quad \ldots\ldots\ldots\ldots\ldots\ldots\ldots\ldots\ldots\ldots (3.2)$$

and a = amplitude of sinusoidal input

$$F_d' = \begin{cases} F_{1,i}, & \phi_i > 0 \\ F_{2,i}, & \phi_i < 0 \end{cases} \quad \ldots\ldots\ldots\ldots\ldots\ldots\ldots\ldots\ldots\ldots (3.3)$$

where ϕ_i corresponds to the condtion function of the ith system type.

The equations are a generalized form of Equations (2.3)-(2.8). The zero-crossing of the condition function ϕ_i determines the switching point for the damping force function. Table 3.1 summarizes the damper forces for the 6 types of systems.

Table 3.1 Summary of Damper Forces

Type, i	ϕ_i	$F_{1,i}$	$F_{2,i}$
1	$\dot{x}.(\dot{x} - \dot{y})$	$2\zeta\omega_n\dot{x}$	0
2	$\dot{x}.(\dot{x} - \dot{y})$	$2\zeta\omega_n(\dot{x} - \dot{y})$	0
3	$-(x - y).(\dot{x} - \dot{y})$	$-\alpha\omega_n^2(x - y)$	0
4	$-(x - y).(\dot{x} - \dot{y})$	$2\zeta\omega_n(\dot{x} - \dot{y})$	0
5	$(\dot{x} - \dot{y})$	F_0	$-F_0$
6	$V_s - (\dot{x} - \dot{y})$	$2r_1\omega_n(\dot{x} - \dot{y})$	$2r_2\omega_n(\dot{x} - \dot{y})$

It is possible to solve these ordinary differential equations (ODE) using numerical integration algorithms with error control, such as a Predictor-Corrector algorithm [54]. As the step size chosen by the integration algorithm is controlled by the current estimate of truncation error, it will adjust the step size sufficiently to overcome the discontinuity. But in the present application this process has two major drawbacks.

1) The algorithm will move around the discontinuity, using large number of function evaluations before a

step size is found which crosses the discontinuity with satisfactory accuracy [52].

2) The actual time at which the discontinuity occurs may not be used as an integration point. Therefore the values of the response variables at this instant will not be available for processing (e.g. calculation of peak forces and accelerations).

Several researchers have studied the problem of numerical integration of ODE with discontinuities [52, 53, 55, 56]. Their basic approach is to incorporate a zero-finder in the integration procedure. At each integration step a test is performed to detect the change in sign of the condition function. If no change occurs the integration proceeds. Otherwise a zero-finder determines accurately the time, t^*, when the condition function is zero. The integration then stops with the old set of system functions and restarts with the appropriate new set.

Carver [52] treated the condition functions the same way as the system function in an expanded system. This requires the time derivative of ϕ to be continuous, and is efficient only when the system is large and the number of condition functions small. Ellison [55], Li, et al. [56] and Borthwick [53] have used Hermite and/or inverse interpolation formulae as zero-finders depending on accuracy requirements. They have obtained good results with high efficiency.

However the Hermite interpolation requires the derivative of the condition function.

In the present study it is desired to have an effective algorithm which can handle all the six types of semi-active control schemes. The method suggested by Li, et al. [56] was found to be very efficient. However, this is not suitable for the Type 6 system because its condition function has discontinuous time derivative. Therefore some efficiency is sacrificed in favour of a more general method and a bisection algorithm [51] is used as the zero finder. This does not require the time derivative of ϕ and will always converge to the solution.

3.3 BIFURCATION ANALYSIS

Bifurcation or branching is a phenomenon that occurs in nonlinear problems, albeit a rare one. In the case of Type 4 semi-active system, it was observed in simulation run that the solution exhibited a drift beyond a certain frequency. This suggested a bifurcation problem. It is not easy to examine bifurcation and stability problems using simulation techniques. Therefore the study was done with the help of a bifurcation analysis software package called AUTO [57]. Type 3 and Type 4 systems were analyzed this way. AUTO solves the system as a boundary value problem instead of using simulation.

3.3.1 Problem Description

AUTO is a subroutine package for the automatic bifurcation

analysis of autonomous systems of ordinary differential equations. Using AUTO it is easy to study the system behaviour as different parameters are varied. Since the differential equations need to be continuous and autonomous, the equations need to be modified. The discountinuity in the above equations will be approximated using an inverse tangent function. For example, a step discontinuity as shown in Figure 3.1 (a) can be approximated by the equation,

$$c = c_1 \left[\arctan(\phi r) + \frac{\pi}{2}\right] \quad \ldots\ldots\ldots\ldots\ldots\ldots\ldots (3.4)$$

where r is called the 'homotopy' parameter. When $r = \infty$, the above function is identical to the step discontinuity. Figure 3.1 (b) shows this function plotted for r = 100.0.

AUTO also requires that the system of equations be autonomous, which means that the forcing term in Equation (3.2) cannot be used. Instead, two more differential equations are added whose solution can be used to produce the forcing function. These coupled nonlinear equations are

$$\begin{aligned} \dot{p} &= p + \omega q - p(p^2 + q^2) \\ \dot{q} &= q - \omega p - q(p^2 + q^2) \end{aligned} \quad \ldots\ldots\ldots\ldots\ldots\ldots\ldots (3.5)$$

They have the solution

$$\begin{aligned} p &= \sin(\omega t) \\ q &= \cos(\omega t) \end{aligned} \quad \ldots\ldots\ldots\ldots\ldots\ldots\ldots (3.6)$$

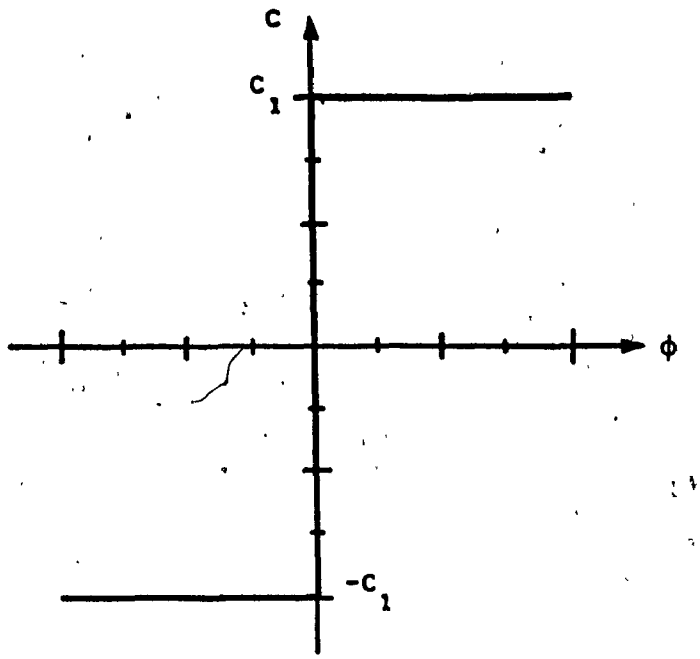

Fig. 3.1 (a): Step Discontinuity

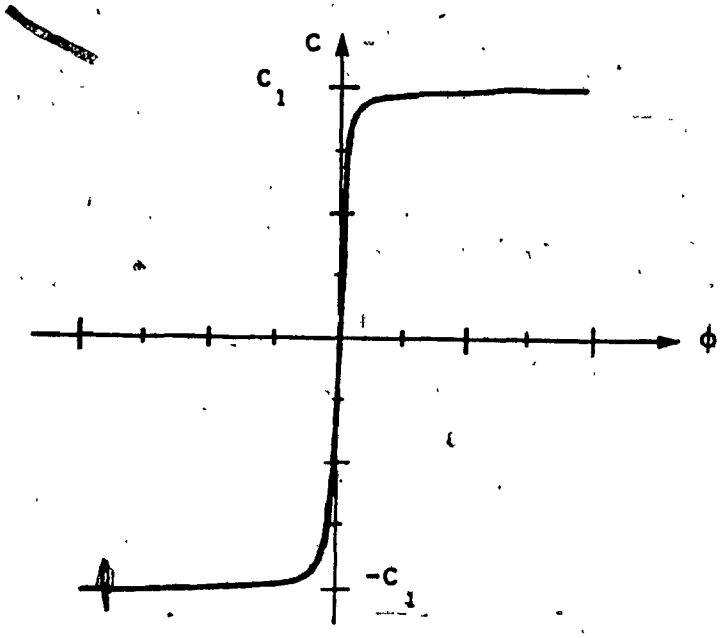

Fig. 3.1 (b): Approximation of Step Discontinuity Using a Continuous Function

Note that this pair of equations are decoupled from the system equations and they are shown to be stable [58].

From Equation 3.1 and 3.5 the expanded systen can be written as four simultaneous nonlinear ordinary differential equations, namely,

$$\begin{aligned}
\dot{x} &= v \\
\dot{v} &= -F_d' - \omega_n^2(x - ap) \\
\dot{p} &= p + \omega q - p(p^2 + q^2) \\
\dot{q} &= q - \omega p - q(q^2 + q^2)
\end{aligned} \qquad \ldots\ldots\ldots\ldots\ldots\ldots \quad (3.7)$$

3.3.2 Solution Scheme

To find the frequency domain performance, ω is treated as free parameter. The equation (3.7) is of the form

$$\underline{u}'(t) = \underline{F}(\underline{u}(t),\omega)) \qquad \ldots\ldots\ldots\ldots\ldots\ldots\ldots\ldots \quad (3.8)$$

In general, the period of the solution ρ may be different from the period of excitation ω. Finding ρ-periodic solutions of (3.8) is equivalent to finding 2π-periodic solutions, and ρ of the boundary value problem

$$\begin{aligned}
\underline{u}'(t) &= \frac{\rho}{2\pi}\,\underline{F}(\underline{u}(t),\omega)) \\
\underline{u}(0) &= \underline{u}(2\pi)
\end{aligned} \qquad \ldots\ldots\ldots\ldots\ldots\ldots \quad (3.9)$$

The difficulty in solving (3.9) is that $\underline{u}(t)$ is not unique, because if $(\underline{u}(t),\rho,\omega)$ is a solution, then $(\underline{u}(t + \sigma),\rho,\omega)$ is also a solution for any σ. This indeterminacy is removed by 'aligning' the the j^{th} solution with respect to the $(j - 1)^{th}$ solution along the time axis. This adds another equation,

$$\int_0^{2\pi} (\underline{u}_j(t) - \underline{u}_{j-1}(t))^T \underline{u}'_j(t)\, dt = 0 \quad \ldots\ldots\ldots\ldots \quad (3.10)$$

This way if the solution points $(\underline{u}_i, \rho_i, \omega_i)$, $i = 1, 2, \ldots j-1$, are computed, one proceeds to computing the j^{th} solution point $(\underline{u}_j, \rho_j, \omega_j)$. ω is not used as continuation parameter because of the possibility of encountering limit points. Using the general pseudo-arclength continuation scheme [59], another equation is added treating ω as an unknown.

$$\int_0^{2\pi} (\underline{u}_j(t)-\underline{u}_{j-1}(t))\dot{\underline{u}}_{j-1}(t)dt + (\rho_j-\rho_{j-1})\dot{\rho}_{j-1} + (\omega_j-\omega_{j-1})\dot{\omega}_{j-1} = \Delta s \quad (3.11)$$

where "." denotes differentiation with respect to the arclength parameter s.

3.3.3 Stability of Periodic Solutions

Let $(\underline{u}, \rho)$ be a solution and consider the linearization

$$\underline{v}'(t) = \frac{\rho}{2\pi} F_u(\underline{u}(t),\omega)\underline{v}(t)$$
$$\underline{v}(0) = \underline{v}(2\pi) \qquad \ldots\ldots\ldots\ldots\ldots\ldots \quad (3.12)$$

If $V(t)$ is the fundamental solution matrix of the above system (note that $V(t)$ is 2π-periodic), with $V(0) = \tilde{I}$, the identity matrix, then,

$$\underline{v}(2\pi) = V(2\pi)\underline{v}(0)$$
$$\underline{v}(m2\pi) = (V(2\pi))^m \underline{v}(0) \qquad \ldots\ldots\ldots\ldots\ldots\ldots \quad (3.13)$$

The solution is stable, if the eigenvalues of $V(2\pi)$ lie inside the unit circle, except for the one eigenvalue which will always be at 1. The eigenvalues of $V(2\pi)$, which determine the stability, are called the Floquet Multipliers.

Change of stability happens when one the following cases occur:

1. An eigenvalue crosses the unit circle through 1.

2. An eigenvalue crosses the unit circle through -1.

3. Complex conjugate pair through $e^{\pm 2\pi i\theta}$, θ rational.

4. Through $^{\pm 2\pi i\theta}$, θ irrational.

In case 1, when there is a double eigenvalue at 1, a variety of cases may occur; there may be a bifurcation. In case 2, there will be a period doubling bifurcation. Cases 3 and 4 lead to bifurcations to invarient tori.

3.4 PERFORMANCE CHARACTERIZATION

Since the semi-active system is nonlinear with step changes in damper force, the acceleration response will have discontinuities. Previous researchers have used displacement transmissibility (ratio of the peak displacement response to the input amplitude) to characterize the suspension performance. Since the human body or a suspended mass is sensitive to inertial forces, the characterization in terms of acceleration would be more appropriate.

In this study the ratio of the root-mean-square (RMS) value of the response acceleration to the RMS value of the input acceleration is taken as the transmissibility. The various types of semi-active schemes will be judged on this basis. The acceleration mean square value of a periodic signal with period τ is

$$A^2 = \frac{1}{\tau} \int_{t=to}^{to+\tau} [\ddot{x}(t)]^2 \, dt \quad \ldots\ldots\ldots\ldots\ldots\ldots\ldots\ldots (3.14)$$

In the computer program the integration is carried out using trapezoidal rule [51]. For the input $y = a \sin \omega t$, the transmissibility is

$$T = \frac{\sqrt{2}A}{a\omega^2} \quad \ldots\ldots\ldots\ldots\ldots\ldots\ldots\ldots \quad (3.15)$$

The use of RMS value is the standard pratice in random vibration analysis. There, the area under a PSD curve is equal to the mean square value of that signal [60]. It can be shown using Parseval's Theorem that this is also equal to the expression in Equation (3.14). Therefore, in the experimental investigation presented in Chapter 5, a FFT analyzer was used to calculate the RMS value of the acceleration signal using the area under its PSD curve.

Analysis was carried out for the frequency range 0.1 to 10.0 Hz. This was based on the fact that most of the ground input energy for on-road and off-road terrains fall within this band [12].

3.5 CONCLUSION

The procedure for solving the semi-active system equations are presented. Computer simulation is used for all cases. Type 3 and 4 systems are also studied using a bifurcation analysis software package. The performance of the various semi-active vibration isolation schemes are characterized by acceleration transmissibility plots. For this the ratio of the RMS value of the response acceleration to the RMS value of the base acceleration excitation is computed. The results are presented and discussed in the following chapter.

CHAPTER 4

COMPUTER RESULTS AND DISCUSSION

4.1 INTRODUCTION

The governing equations of the six types of semi-active isolators and the solution scheme were presented in the previous chapters. The results are given in this chapter. These are detailed for each type seperately. The performance of the various semi-active schemes are compared with that of active and passive isolators. For each system a set of basic parameter values are established. The effect of varying some relevant parameters are compared with the 'basic system'. Comparison between the various types are made whenever appropriate. The results are summarized in the concluding section.

4.2 TYPE 1 SEMI-ACTIVE SYSTEM

The basic set of parameters for this system are $\omega_n = 1.0$, $\zeta = 0.707$ and $a = 1.0$. Thus, this semi-active scheme attempts to emulate an optimum active isolator. Figures 4.1, 4.2 and 4.3 show the steady state response from simulation for the frequency ratio (ω/ω_n) of 0.5, 1.0 and 5.0. The time scale is normalized with respect to the period of oscillation. It can be verified that the damper force conforms to Equation (2.3). Figure 4.1 clearly shows the three regions where the damper force is (a) proportional to absolute velocity, (b) equal to zero and (c) the region where lock-up occurs. Lock-up condition does not occur at high frequencies.

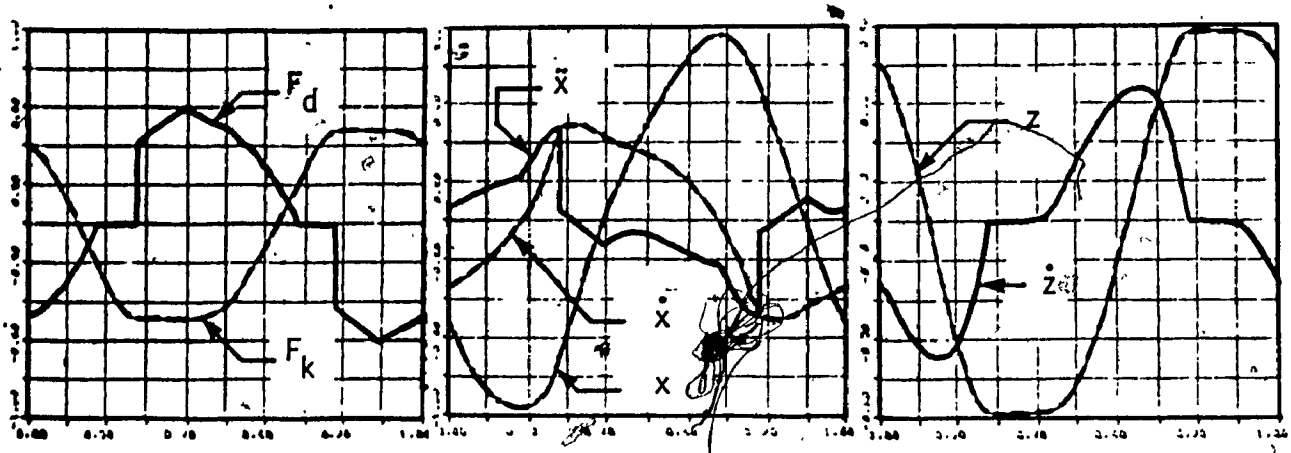

Fig. 4.1: Steady-State Response of Type 1 System at $\frac{\omega}{\omega_n}$ =0.5

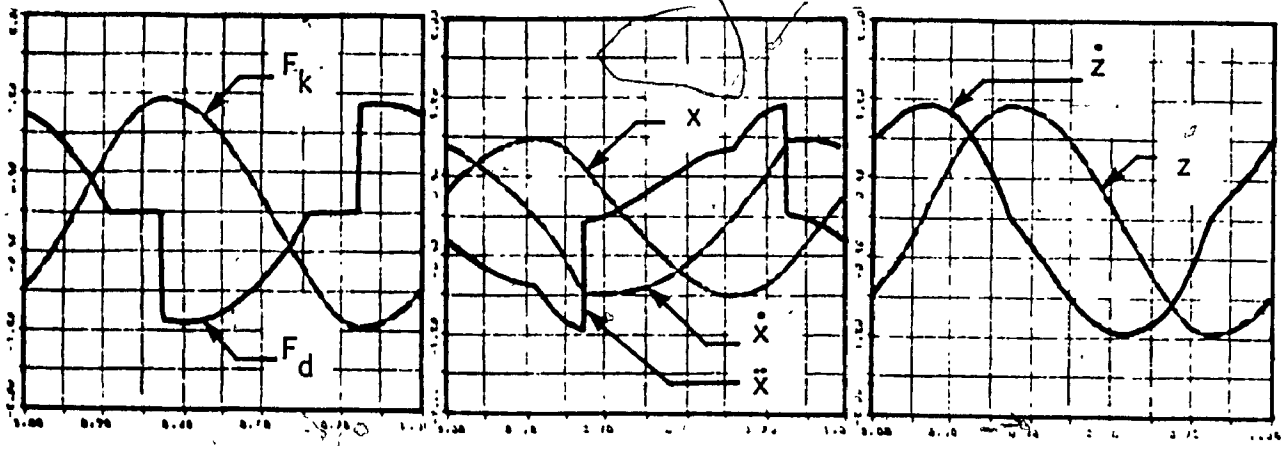

Fig. 4.2: Steady-State Response of Type 1 System at $\frac{\omega}{\omega_n}$ =1.0

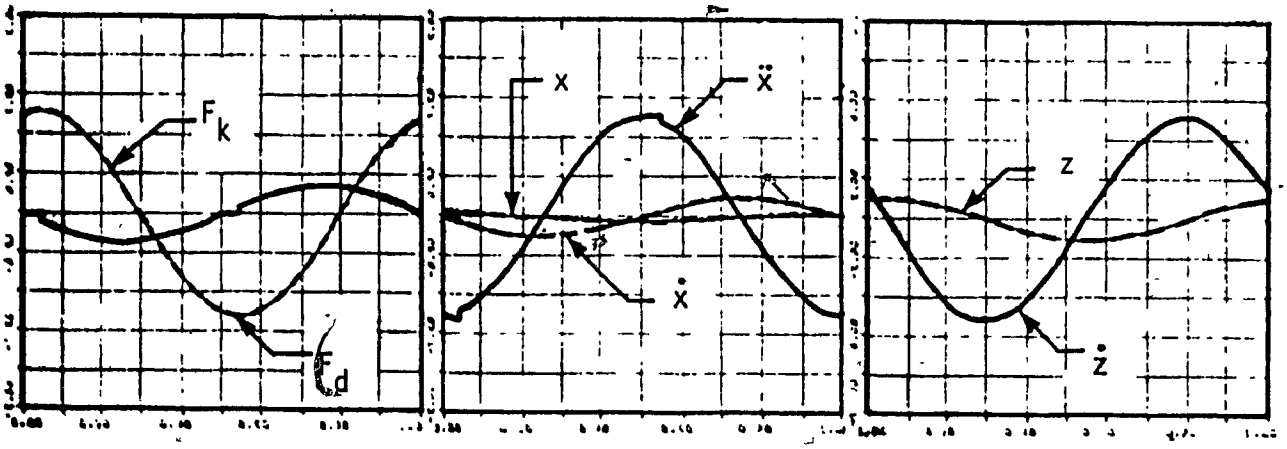

Fig. 4.3: Steady-State Response of Type 1 System at $\frac{\omega}{\omega_n}$ =5.0

The sudden changes in damper force gives rise to sharp acceleration peaks. Although the displacement response is close to being sinusoidal, the acceleration and velocity are not. Figure 4.4 shows the peak amplitude transmissibility of acceleration, velocity and displacement. One is higher than the other in the same order. Especially at lower frequencies, the acceleration isolation is not as good as displacement isolation. However, as described in section 3.3, transmissibilities based on RMS values rather than on peak vlues are used to characterize the system performance. The RMS transmissbility plot is shown in Figure 4.5. It is apparent by comparing this with Figure 4.4 that RMS acceleration transmissbility is lower than the peak-acceleration transmissiblity. However it is still higher than displacement or velocity transmissibility.

Figure 4.6 shows the transmissibility of Type 1 system superposed on that of active and passive systems. The semi-active system has a performance close to that of a fully active system. Although the active system does not amplify the input at any frequency, Type 1 system does so upto a frequency ratio of 0.8. However, the amplification is not large. Above a frequency ratio of 2, the semi-active and active systems have almost identical performance.

In comparison with passive isolators, the semi-active system is clearly superior. Its high frequency performance is better than that of an undamped passive isolator. However, its low frequency performance is slightly worse than that of any passive system below a

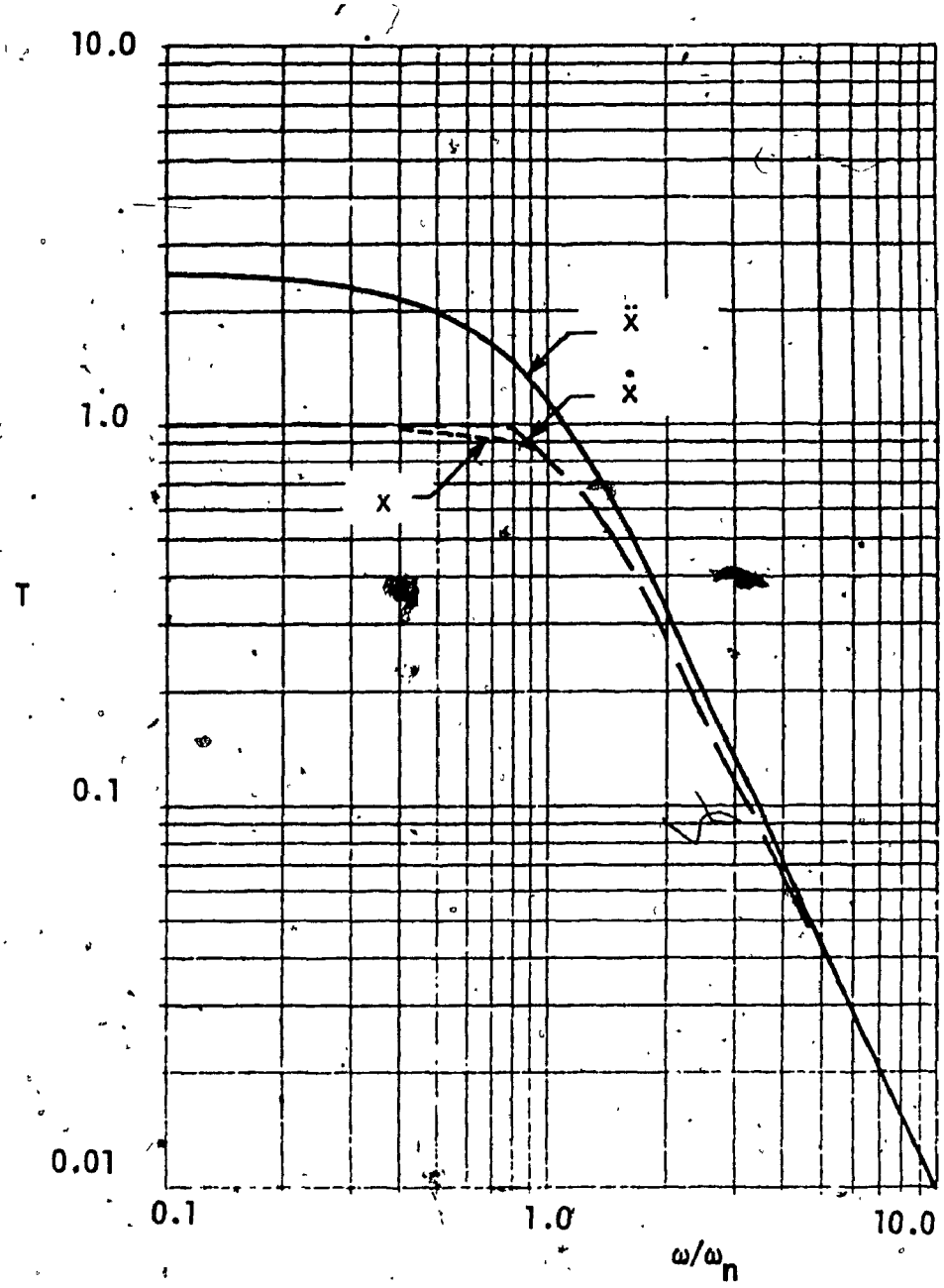

Fig. 4.4: Peak Transmissibility of Type 1 System

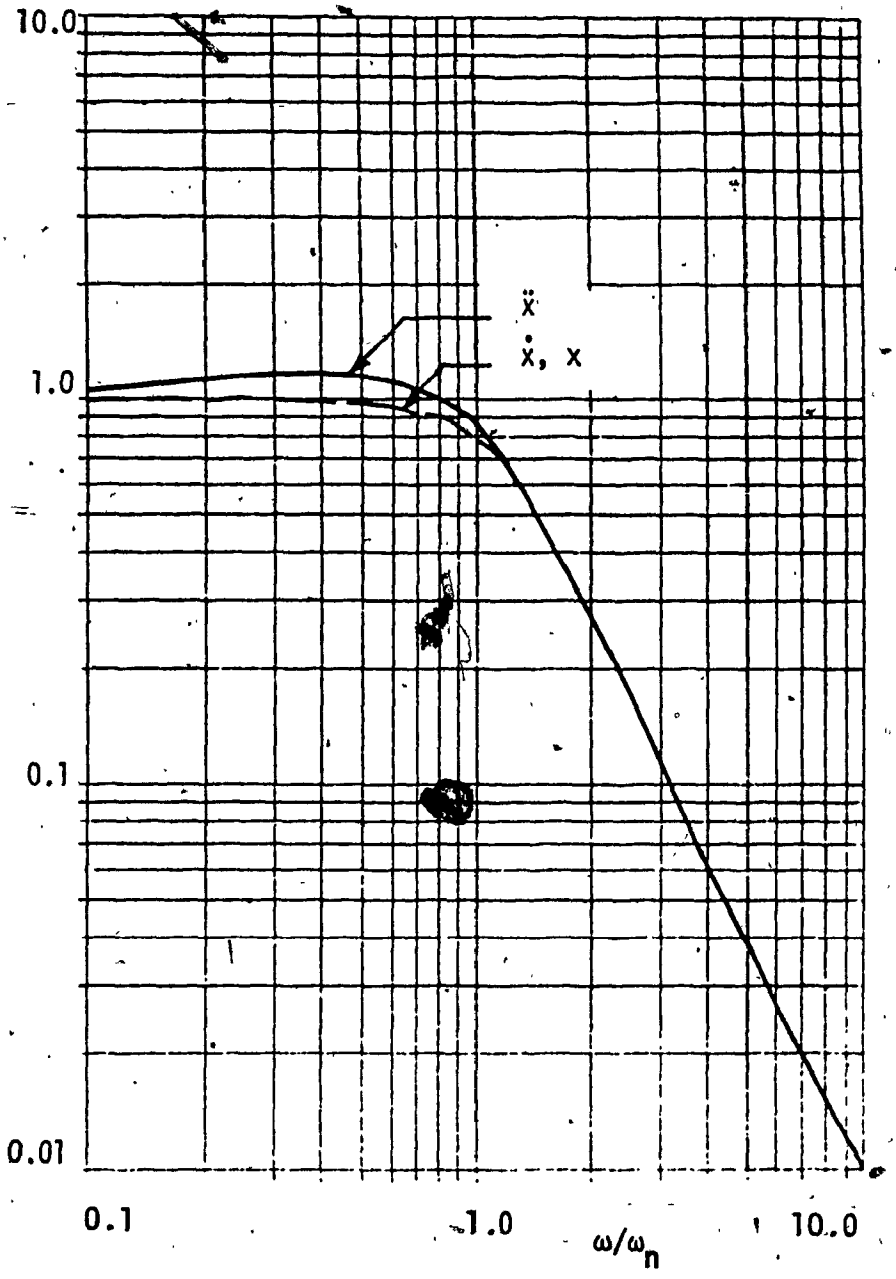

Fig. 4.5: RMS Transmissibility of Type 1 System

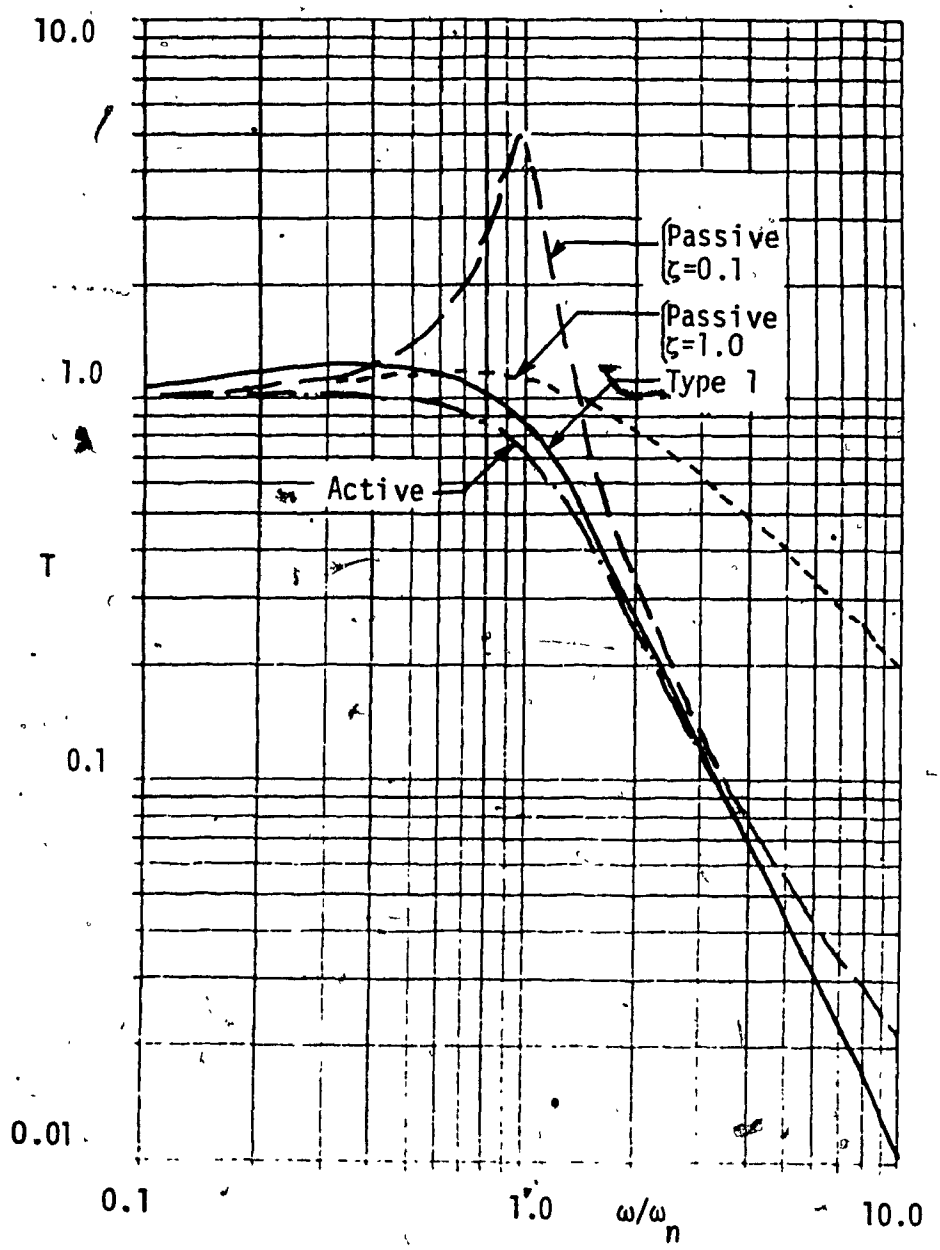

Fig. 4.6: Comaparison of RMS Acceleration Transmissibilities of Type 1 Semi-Active System with Active and Passive Systems

frequency ratio of 0.4 by a relatively insignificant amount.

The reason why the Type 1 semi-active system has poor performance at the very low frequency end is as follows. The control scheme forces the isolator to lock-up for parts of the cycle. The switching between various force levels causes acceleration peaks. Thus the performance is degraded. This fact is made clearer if one looks at the peak acceleration transmissibility in Figure 4.4.

The performance is not influenced by changes in the natural frequency or excitation amplitude. The only parameter of importance is the damping ratio, ζ. Figure 4.7 shows the effect of ζ on the RMS acceleration transmissibility. The trend is similar to the active isolator case. Lower damping gives worse performance. However it should be noted that the performance degradation due to switching phenomenon at very low frequencies worsens with higher damping. This is to be expected since the damper force will be relatively more significant than the spring force and any irregularities in it will have a greater effect on the mass acceleration.

In conclusion, the Type 1 semi-active scheme is capable of achieving a performance comparable to that of an active system. The semi-active isolator with a damping ratio of 0.707 comes very close to reproducing the performance of an optimum active damper except at low frequencies. The acceleration isolation at the lower frequency end is somewhat degraded due to the damper force discontinuities.

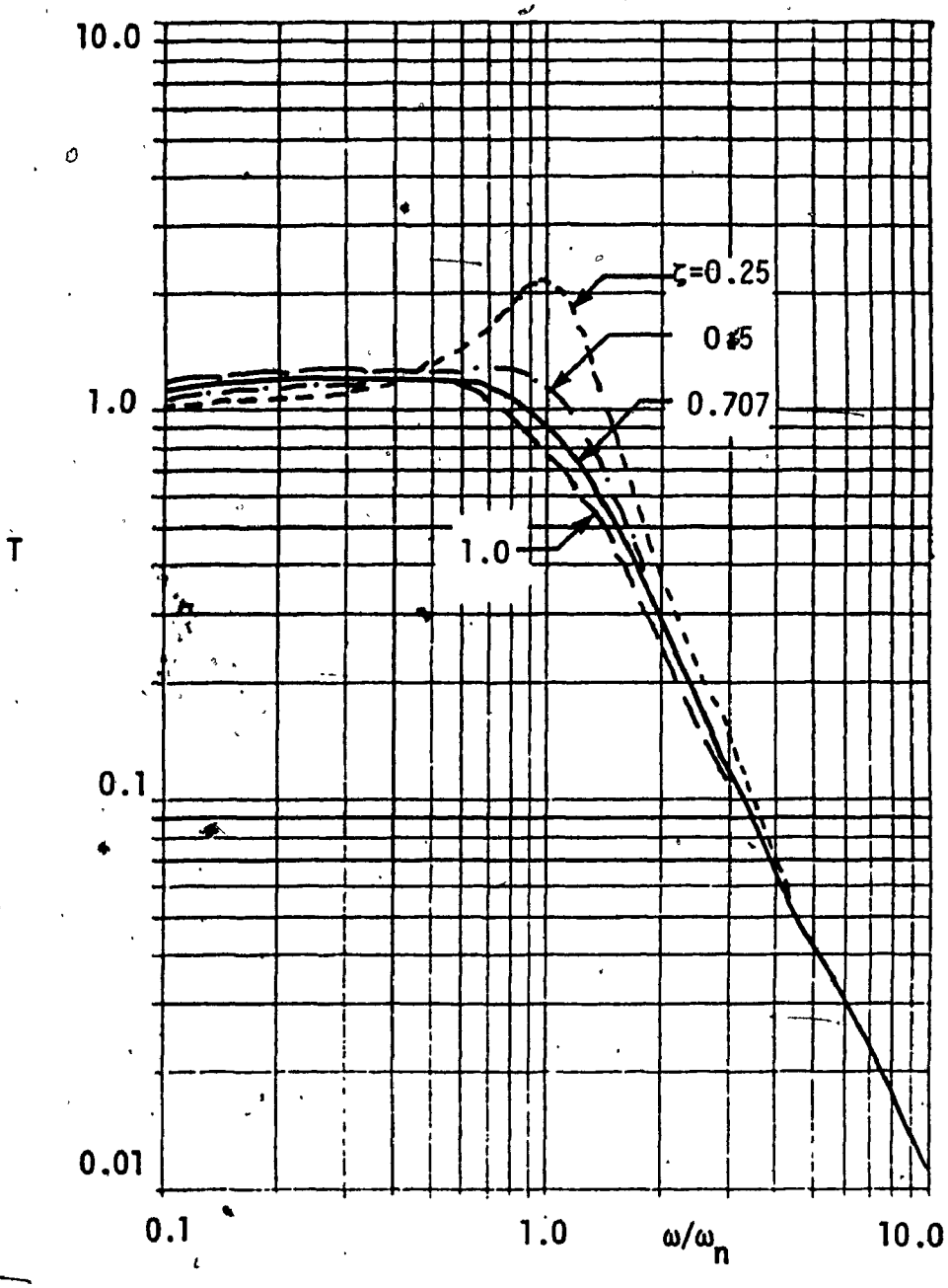

Fig. 4.7: Type 1 System RMS Acceleration Transmissibility for Variation in ζ

This performance drawback was not apparent from the previously reported work [20-25]. Displacement transmissibility, which was used to characterize the isolator performance by these researchers, does not show this phenomenon.

4.3 TYPE 2 SEMI-ACTIVE SYSTEM

This is an on-off version of Type 1 system. The basic set of parameters are the same as before ($\omega_n = 1.0$; $\zeta = 0.707$, and $a = 1.0$). When simulation is carried out under the same initial conditions as before, it was found that the system did not have a solution at the starting frequency $\frac{\omega}{\omega_n} = 0.1$; the initial value problem is stuck at the point where the condition function reaches zero. The reason for this situation was discussed in detail in chapter 2. It is entirely possible that solution might exist for the same frequency for a different set of initial conditions. Another trial run indicated that this was indeed true. In this case, solutions were obtained for discrete frquencies only upto $\omega/\omega_n = 1.0$. However, spot checks revealed that solution did exist for certain higher frequencies.

Thus it is evident that the Type 2 system described by the set of differential equations set out earlier leads to physically infeasible situations. A physical system must of course exhibit finite response quantities for all time. When one says that a set of differential equations do not have a solution, it only means that the mathematical system does not have a physical counterpart. Or, in other words, it will be impossible to construct a physical system

which will be exactly described by this kind of differential equations.

The differential equations describing Type 2 system (and all others as well) require instantaneous changes in damper force. This, in turn, requires a controller with zero response time, which is physically impossible. The actual delays involved in the 'on-off' semi-active controller and the dynamics of the valves will determine the exact nature of the system behaviour. In reality, the on-off valve will 'chatter' when the switching is 'unstable'. This behaviour is complex and requires a detailed understanding of all the physical components involved. Since the purpose of this study is to examine semi-active suspensions in a general way, control circuit delays, valve dynamics etc. were not taken into account. However, in the semi-active control schemes which have stable switching characteristics this idealization is quite realistic.

For reasons outlined above, the Type 2 semi-active scheme as described by equations is deemed to be infeasible. Therefore no further analysis was carried out.

4.4 TYPE 3 SEMI-ACTIVE SYSTEM

This innovative control scheme is based on relative velocity and relative displacement measurements. When these quantities have the opposite signs, the damper force opposes the spring force with an equal magnitude. Otherwise the damper force is zero.

The basic set of parameters are: ω_n = 1, the gain α = 1 and a = 1. Figure 4.8 through 4.10 show the steady-state response at 3 frequencies. At $\frac{\omega}{\omega_n}$ = 0.5 (Figure 4.8) the damper operates in three phases: (a) exactly opposing the spring force, (b) zero force and (c) lock-up force. The lock-condition occurs only at low frequencies. This type of system has a unique behaviour in that for nearly half of the time the mass acceleration is zero. This in turn leads to good isolation characteristics.

Figure 4.11 and 4.12 show the peak and RMS transmissibilities repectively of Type 3 system. The peak acceleration transmissibility is higher than the displacement and velocity transmissibilities. This will in fact be the case for most semi-active systems because of the discontinuities in the damper force. The RMS transmissibility shows the excellent isolation characteristics of this system. The RMS transmissibility has a peak value of 1.84 at $\frac{\omega}{\omega_n}$ = 0.5 and reduces to 0.007 at $\frac{\omega}{\omega_n}$ = 10.

Comparison of this system to active and passive isolators is shown in Figure 4.13. Compared to the passive isolator, Type 3 system has a far superior performance for $\frac{\omega}{\omega_n}$ greater than 0.95. At $\frac{\omega}{\omega_n}$ = 10, the isolation is almost 1.5 times better than that of an undamped passive isolator. However, there is a price to be paid in terms of inferior low frequency performance. But there is a

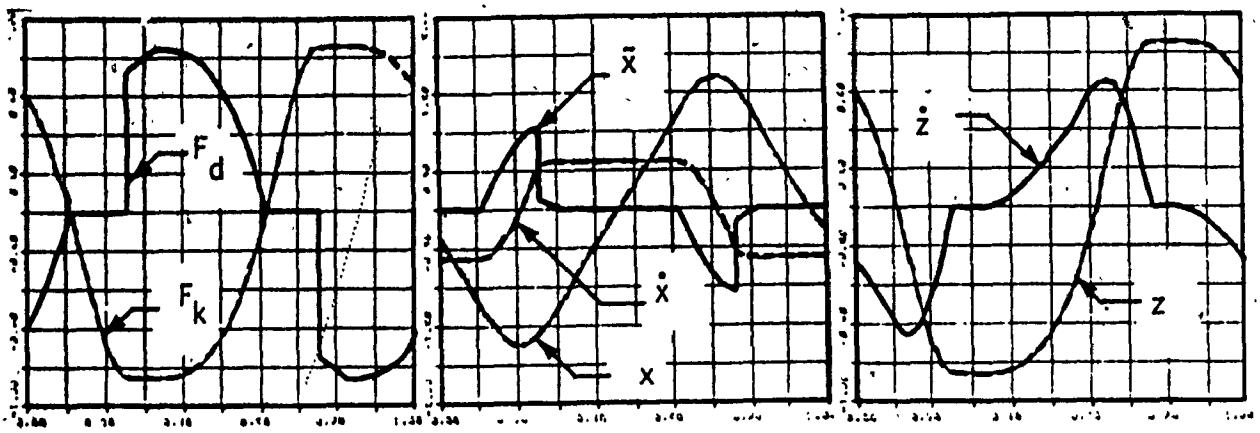

Fig. 4.8: Steady-State Response of Type 3 System at $\frac{\omega}{\omega_n}$=0.5

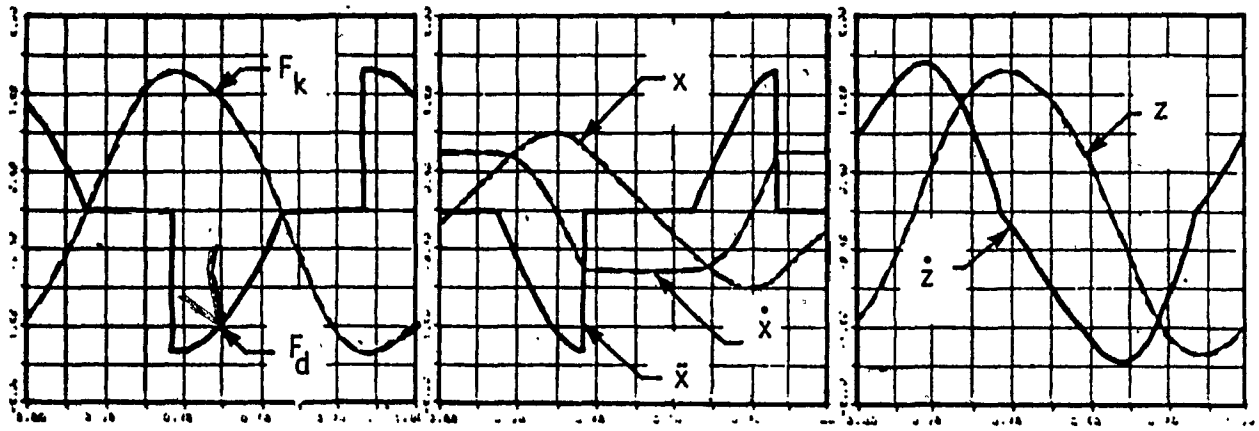

Fig. 4.9: Steady-State Response of Type 3 System at $\frac{\omega}{\omega_n}$=1.0

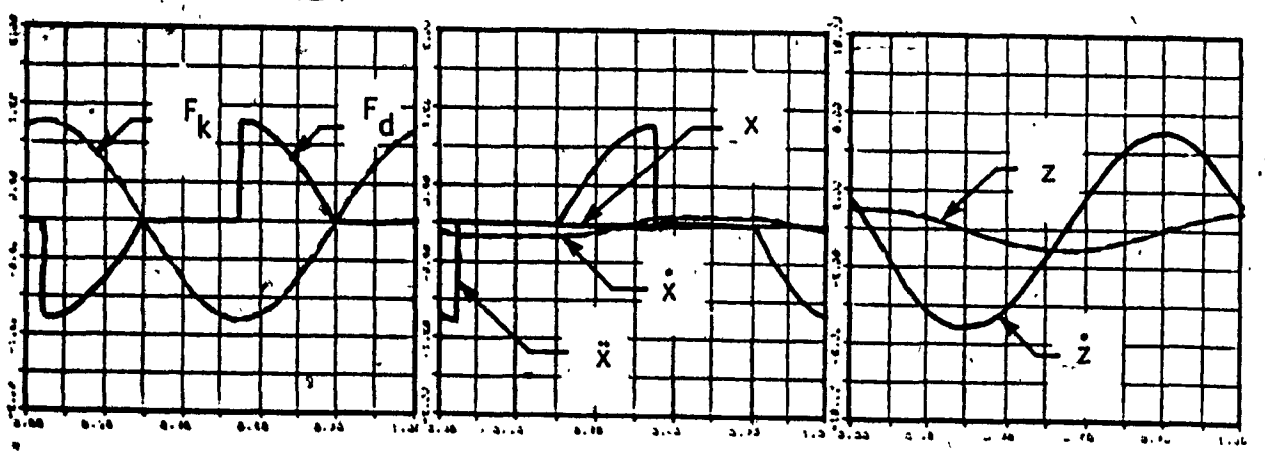

Fig. 4.10: Steady-State Response of Type 3 System at $\frac{\omega}{\omega_n}$=5.0

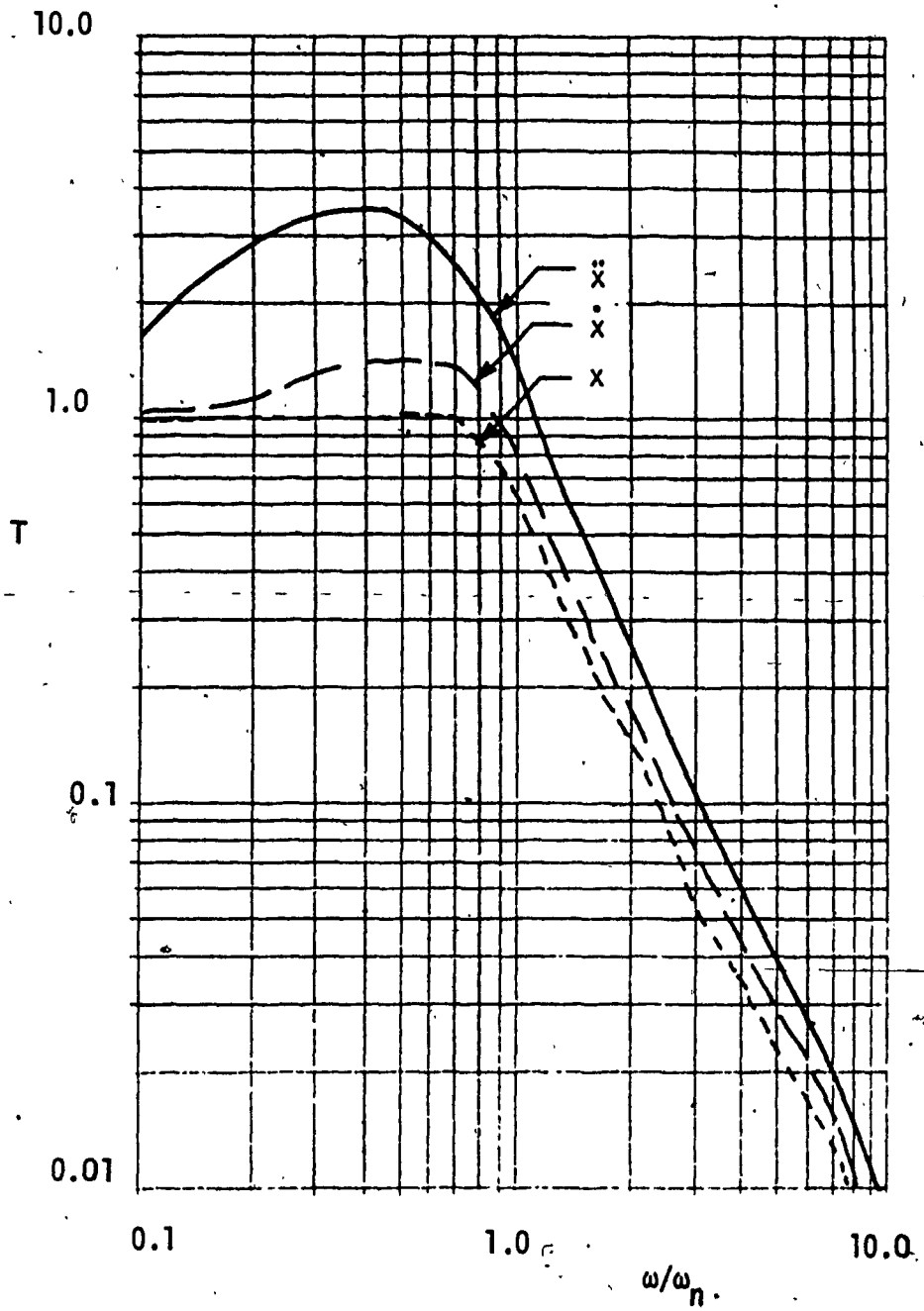

Fig. 4.11: Peak Transmissibility of Type 3 System

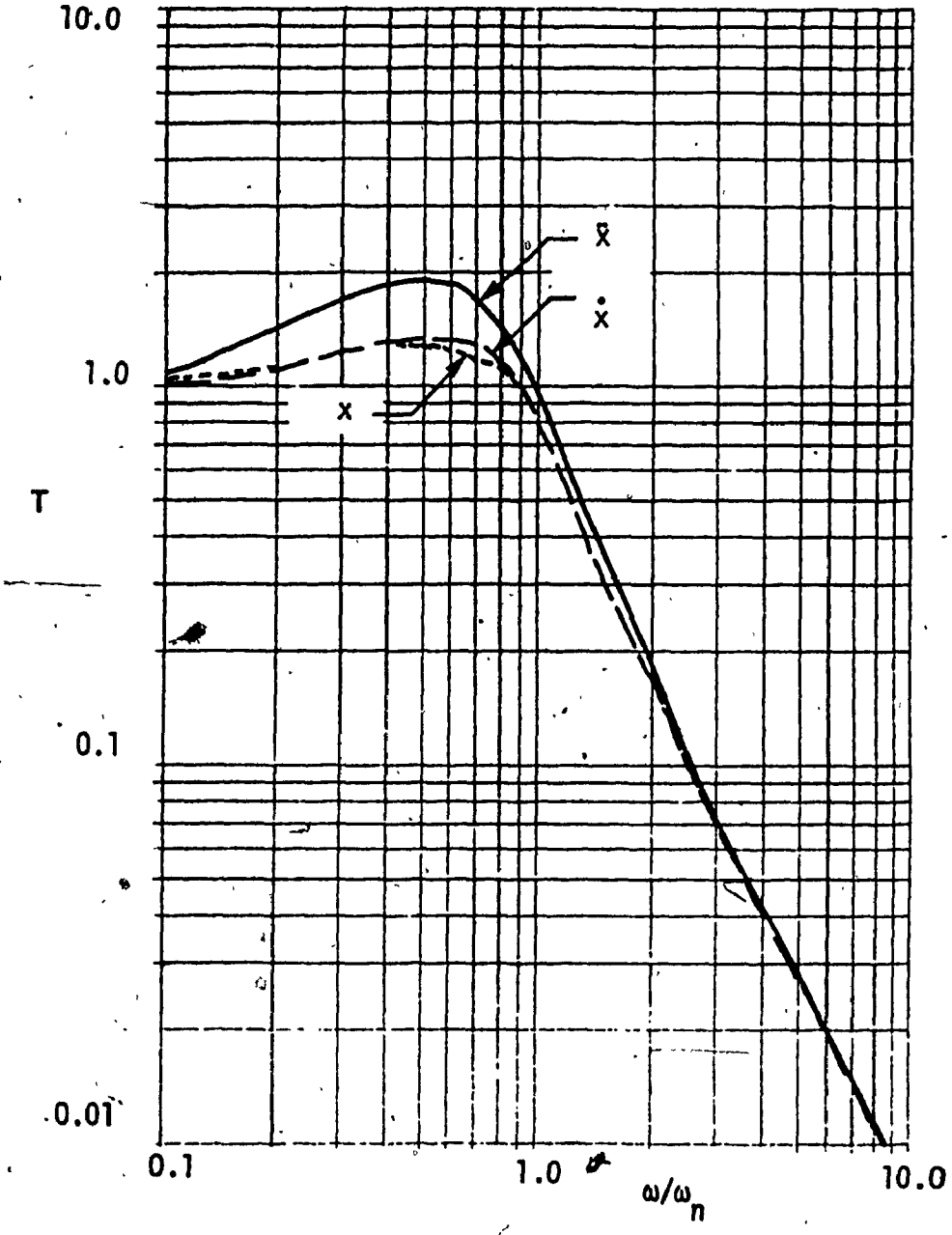

Fig. 4.12: RMS Transmissibility of Type 3 System

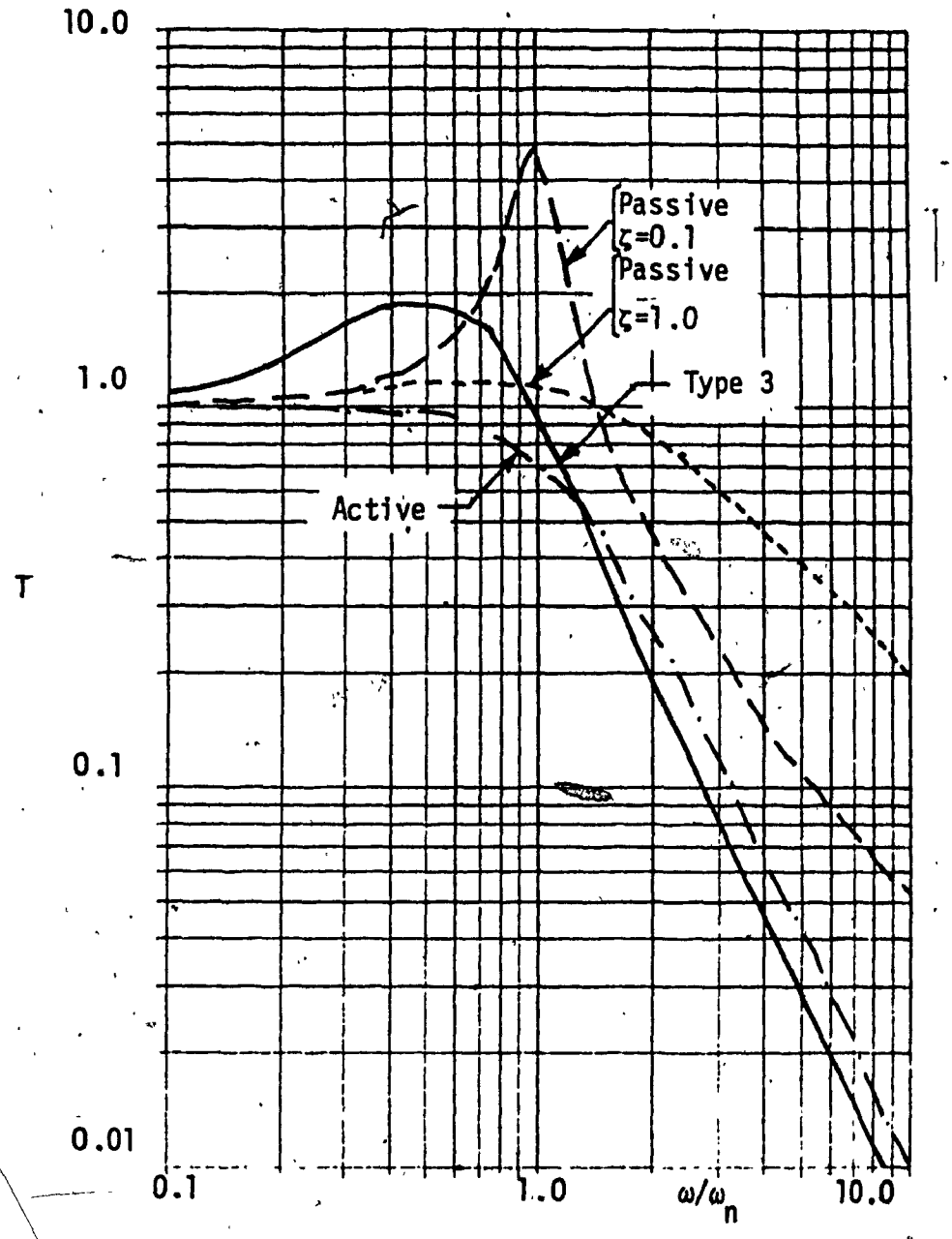

Fig. 4.13: Comparison of RMS Acceleration Transmissibilities of Type 3 Semi-Active System with Active and Passive Systems

consolation that there is an effective lowering of the system natural frequency. Figure 4.13 also shows that Type 3 system is also superior to be the optimum active isolator for $\frac{\omega}{\omega_n} > 1.24$. This result is extremeley encouraging because it is achieved through semi-active control.

Variations in excitation amplitude, a, or the system undamped natural frequency, ω_n do not affect the performance. But the damper force gain, α is an important parameter. When looking at the steady-state time plots of the system, it is felt that a larger than unity value of α will give better isolation. To test this, α was set to 2.0 and simulation was carried out. But the computer run indicated that the system failed to achieve periodic oscillations.

It was recongnized that the periodic solutions may be unstable at certain values of gain. To study this in more detail, the software package AUTO [47] was used. As described in chapter 3, AUTO solves the system equations as a boundary value problem. The pertinent details of this analysis were given in chapter 3. One approximation involved in the system equations is that the discontinuous damper force function was replaced by a continuous one using the inverse tangent function (see chapter 3). It was seen that with the 'homotopy' parameter equal to 100, the solution from AUTO is almost indentical to that from simulation. Figure 4.14 shows the solution form AUTO for ω = 0.5 and a = 1.1902. Comparing this with the simulation results, it was seen that the approximation is acceptable. Even the lock-up condition is closely followed.

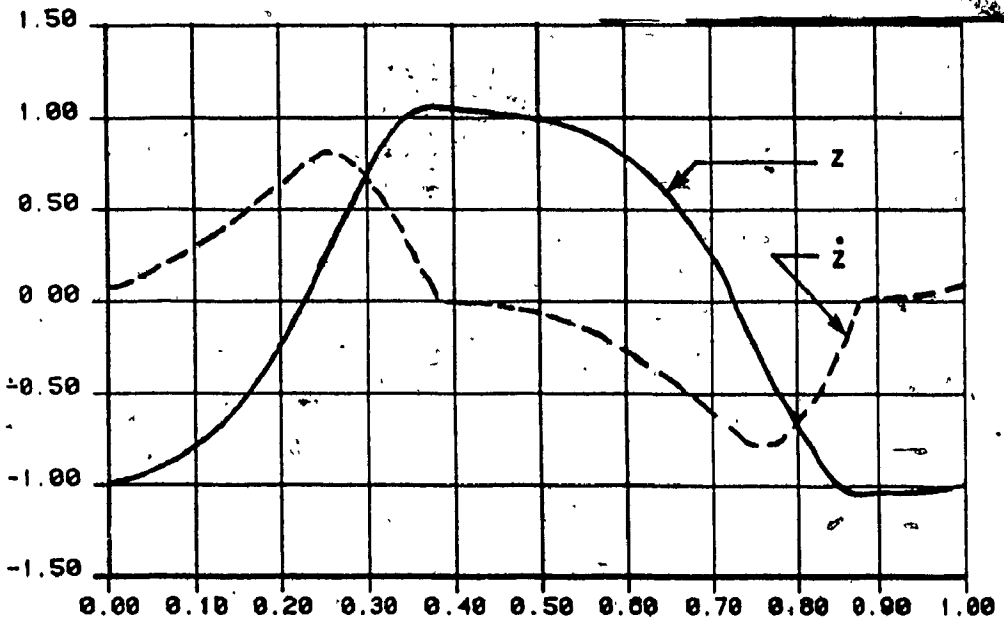

Fig. 4.14 (a): z and ż Response Using AUTO

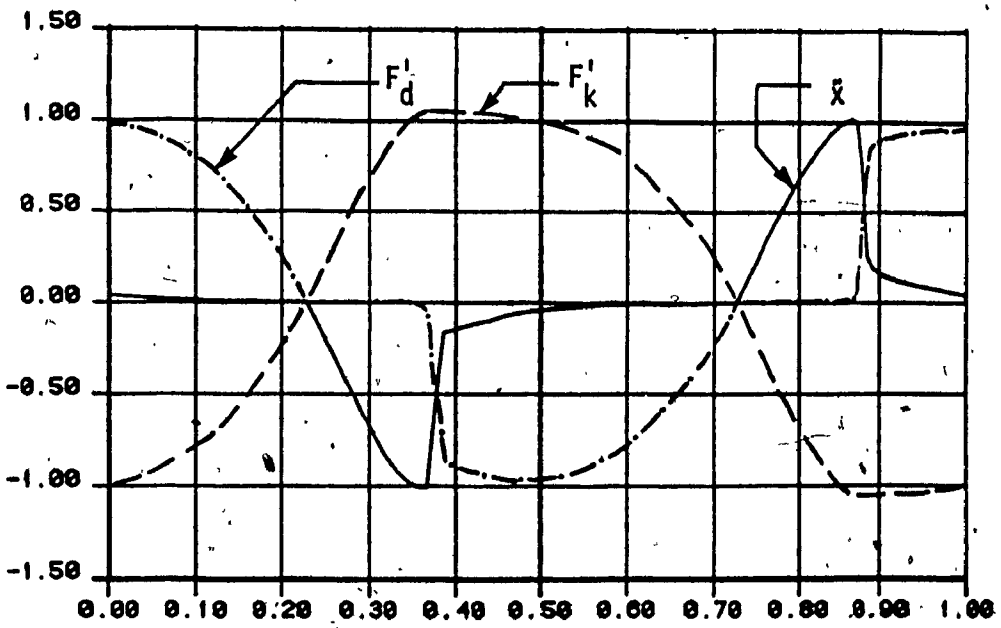

Fig. 4.14 (b): F'_d, F'_k, and $\ddot{x}$ Response Using AUTO

Figure 4.15 shows the peak value of displacement response at $\omega = 0.5$ when α is varied form 1.00 to 2.00. It should be noted that for the value of gain upto 1.5, the response peak decreases. However, the solutions lose stability for $\alpha > 1.4$. This means that they will not persist under perturbations. Numerical integration in simulation techniques inherenly involves perturbations due to round-off errors. Therefore the unstable solutions are never obtained in simulation.

Using AUTO it is normally possible to accurately determine the point where stability changes (bifurcation point). It is also possible to trace out this bifurcation point as a function of two system parameters. However, in this case, because of the high degree of nonlinearity in our system the software package had convergence difficulties in trying to trace out the bifurcation point as a function of α and ω. Therefore, 'slices' of this trace was obtained at different frequencies. This shows that the upper bound on α for stable solutions to exist increases as the frequency in increased. Table 4.1 shows these results.

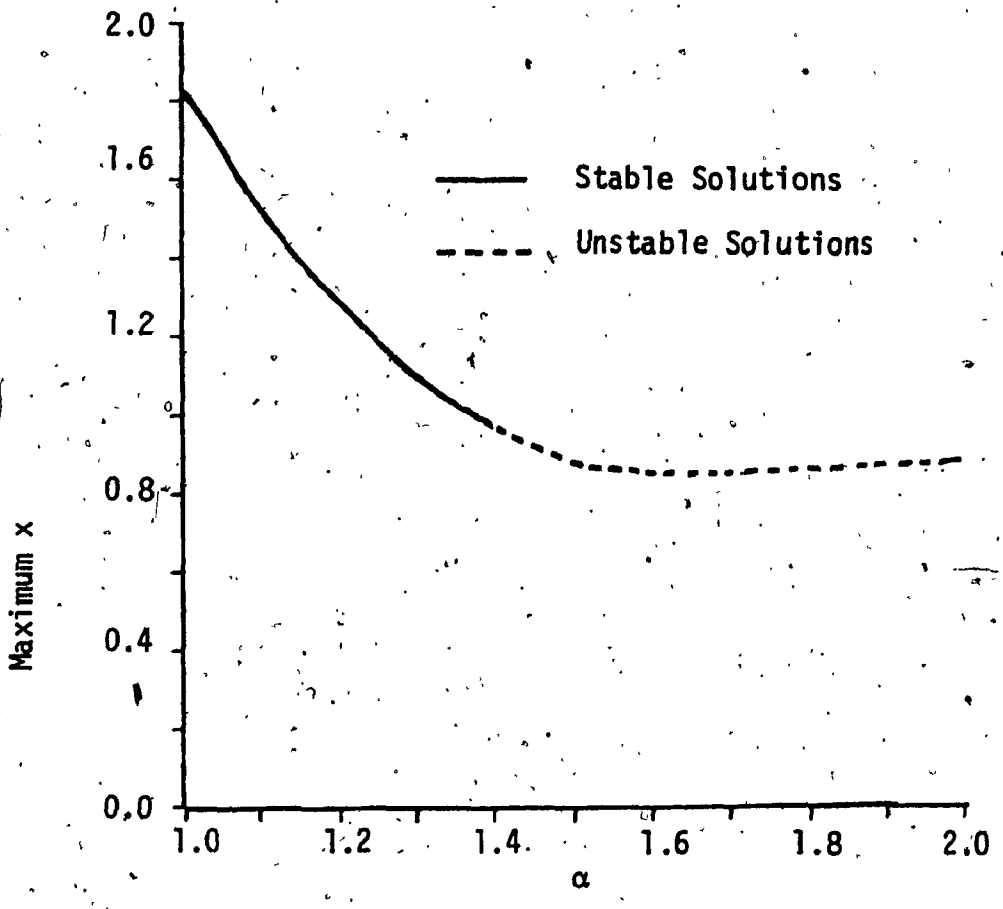

Fig. 4.15: Variation of Peak Displacement Response with α at $\frac{\omega}{\omega_n} = 0.5$

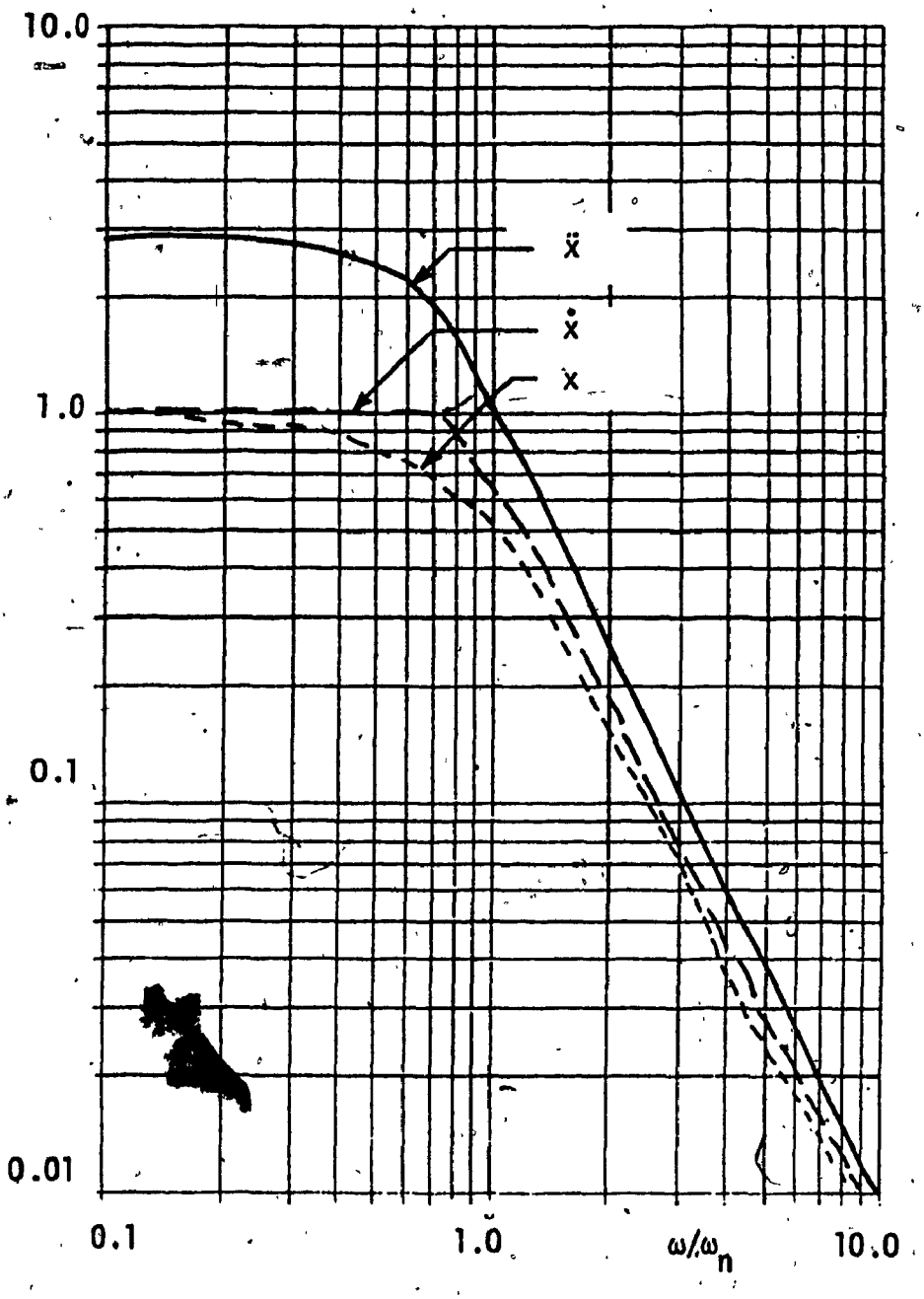

Fig. 4.16a: Peak Transmissibililty of Type 3 System for α=1.3

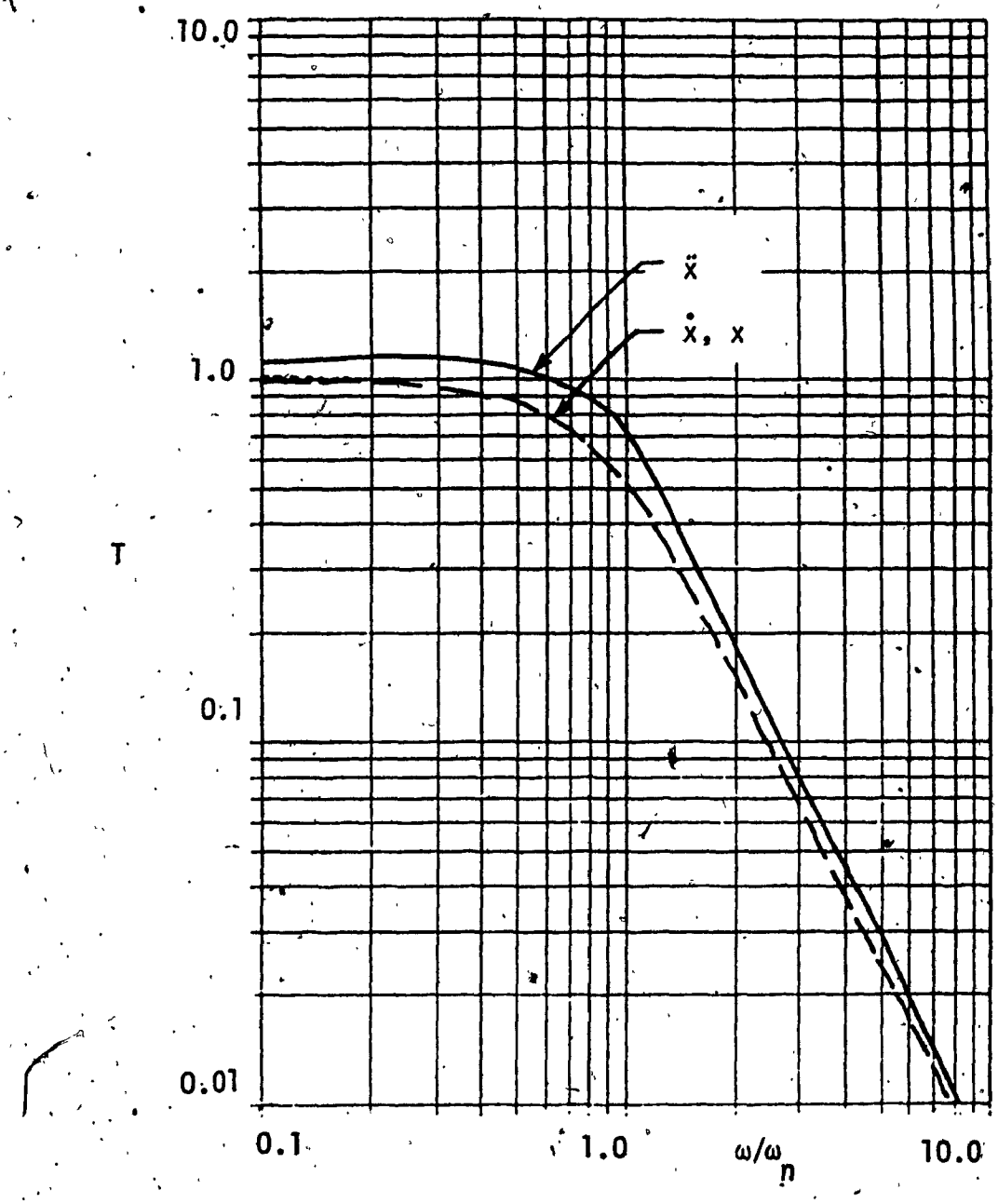

Fig. 4.16b: RMS Transmissibility of Type 3 System for α=1.3

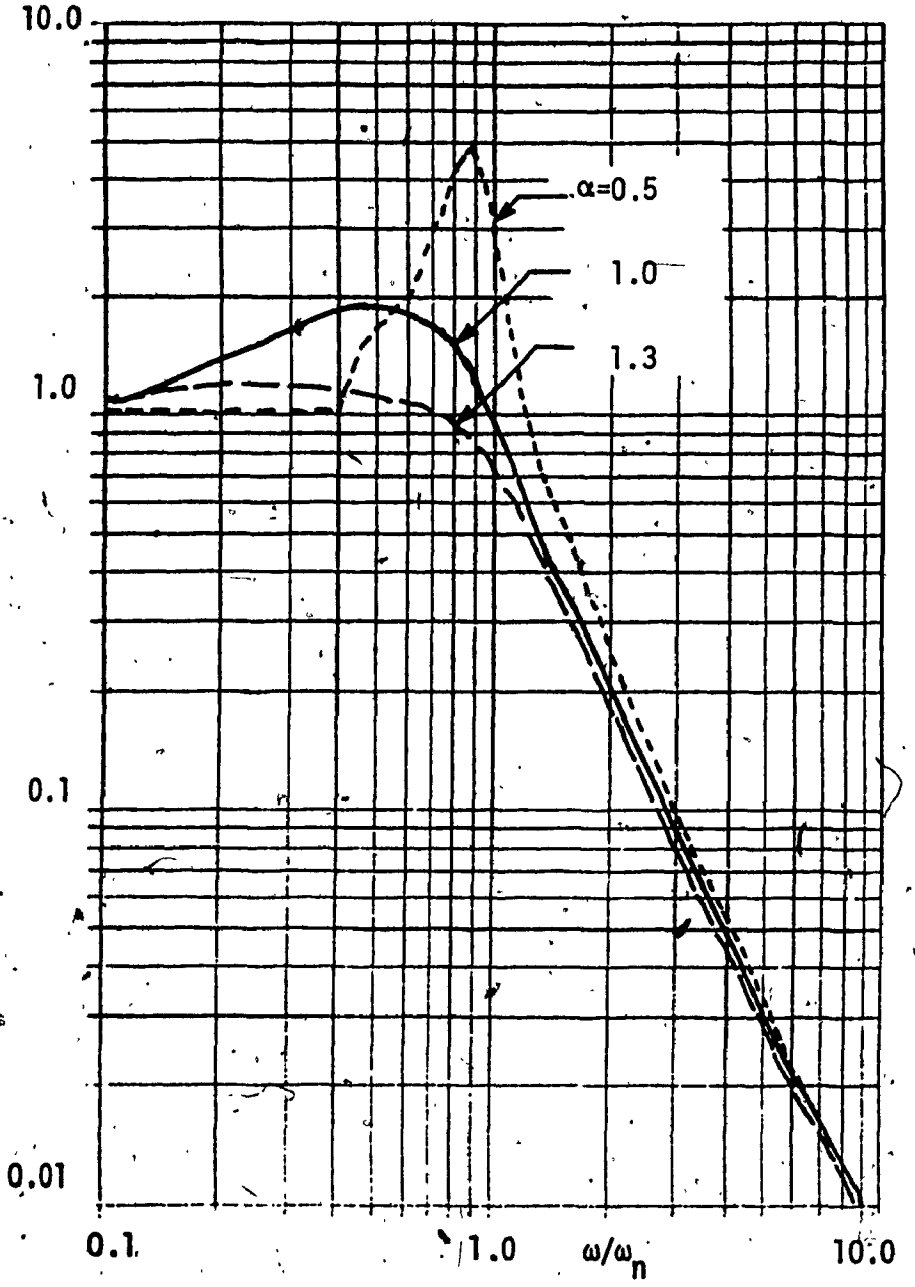

Fig. 4.17 Type 3 System RMS Acceleration Transmissbility for Variation in α

Table 4.1: Upper Bound on α for Stable Solutions

Frequency Ratio, ω/ω_n	α
0.5	1.366
1.02	1.474
2.55	1.857
3.96	1.86
6.384	1.88
10.0	2.00

Simulation was carried out with $\alpha = 1.3$. Figure 4.16 (a) and 4.16 (b) shows the transmissibility plots. It is obvious that this value of α gives a better performance than the unity gain system (Figures 4.11 and 4.12). The RMS acceleration transmissibility has a peak of 1.19, but outperforms even active suspensions at high frequencies. Figure 4.17 shows the transmissibility for various values of the gain α. As α is decreased, resonant peak increases. As α is increased, performance improves. However, there is a limit on α for stability as established earlier.

4.5 TYPE 4 SEMI-ACTIVE SYSTEM

Type 4 condition function is the same as in Type 3, with the damper force control based on on-off switching. The basic set of system parameters is the same as for Type 1 and 2, namely $a = 1.0$, $\omega_n = 1.0$ and $\zeta = 0.707$. Figure 4.18 through 4.20 show the

steady-state response of the system. The damper force is either zero or proportional to the relative velocity depending on whether the relative displacement and velocity have the same sign or not. The interesting thing to note is that Figure 4.20 shows that the steady-state displacement oscillates about a non-zero mean.

Figure 4.21 and 4.22 show the peak and RMS transmissibilities of this system. It is clear from the RMS displacement transmissibility curve that above $\omega/\omega_n = 2.5$, the steady-state solutions show a drift. This may not be tolerated in practical applications. Furthermore, as can be seen from Figure 4.22, when the drift occurs the relative displacement is always positive and the damper simply acts like a one-way valve dashpot. The acceleration transmissibility is very close to that of a passive system with $\zeta = 0.4$. Therefore, even if the drift is tolerated, there is little improvement in performance.

This system was also studied using the software AUTO. It was seen that the drift is indeed a bifurcation phenomenon. Figure 4.23 shows the bifurcation diagram which has the peak value of the displacement response plotted against the frequency ratio. The system parameters are $a = 1.146$, $\frac{\omega}{\omega_n} = 1.0$ and $\zeta = 0.5$. Solution branch 1 has a bifurcation point at label 5. Beyond this point the solutions on this branch are unstable. The two branches that lead from the pitch fork bifurcation at label 5 are stable. Figure 4.24 shows the orbits at the labels marked 9, 6 and 14 in Figure 4.23.

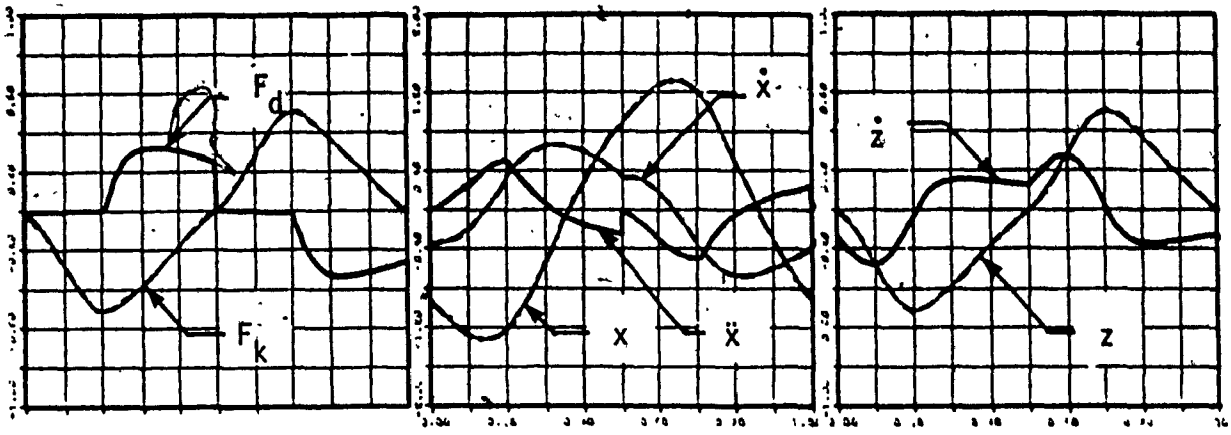

Fig. 4.18: Steady-State Response of Type 4 System at $\frac{\omega}{\omega_n}$=0.5

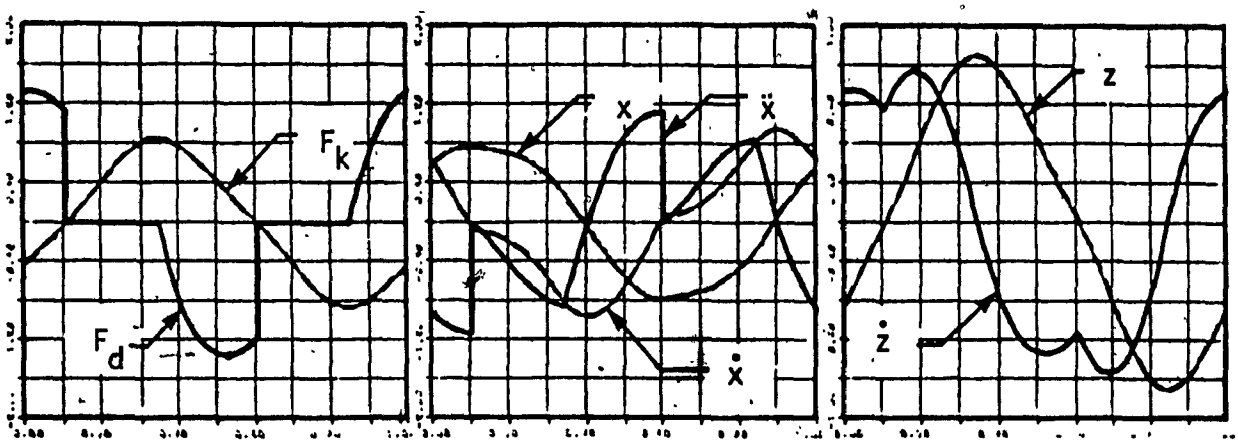

Fig. 4.19: Steady-State Response of Type 4 System at $\frac{\omega}{\omega_n}$=1.0

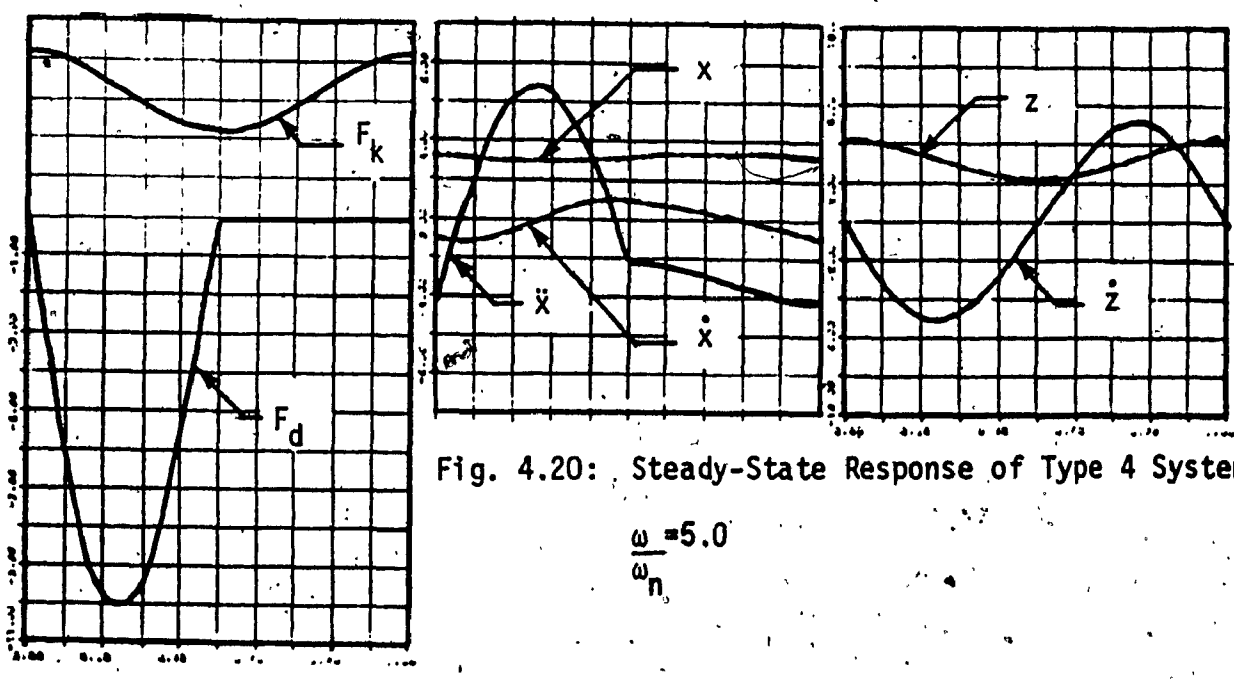

Fig. 4.20: Steady-State Response of Type 4 System at $\frac{\omega}{\omega_n}$=5.0

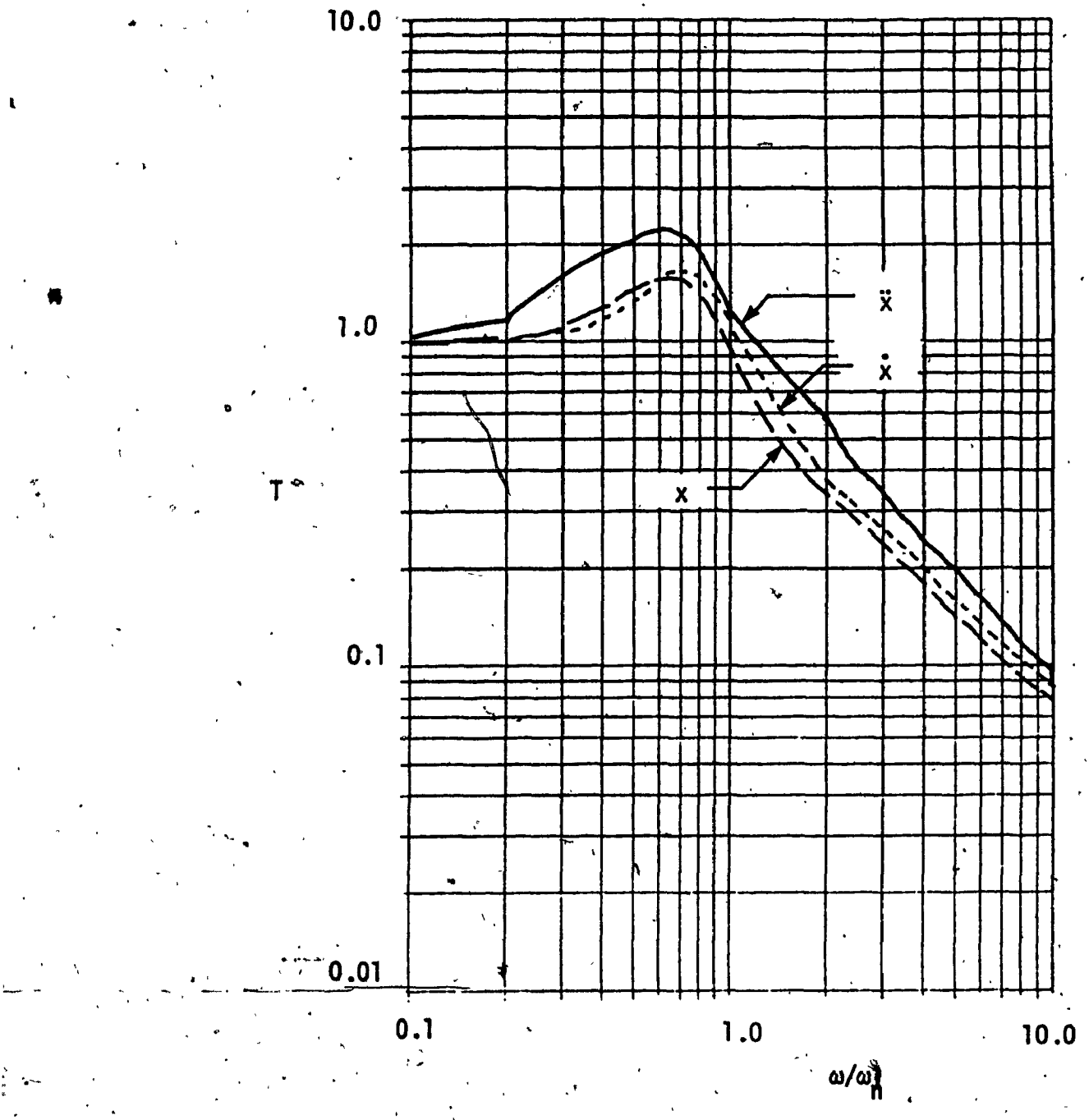

Fig. 4.21: Peak Transmissibility of Type 4 System

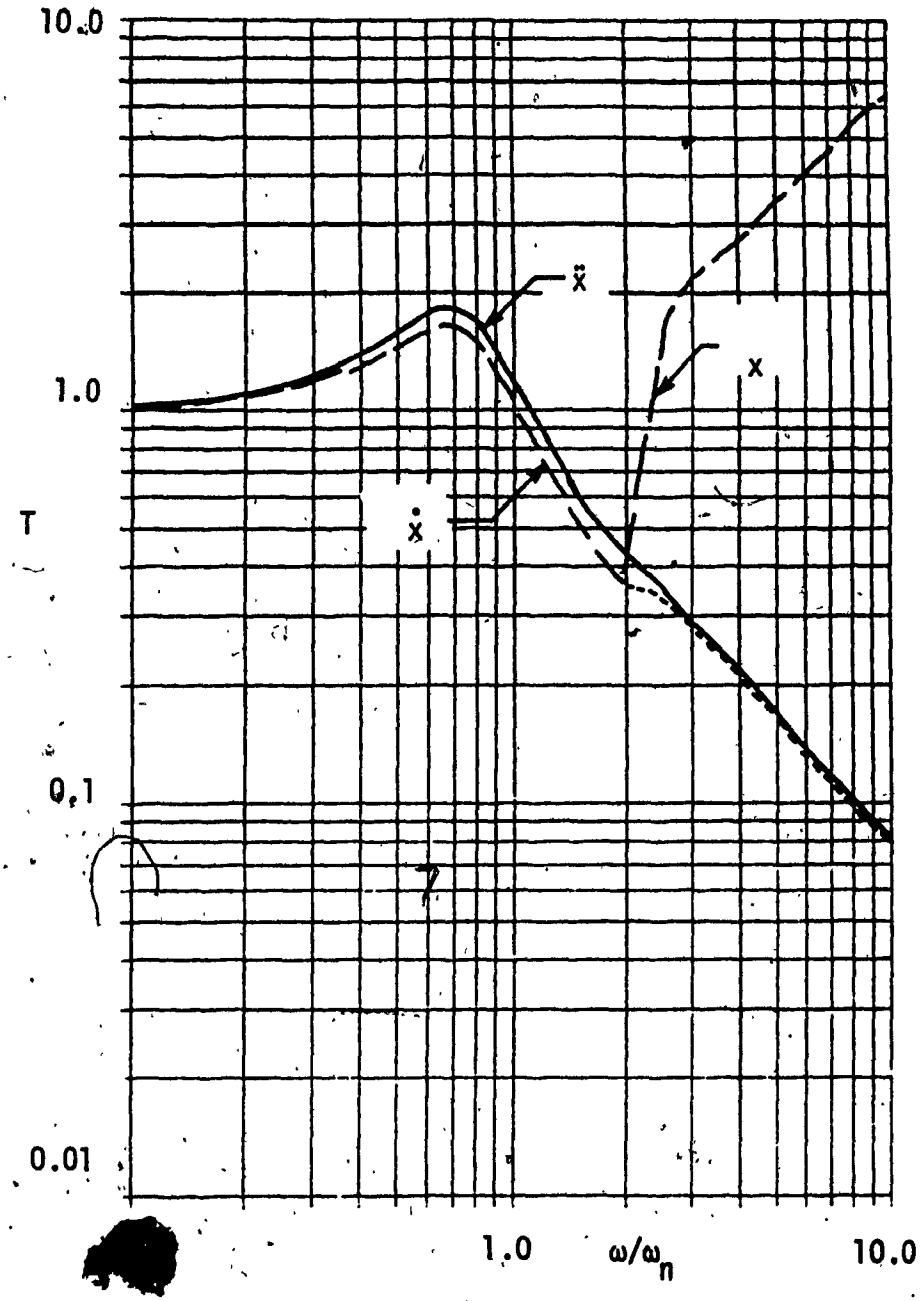

Fig. 4.22: RMS Transmissibility of Type 4 System

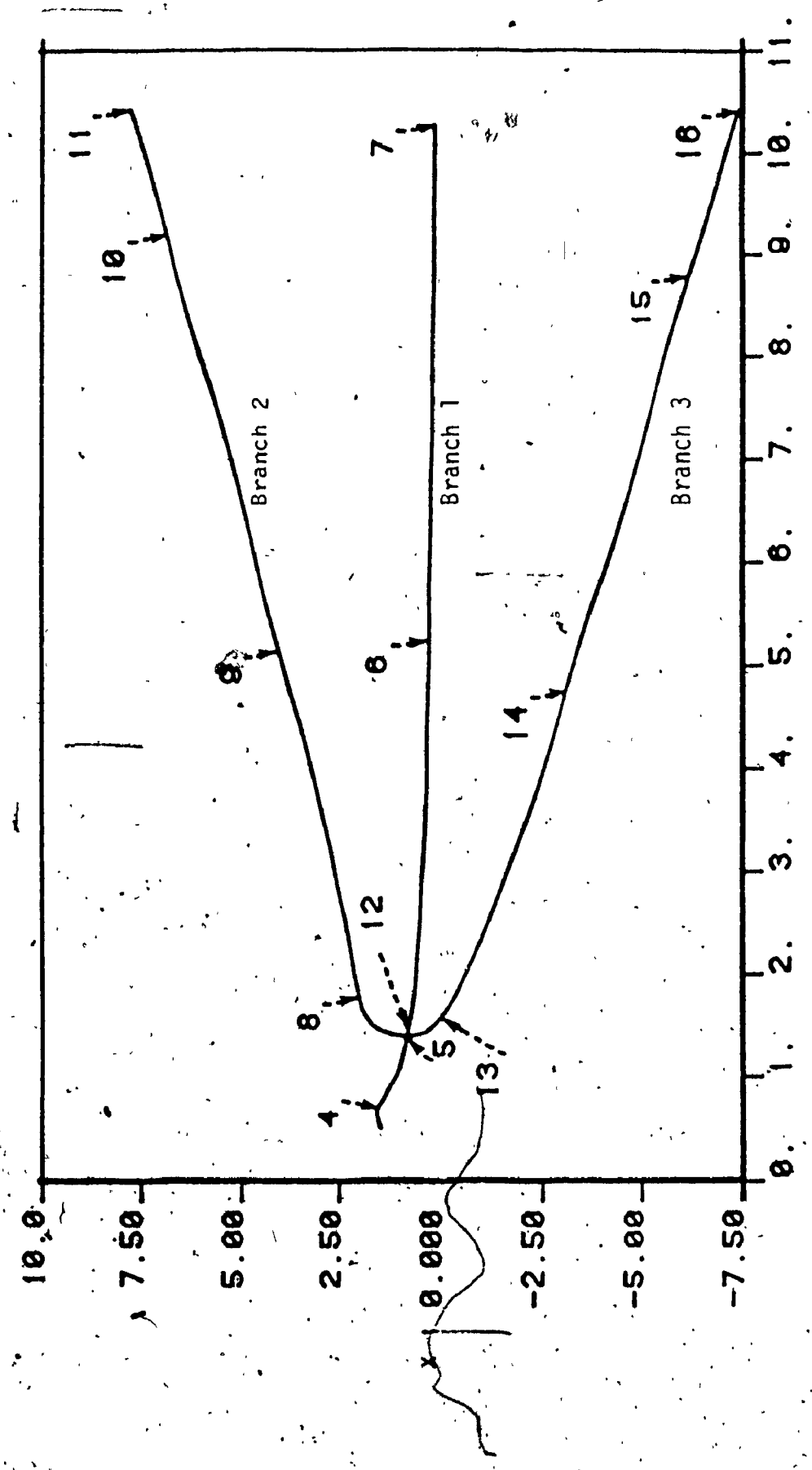

Fig. 4.23: Bifurcation Diagram of Type 4 System Response

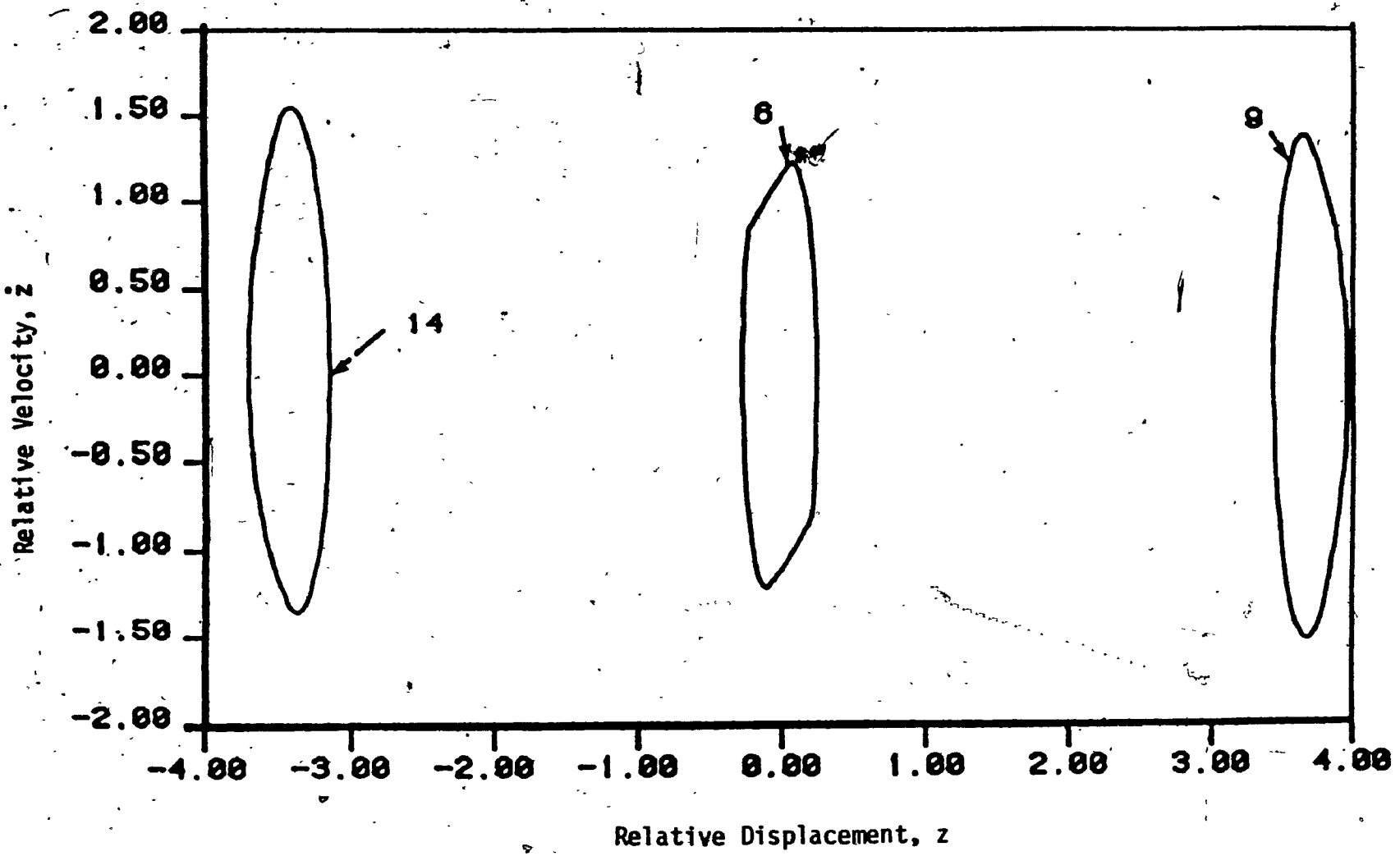

Fig. 4.24: Orbits of Solutions at Labels 6,9 and 14 of Fig. 4.23

This clearly shows the stable vibration occurring about a non-zero mean. The solution along branch 3 are mirror symmetry of solutions along branch 2. At a given frequency, there are two possible stable solutions. Which one of these is attained in practice or simulation depends on the initial conditions or the perturbations.

The frequency at which drift occurs as seen from simulation was higher than that determined by AUTO. This could be because near this frequency the drift occurs so slowly that the simulation does not detect it. The drift frequency ratio is not affected by variations in ω_n. It increases with decreasing values of ζ and decreasing values of a.

4.6 TYPE 5 SEMI-ACTIVE SYSTEM

This type of system employs a Coulomb friction damper. The idealization is made that the kinetic and static friction have the same value. The basic system parameters are chosen as a = 1.0, ω_n = 1.0 and F_o = 1.0.

Up until $\frac{\omega}{\omega_n} = 1$, system is locked up and no relative motion exists between the base and the mass. At $\frac{\omega}{\omega_n} = 1$ it exhibits "stick-slip" motion. At this stage damper causes lock-up for some time and motion occurs for some time as shown is Figure 4.25. At high frequencies lock-up does not occur (Figure 4.26). The solution obtained from simulation shown is Figure 4.26 has also been observed in laboratory.

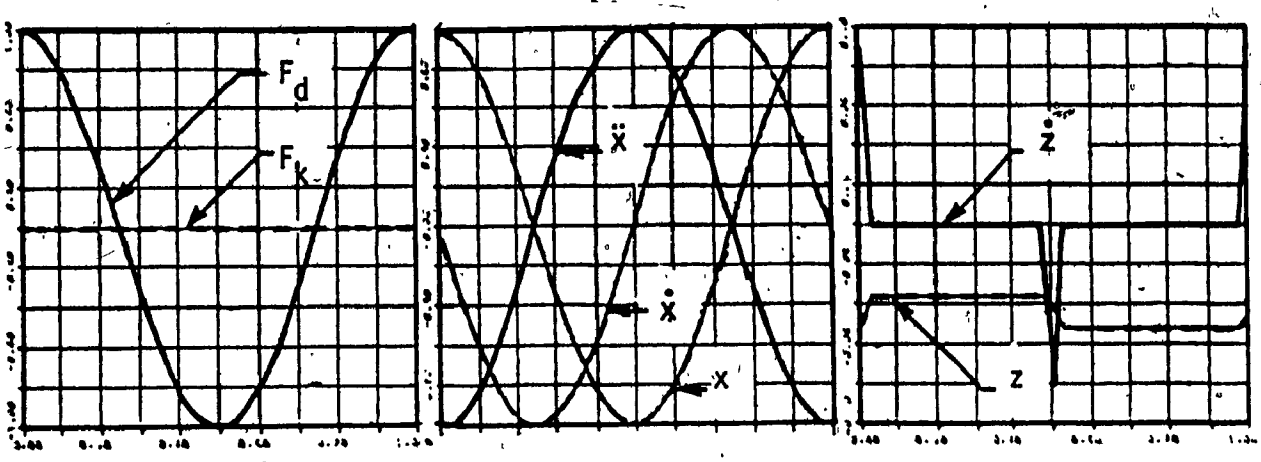

Fig. 4.25: Steady-State Response of Type 5 System at $\frac{\omega}{\omega_n}$=1.0

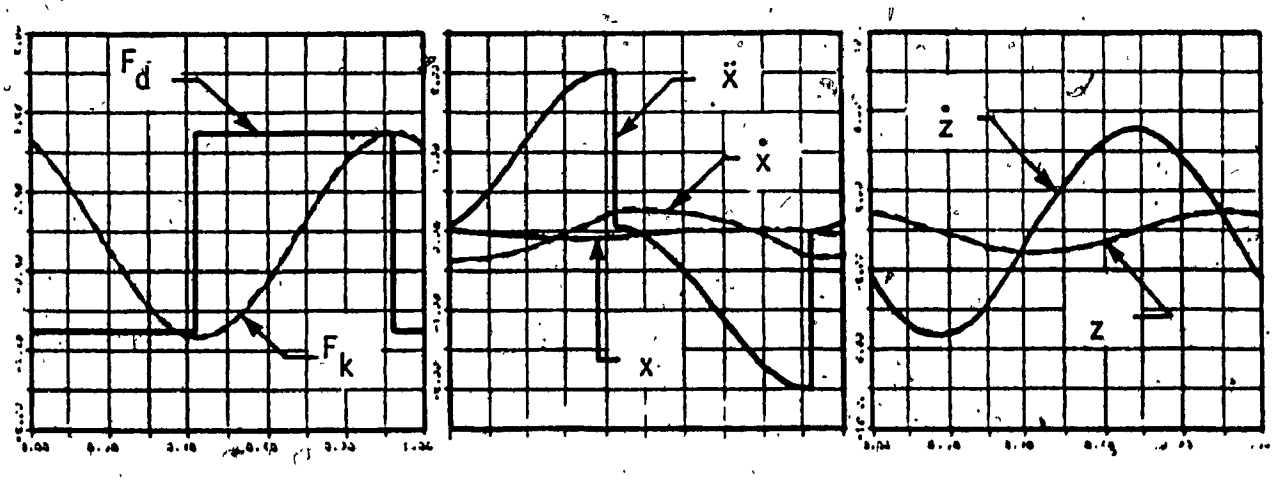

Fig. 4.26: Steady-State Response of Type 5 System at $\frac{\omega}{\omega_n}$=5.0

Figure 4.27 and 4.28 show the peak and RMS transmissibilities of this system. They show unity transmissiblity until $\frac{\omega}{\omega_n} = 1.0$ due to lock-up and then a small dip followed by a small peak. Thereafter the transmissibility drops by a steady rate of 40 db/decade. The peculiar dip that follows the lock-up stage has also been observed in laboratory experiments [43].

Comparing this with active and passive isolators as shown in Figure 4.29, it is easy to explain why the Coulomb friction damper is judged to be 'optimum'. It provides excellent isolation at high frequencies (very close to that of a passive system with $\zeta = 0.1$) and virtually eliminates resonance peak. However, this is true only for the combination of input amplitude, a, and friction force, F_0 considered.

The effect of varying the friction force, F_0 is shown in Figure 4.30. The break frequency decreases with decreasing F_0. This could lead to very undesirable resonant peaks. The effect of increasing a has the same effect as decreasing F_0 by the same factor. From the system equations it can be seen that the relative motion exists when

$$a\omega^2 > F_0$$

or

$$\omega > \sqrt{\frac{F_0}{a}}$$

Of all the systems considered so far this is the only one

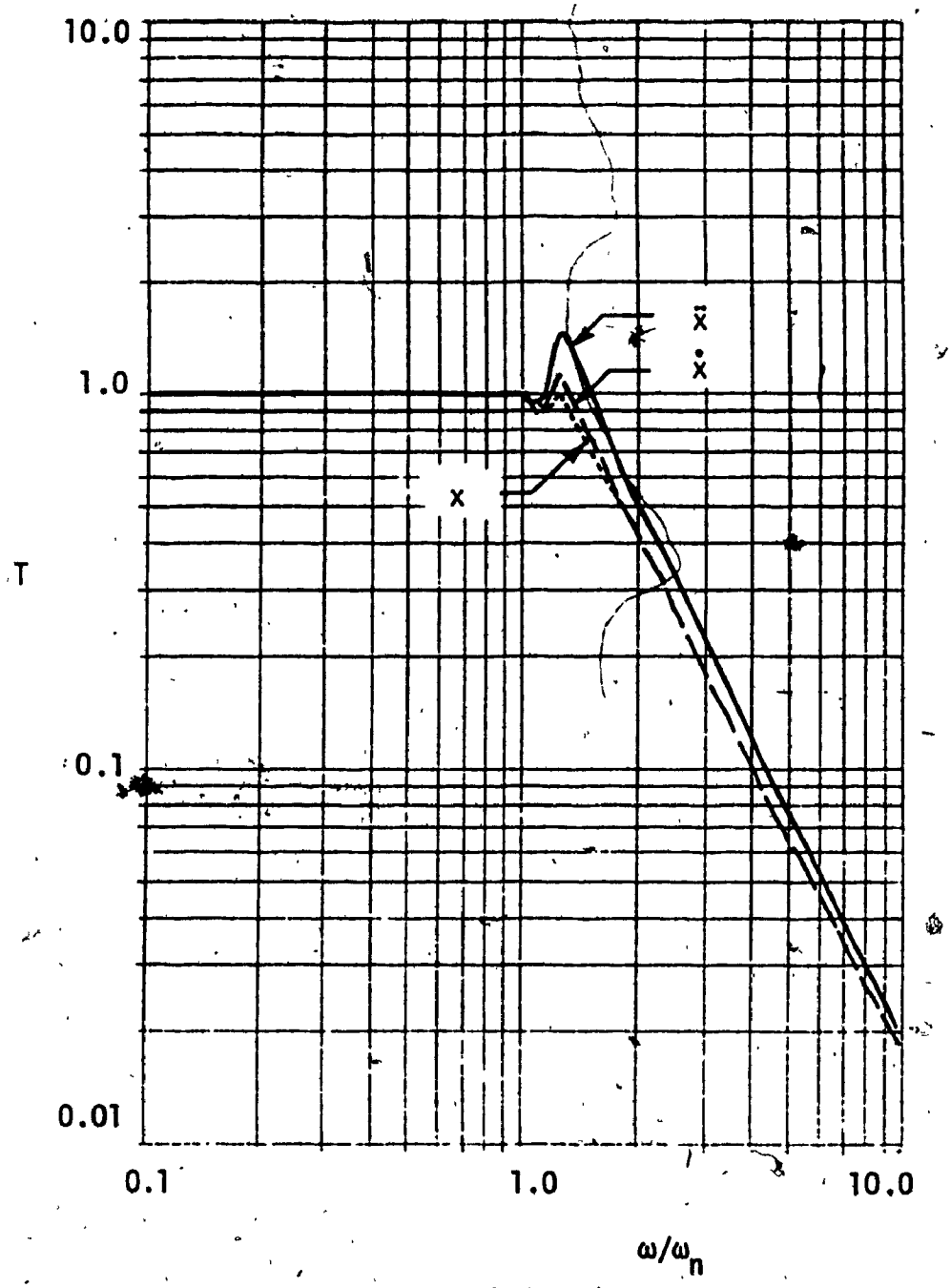

Fig. 4.27: Peak Transmissibility of Type 5 System

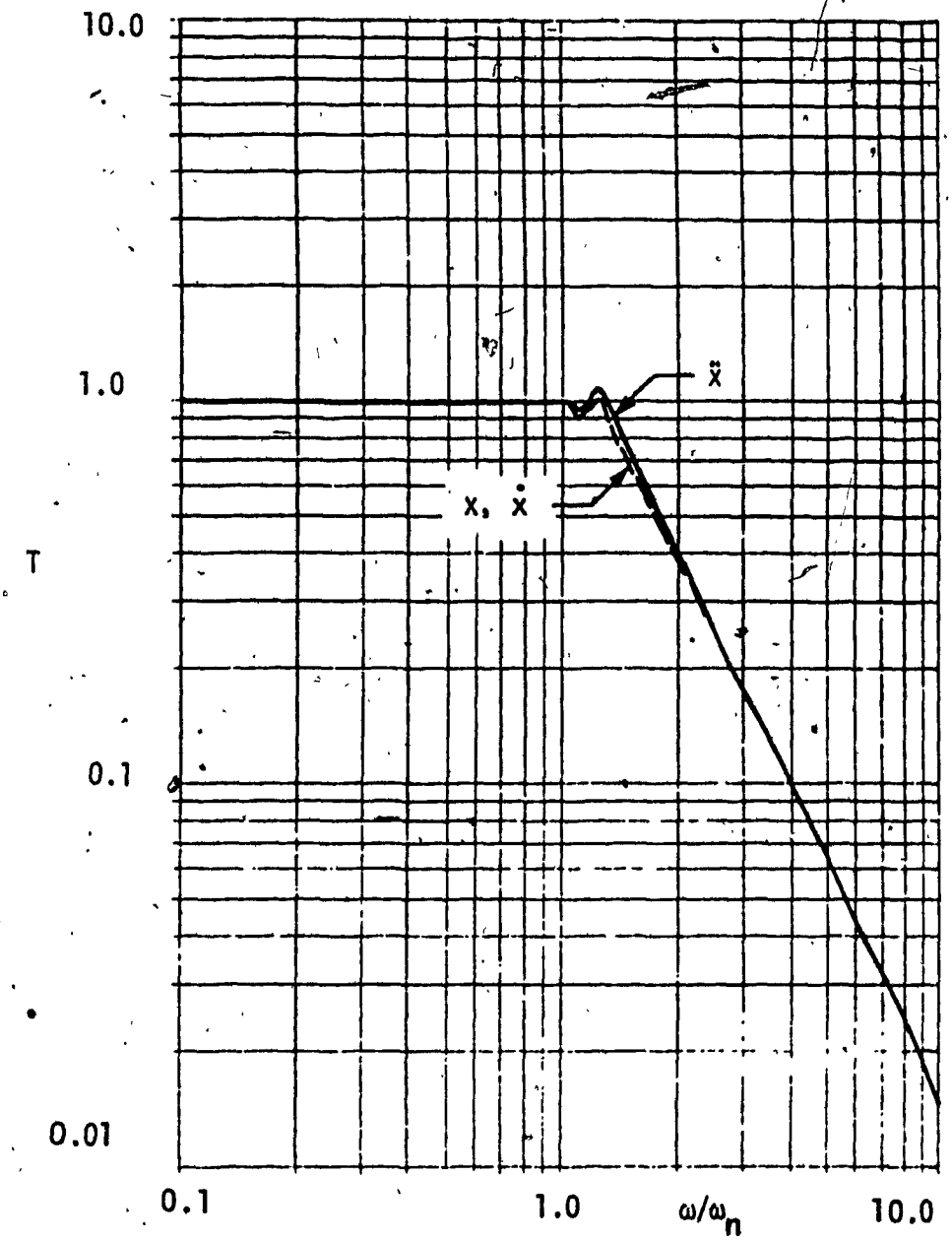

Fig. 4.28: RMS Transmissibility of Type 5 System

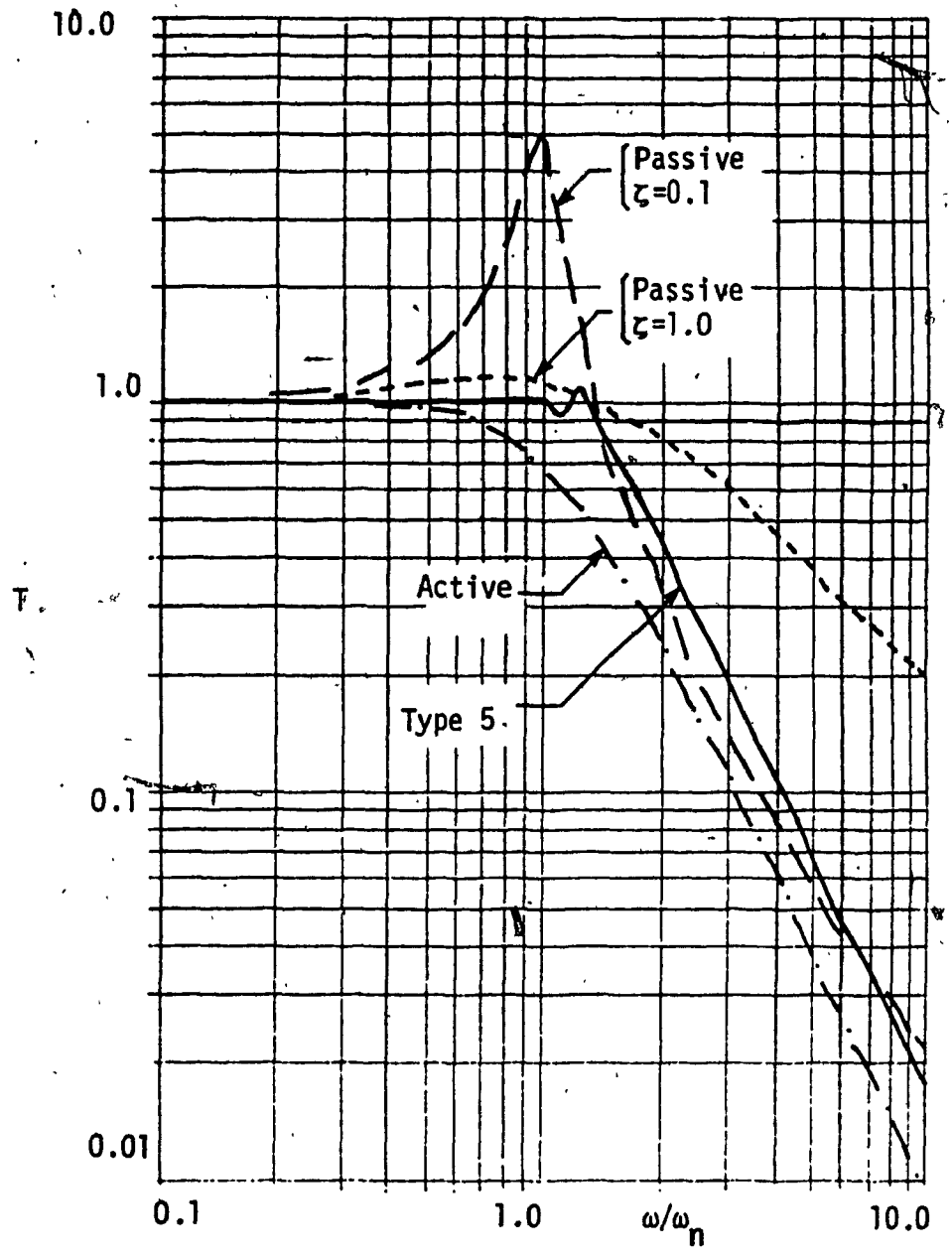

Fig. 4.29: Comparison of RMS Acceleration Transmissibilities of Type 5 Semi-Active System with Active and Passive Systems

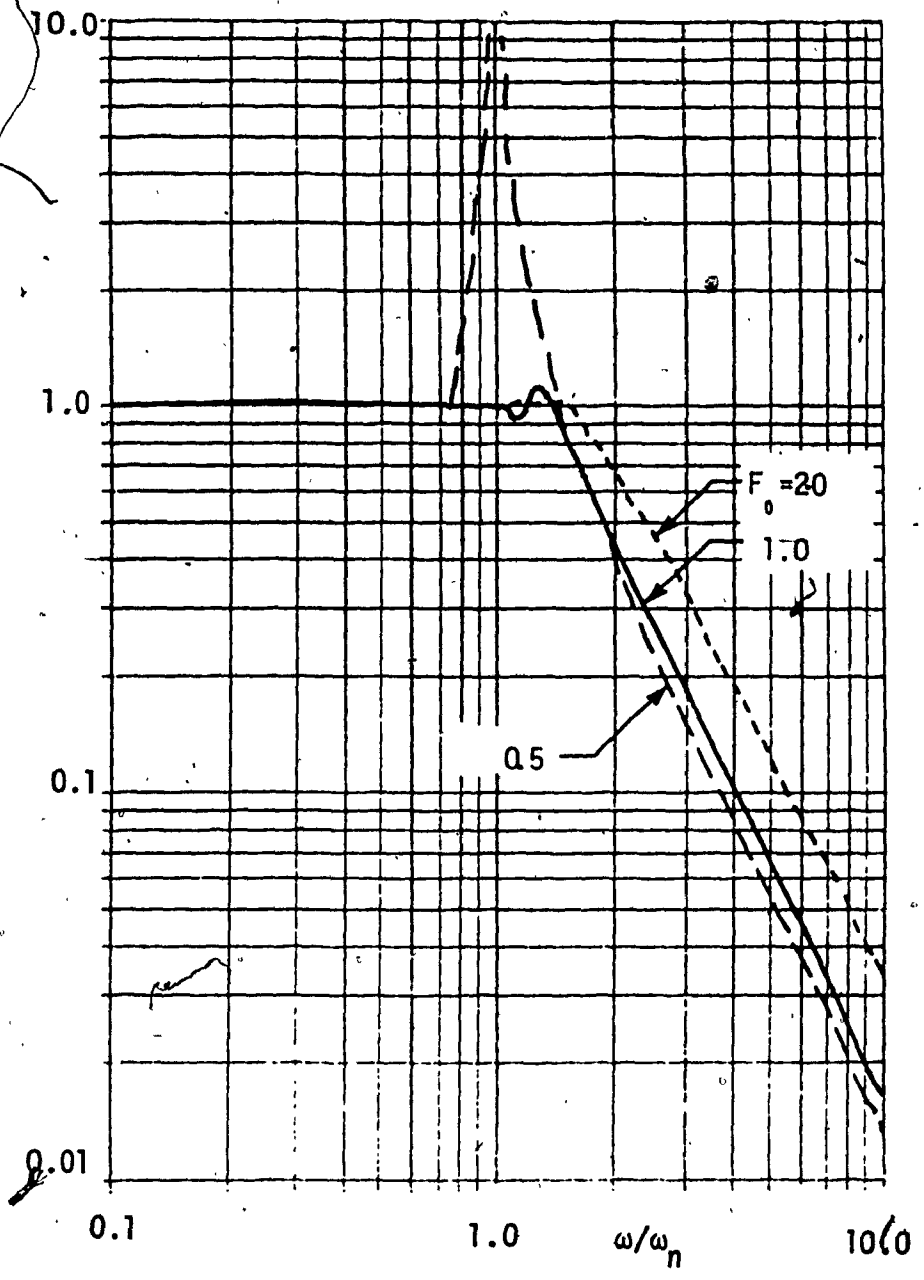

Fig. 4.30: Type 5 System RMS Acceleration Transmissibility for Variation of F_0

(except Type 4 system whose bifurcation point is affected by a) where the transmissibility is affected by the input amplitude.

4.7 TYPE 6 SEMI-ACTIVE SYSTEM

Although the Type 5 system considered in the previous chapter can be implemented using a Coulomb friction damper, it can be thought of as a semi-active damper with orifice area continuously modulated depending on relative velocity to give a constant force. Type 6 system is an on-off version of Type 5. A passive viscous damper is fitted with an on-off value giving two possible damping ratios ζ_1, and ζ_2. The basic parameters are chosen as a = 1.0, ω_n = 1.0 ζ_1 = 1.0, and ζ_2 = 0.1. Then from Equation (2.10), V_s = 0.943.

From simulation it is seen that system acts like a passive isolator with ζ = 1.0 upto $\frac{\omega}{\omega_n}$ = 1.4. From then on the damping value switches between 1.0 and 0.1 depending on the magnitude of relative velocity. Figure 4.31 through 4.33 show the steady-state response just before switching starts ($\frac{\omega}{\omega_n}$ = 1.4), just after switching starts ($\frac{\omega}{\omega_n}$ = 1.42) and also at a high frequency ($\frac{\omega}{\omega_n}$ = 5.0).

Figure 4.34 and 4.35 give the peak and RMS transmissibilities of Type 6 system. The transmissibilities of a passive system with ζ = 1.0 and ζ = 0.1 are also shown in Figure 4.35. It is clearly seen from this figure that the Type 6 semi-active system behaves like a passive system with high damping (ζ = 1.0) upto $\frac{\omega}{\omega_n} = \sqrt{2}$ and as a

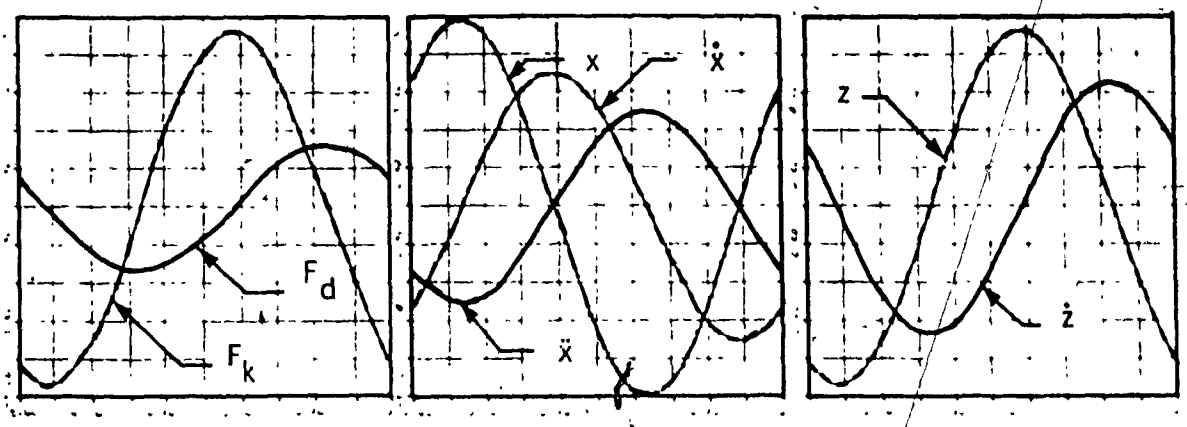

Fig. 4.31: Steady-State Response of Type 6 System at $\frac{\omega}{\omega_n} = 1.4$

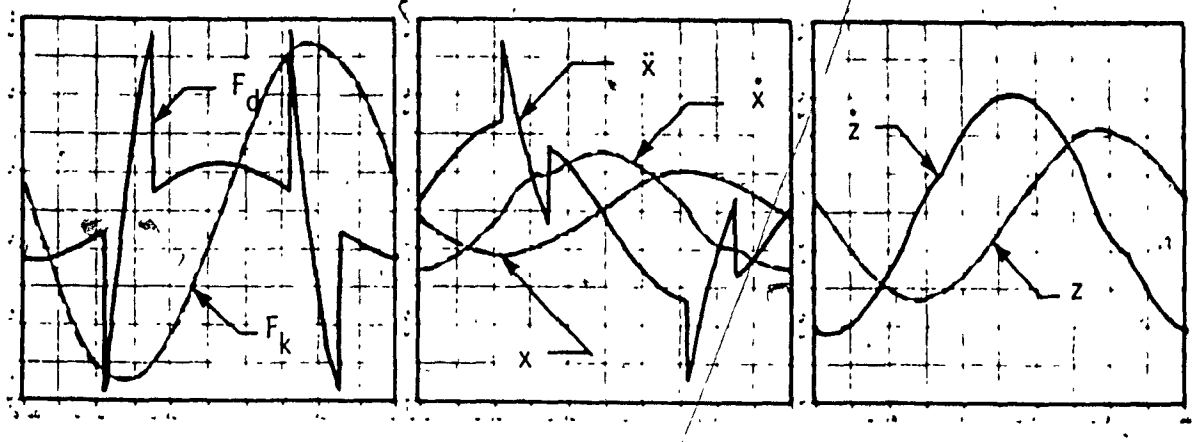

Fig. 4.32: Steady-State Response of Type 6 System at $\frac{\omega}{\omega_n} = 1.42$

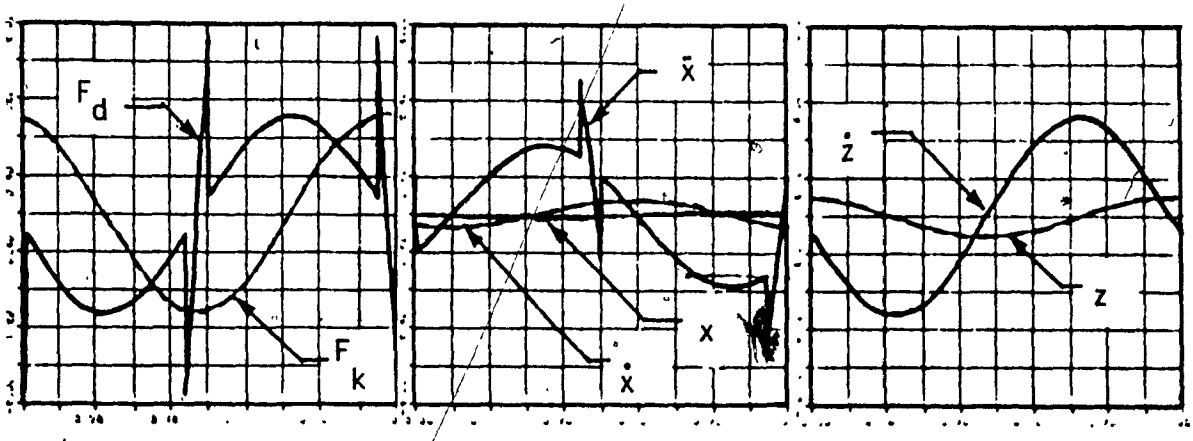

Fig. 4.33: Steady-State Response of Type 6 System at $\frac{\omega}{\omega_n} = 5.0$

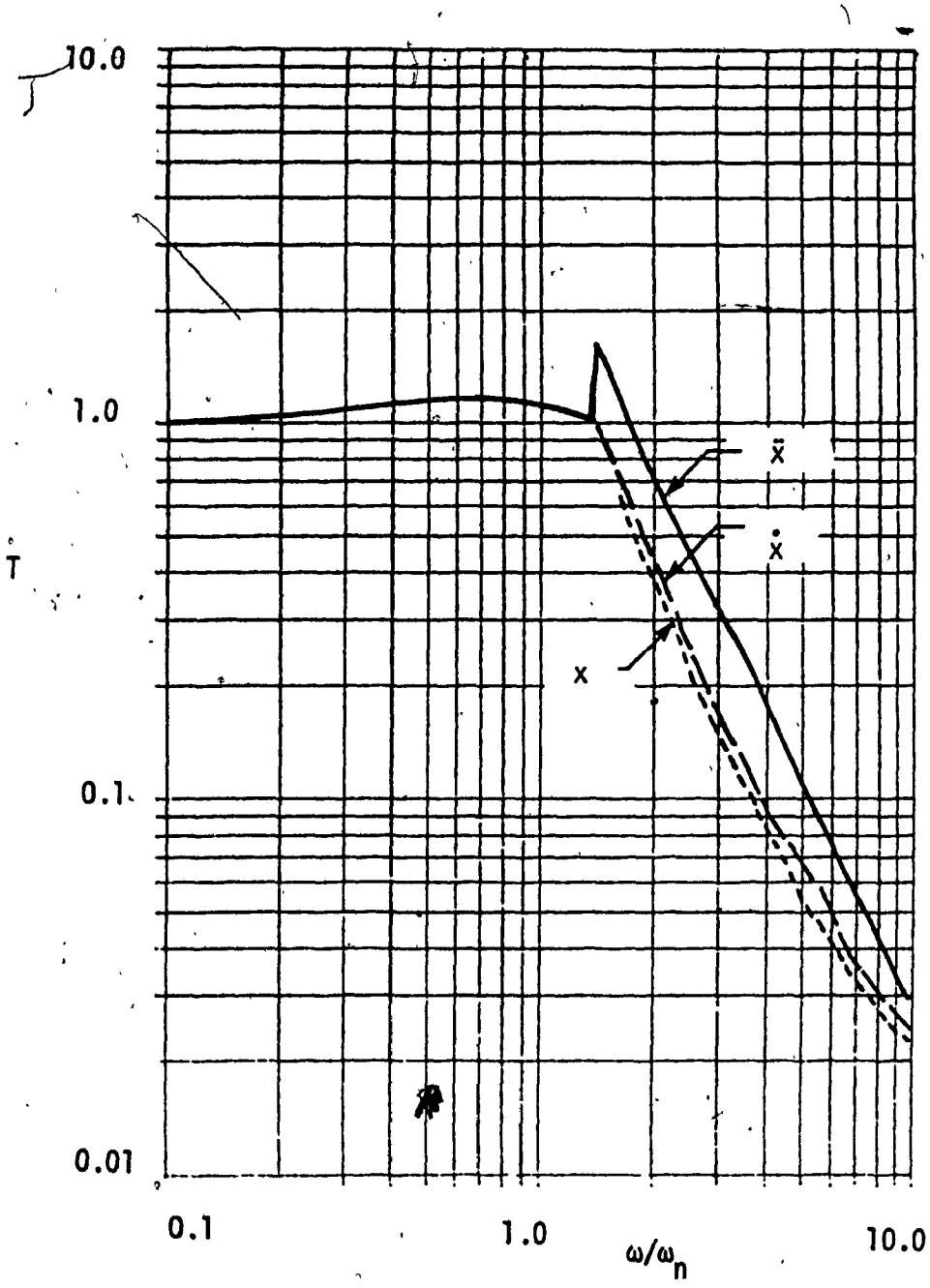

Fig. 4.34: Peak Transmissibility of Type 6 System

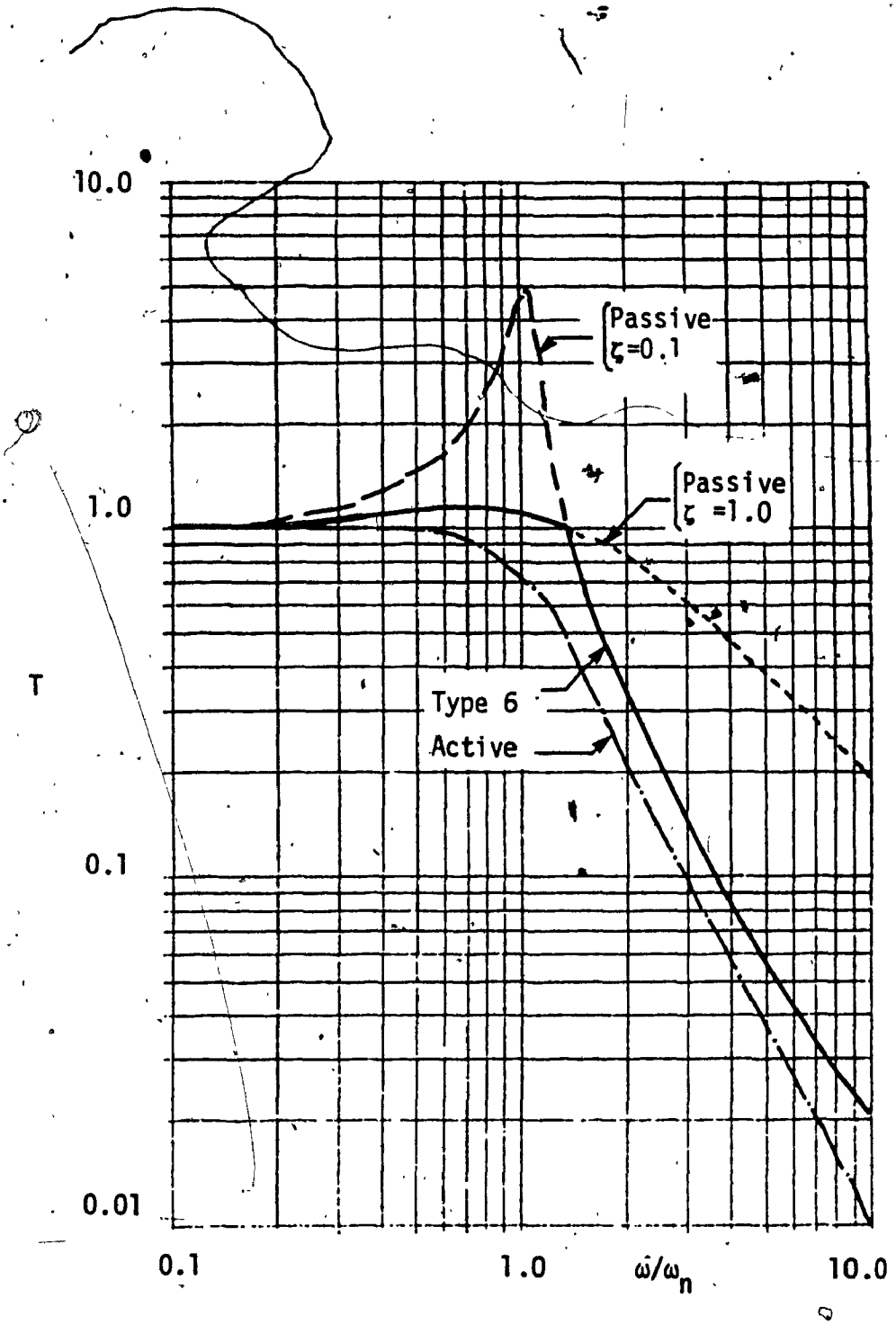

Fig. 4.35: Comparison of RMS Acceleration Transmissibilities of Type 6 Semi-Active System with Active and Passive Systems

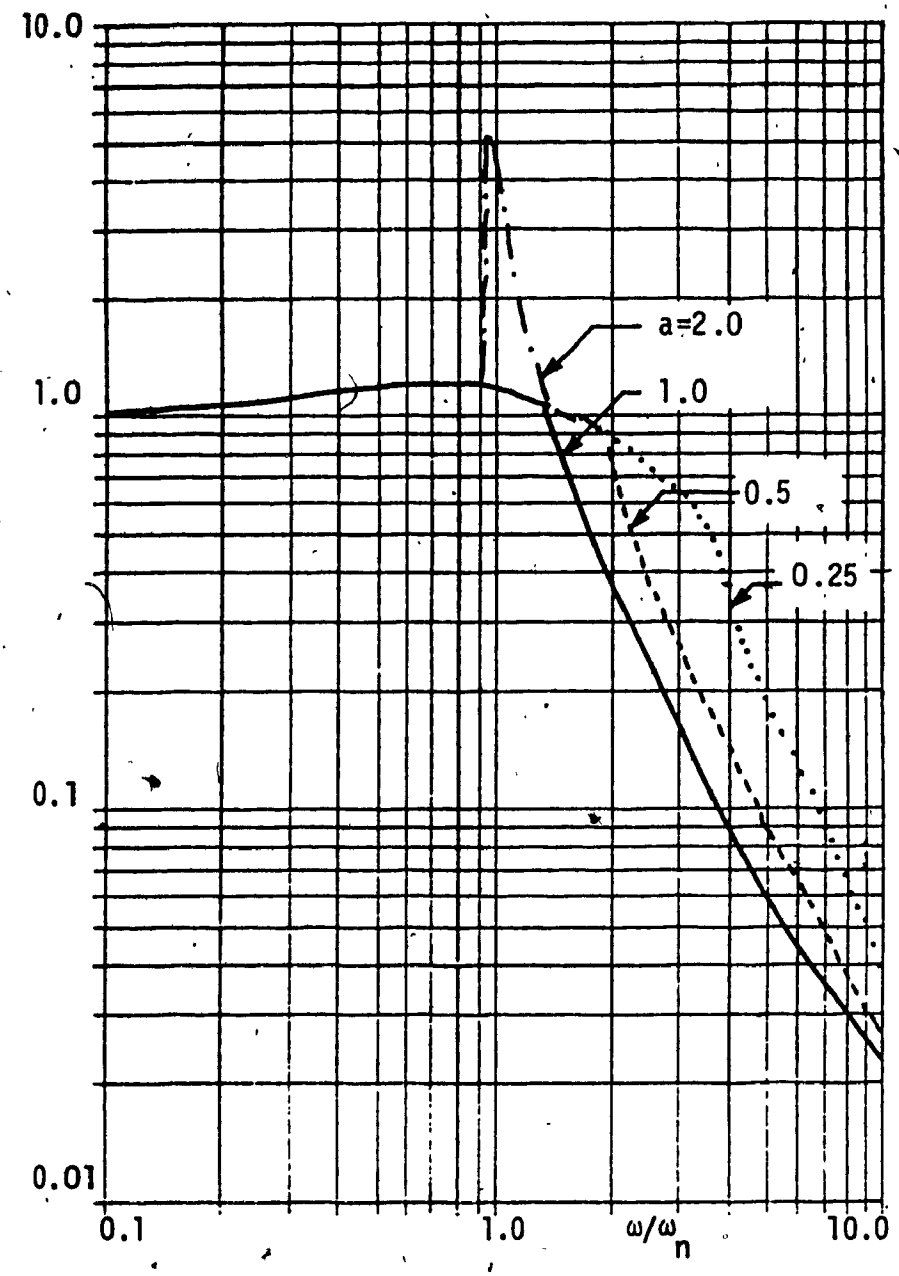

Fig. 4.36: Type 6 System RMS Acceleration Transmissibility for Variation in a

lightly damped passive system ($\zeta = 0.1$) thereafter. This was the performance one was looking for when the Type 6 control scheme was proposed.

It should be remembered that the switching velocity V_s depends on the excitation amplitude, a. Therefore it is important to see the system performance for a fixed V_s and varying a (or vice versa). Figure 4.36 shows this for a = 0.25, 0.5, 1.0 and 2.0. The result is similar to that observed for Type 5 system. When a is decreased the transmissibility breaks from the high damping curve to join the low damping curve at higher frequencies. Thus the performance suffers when one uses amplitudes lower or higher than the one for which the isolator is tuned. The worst low frequency performance occurs for large values of a at resonance. The maximum resonant peak is limited by ζ_2 and is about 5 for $\zeta_2 = 0.1$. From equations (2.9) and (2.10) it can be seen that the transmissibility break from the high damping curve to the low damping one occurs at $\frac{\omega}{\omega_n} = 1$ when

$$a > \frac{4\sqrt{2}}{3} a_s \approx 1.886\, a_s \quad \ldots\ldots\ldots\ldots\ldots\ldots\ldots\ldots (4.3)$$

where a_s is the amplitude level for which the damper was tuned. Thus a band of amplitudes may be indentified for a given system such that the low and high frequency performance is satisfactory.

4.8 CONCLUSION

Computer simulation and bifurcation analysis results for the six

types of semi-active schemes have been presented in the previous sections. The advantages and disadvantages of each type and the comparison of their performance with active and passive isolators are also discussed. These points are summarized here along with some additonal comments.

Type 1 system gives a performance close to that of an active system. The low frequency performance is a little degraded due to acceleration peaks occuring with damper switching. However the major drawback of this scheme is that implementation in vehicle suspensions may be impossible due the difficuly of obtaining accurate absolute velocity measurements. Type 2 system seems to lead to complexities due to force discontinuity. Under certain cases no mathematical solution exists for the system. In practical implementation this may lead to damper valve chatter. A delay may be built into the valve switching to improve the situation.

Type 3 system is based on directly measurable variables of a vehicle suspension. Performance improves as the gain is increased. The upper bound on the gain is determined for stablity. The high frequency performance is better than all the other systems considered. The low frequency performance is comparable to that of Type 1 system when gain is 1.3. Type 4 system exhibits drift at high frequencies. The point of onset of drift can be shifted higher by decreasing the damping ratio. However this leads to high resonant peaks. The overall system performance is judged to be not much better than that of a passive system.

Type 5 system is physically a Coulomb friction isolator. It has been treated as semi-active damper with continuously modulated prifice area. Thus Type 6 system is considered as an on-off version of Type 5. Both systems combine the good low frequency performance of highly damped passive isolator with the good high frequency performance of a lightly damped isolator. However the system must be tuned for a particular excition amplitude. The advantage of Type 6 system over type 5 is that there is no lock-up and the system is returned to static position after any transients. Also, the worst case resonant peak is much lower.

CHAPTER 5

EXPERIMENTAL INVESTIGATION

5.1 INTRODUCTION

Experimental verificaiton of analytical predictions is a necessary step in system design. Theoretical analysis cannot take into account all the non-ideal characteristics of various components. Often this is because these characteristics are not precisely known or understood. Also, even if they are known, their inclusion in the model may make the analysis too complex or difficult to perform. A typical vehicle suspension consisting of a spring and damper has many non-ideal characteristics which were not taken into account in the preceding analysis. These include Coulomb friction, damping nonlinearities, nonlinear spring due to entrapped air column, viscosity change of oil due to temperature variation, etc.. The influence of these on the suspension performance were assumed to be insighificant and tnerefore ignored in the analytical investigation.

The purpose of experimental investigation is to study how feasible a proposed concept is and to evaluate any performance improvement. It should be noted, however, that the test set-up itself may have some characteristics of its own which may vary from the actual environment for which the design is intended. This was the case in this study where the test rig gave rise to some undesirable effects.

Experimental study is carried out for the Type-6 semi-active

system. From the control circuit and suspension hardware point of view, this is the easiest to implement. The analytical studies indicated that this control scheme succeeds in combining the good characteristics of both lightly damped and highly damped passive systems. The experiment was undertaken to see if this was indeed feasible in practice and to identify any special effects caused by the physical components. The following sections detail the experimental procedure and results.

5.2 TEST FACILITIES AND SETUP

The semi-active shock-absorber was tested for two fixed values of damping, and On-Off damping based on Type 6 control scheme. The acceleration transmissibilities were computed for various excitation levels. The hardware used for this procedure is described in this section.

5.2.1 Semi-Active Isolator

In order to relate this work to a practical application, a commercially available suspension unit was used as the basis of a prototype. A 45mm front fork of an off-road motorcycle manufactured by Fox Industries of California was taken and modified to incorporate On-Off damping.

Figure 5.1 shows a schematic of the cross-section of the original unit. A pair of these forks form the front secondary suspension of an off-road motorcycle. A fork consists of two oil filled telescopic tubes with the top one (stanchion tube) sliding inside the lower one (slider). A piston is attached to the lower

end of the stanchion tube. As the piston moves up or down in the slider, the oil flow across the orifice in it creates damping forces. The piston has a one-way valve in it giving less damping in compression than in extention. The Coulomb friction at the oil seals also dampens the motion. Springing action is provided by the coil springs and entraped air column. When the slider moves up onto the stanchion tube, the extra volume of oil displaced by the tube goes through the orifice at the bottom of the damper rod.

The "On-Off" damping was to be provided by an orifice controlled by a solenoid. Since it would be difficult to implement one on the piston, a different method was adopted for modulating the oil flow. Figure 5.2 shows the modified fork. The orifice at the base of the damper rod was made larger and controlled by a solenoid. Large orifices were also made at the top of the damper rod for the oil to travel past the piston when the bottom orifice is open. When the solenoid is on, the orifice in the damper rod base is fully open and most of the oil flow occurs through it with relatively less restriction. When the solenoid is off, this orifice is mostly closed (full closure will cause lock-up) and the oil flowing through it and past the piston creates higher damping. The piston has a small fixed orifice. The solenoid operates on 12V DC and is controlled by an electronic control circuit.

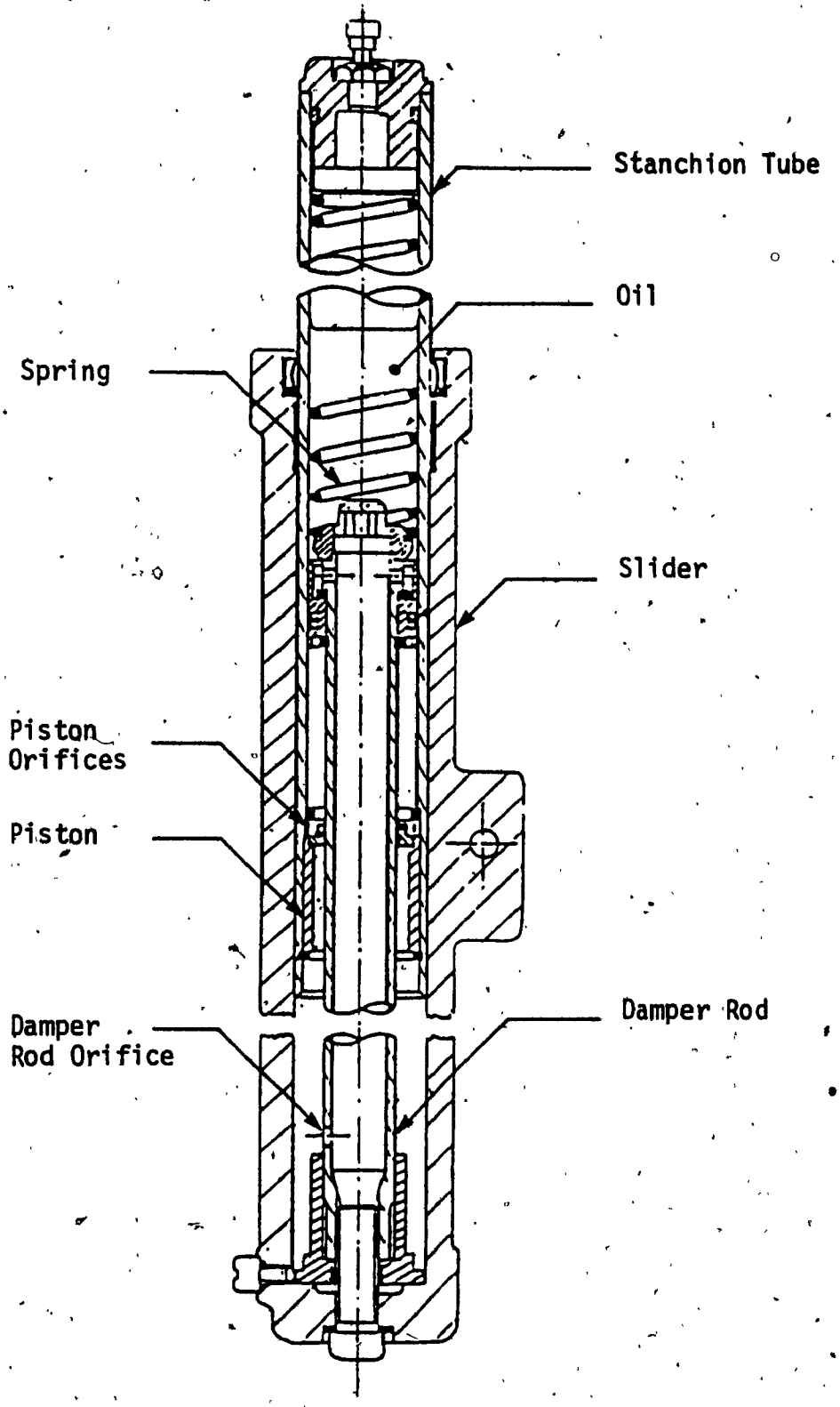

Fig. 5.1: Cross-Section of a Motorcycle Front Fork

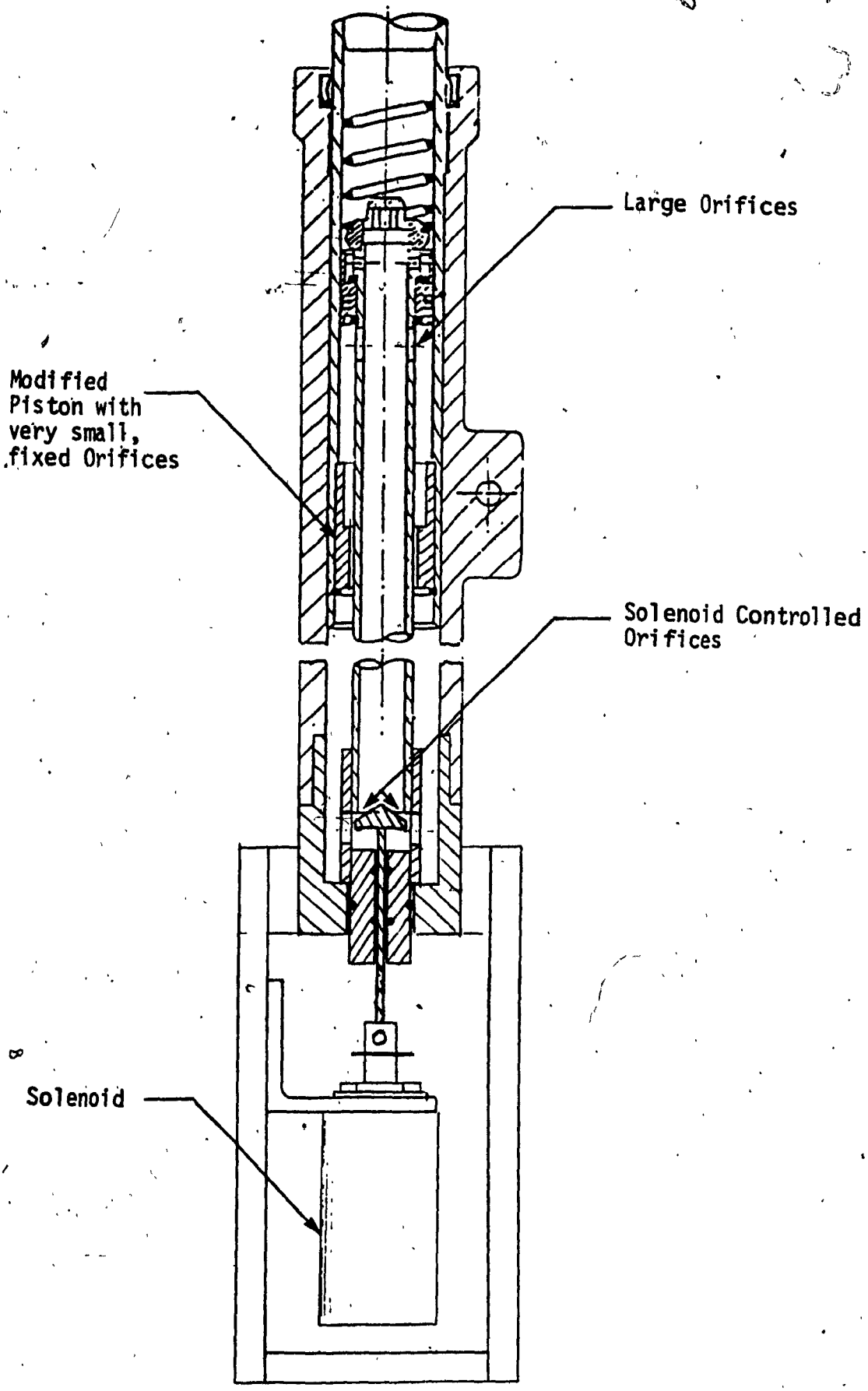

Fig. 5.2: Prototype of On-Off Damping Isolator

5.2.2 Control Circuit

The principle of Type 6 semi-active isolator is that when the magnitude of the relative velocity is above a certain fixed value, the damping should be low and when it is below this value, the damping should be high. As described in the previous section, the damping is low when the solenoid is on and high when off. The control circuit receives the relative velocity from an LVT and operates the solenoid.

5.2.3 Instrumentation

The motion sensors consisted of the following:

- 2 accelerometers (Bruel & Kjaer 4370 peizoelectric, delta shear type) to measure accelerations of the base and mass;
- a linear velocity transducer (LVT) with 102 mm (4") stroke (Robinson Halpern model 240A-4000) to measure relative velocity across the isolator;
- a 406 mm (16") stroke potentiometer (New England Instruments), to measure relative displacement; and
- a Nicolet 660B digital FFT analyser for signal processing.

5.2.4 Input Exciter

The sinusoidal excitation required to determine the frequency response function of the isolator was provided by an electro-hydraulic shaker. This was manufactured by International Scientific Instruments of Japan and is capable of producing large and stable low frequency signals. Sinusoidal displacements of 1 Hz to 8 Hz were used at amplitudes of 12.7 mm (0.5 inch) 19.1 mm (0.75 inch) and 25.4 mm (1.0 inch).

5.2.5 The Sprung Mass

Two steel rods with a total mass of 33.37 kg were attached to the top of the suspension unit. This represents the equivalent mass on one front fork of an off road motorcycle with an average sized rider on board [6]. In order to provide lateral guidance for the mass as it moves up and down, two Thomson linear bearings, attached to a rigid frame were provided.

Figures 5.3 through 5.6 shows the various details of the experimental setup.

5.3 RESULTS AND DISCUSSION

As in the case of analytical results, experimental results are also presented in the form of transmissibility plots. The isolator was excited at discrete frequencies and the transmissibility determined. For a linear system, for a sinusoidal input, the response will also be sinusoidal and the ratio of the peak values

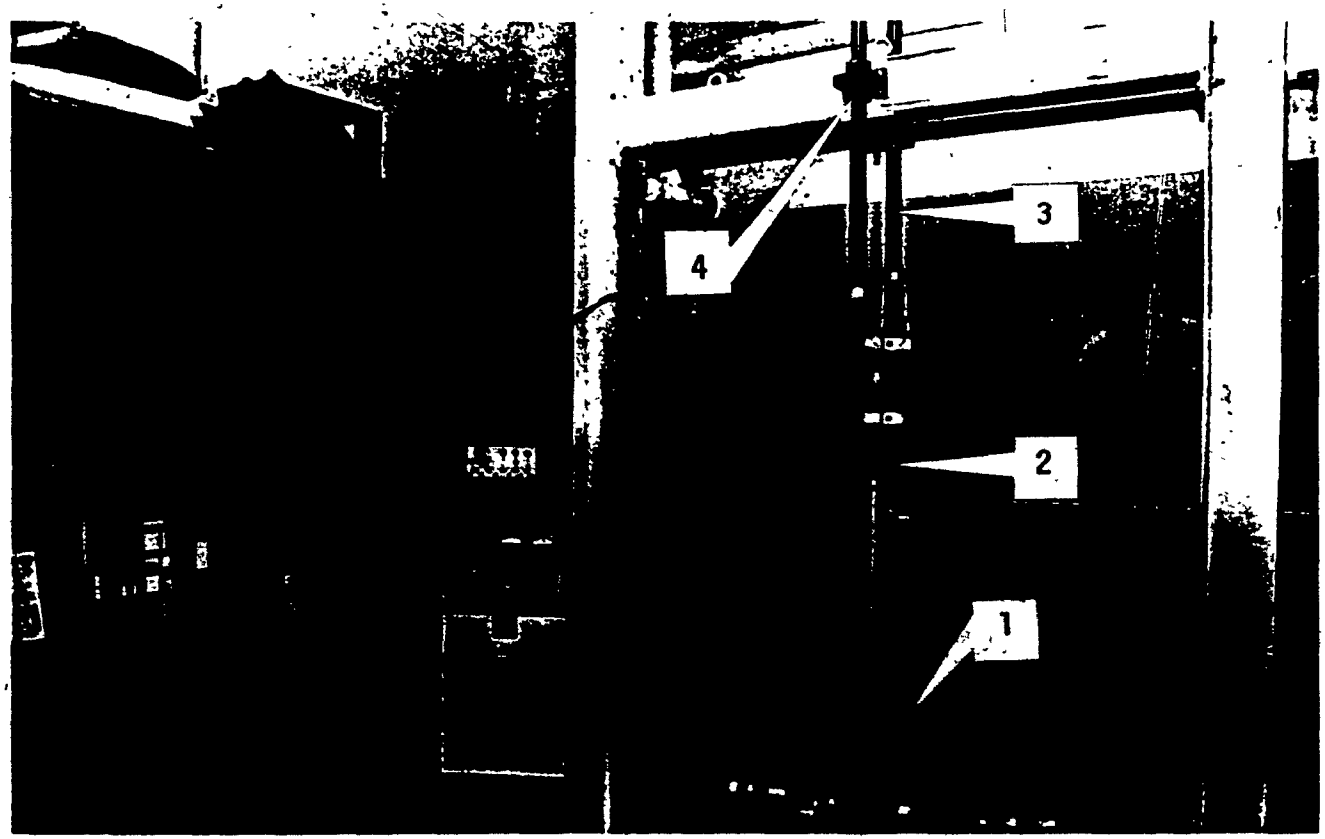

Legend 1: Shaker 2: Shock-Absorber
3: Sprung Mass 4: Linear Bearings

Fig. 5.3: Overall View of Test Setup

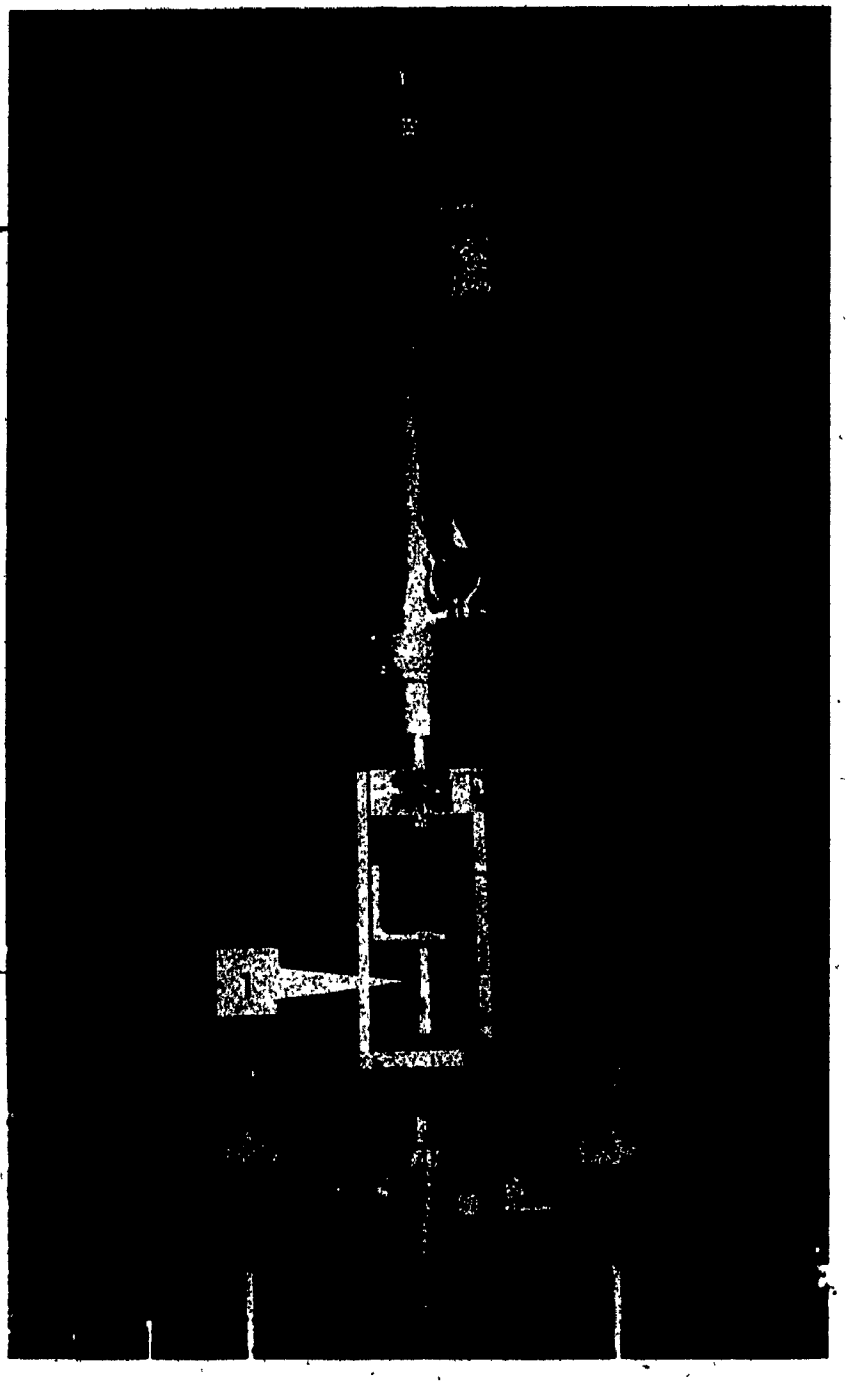

Legend 1: Solenoid

Fig. 5.4: Arrangement of On-off Solenoid

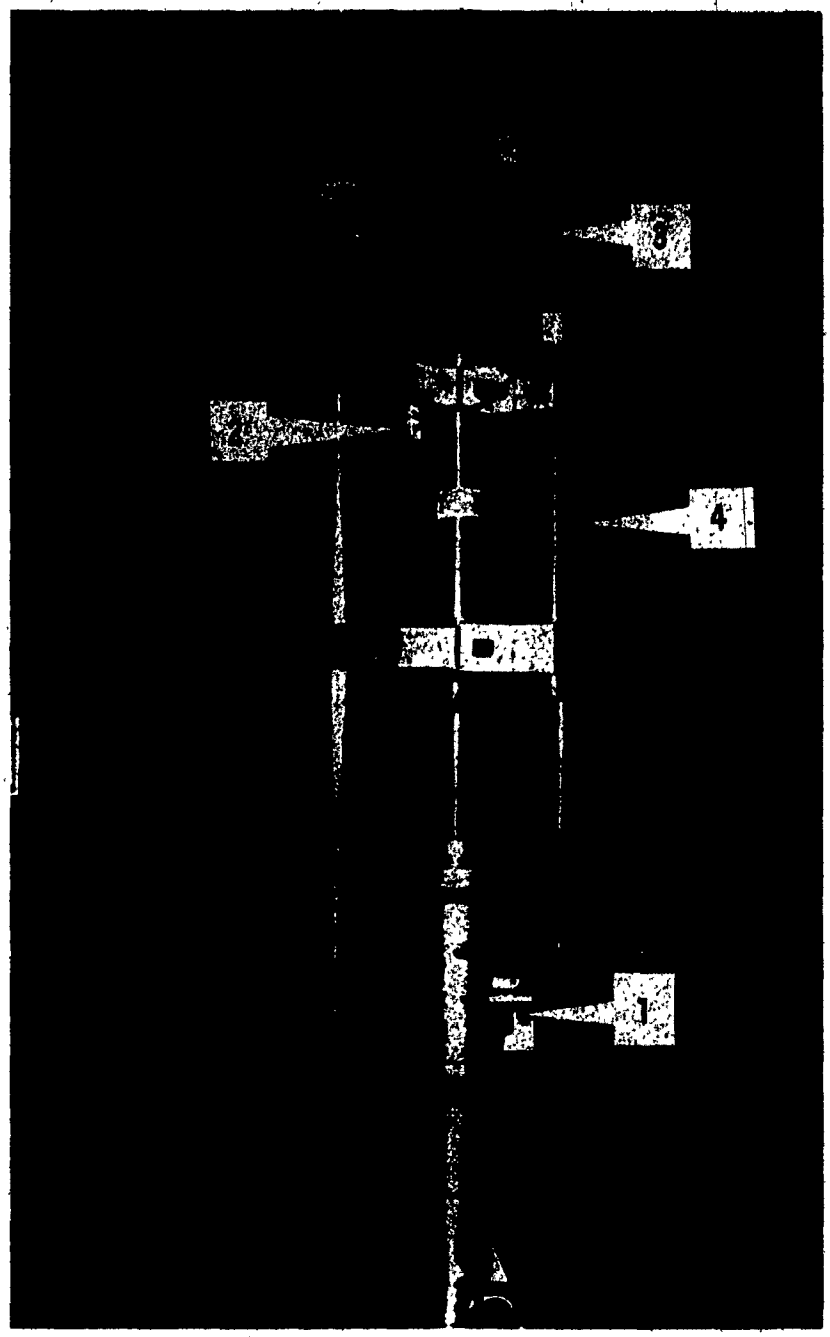

Legend 1: Base Accelerometer 2: Mass Accelerometer
3: Potentiometer 4: Velocity Transducer

Fig. 5.5: Motion Sensor Locations

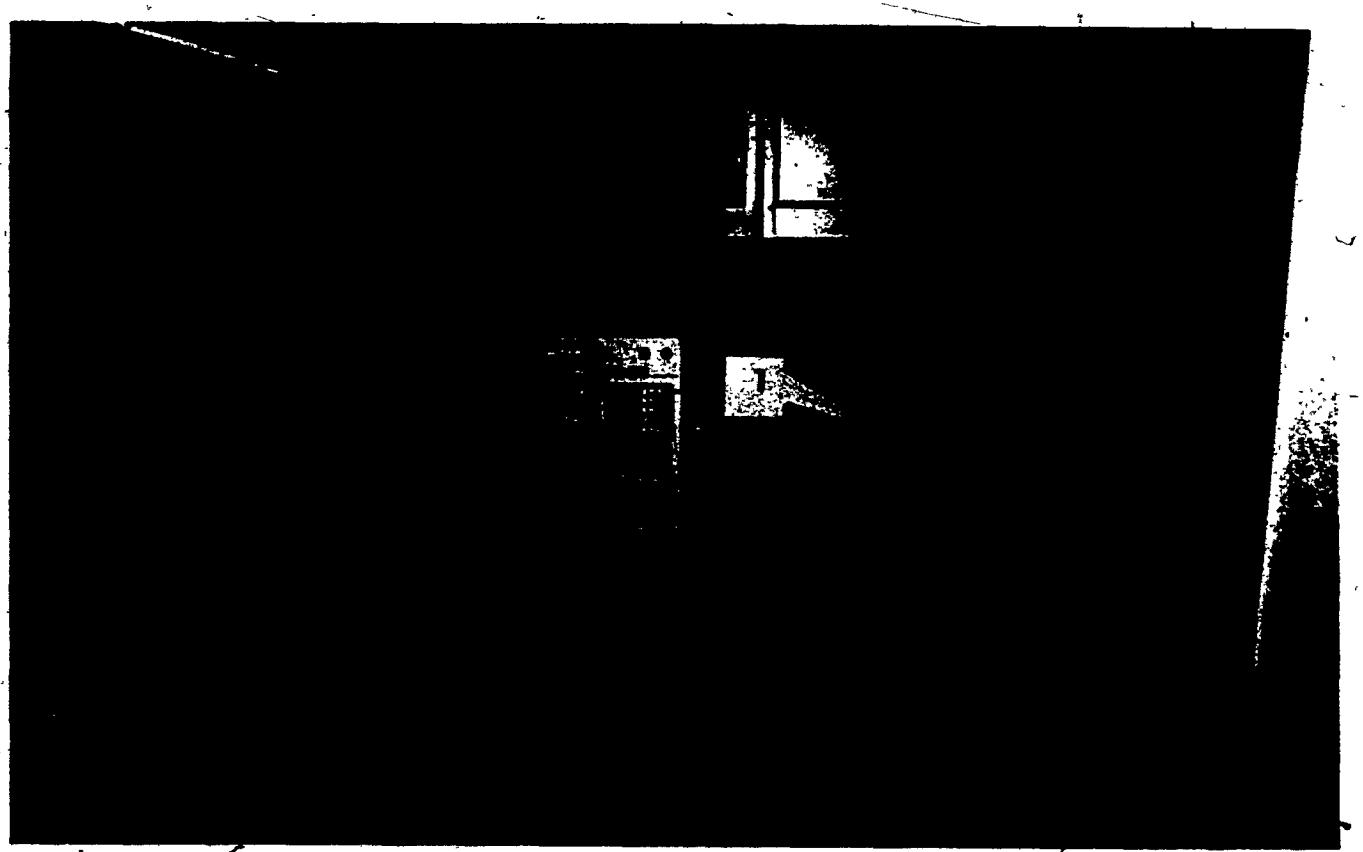

Legend 1: Control Circuit

Fig. 5.6: Controller, Recorders and FFT Analyser

will give the transmissibility. However for a non-linear system the response bandwidth will be larger than the input and therefore the ratio of peak values may not be meaningful. Therefore as in the case of analytical results, ratio of the RMS values of acclerations are presented as the transmissibilty. This was carried out using the FFT analyser within the bandwidth 0.05 to 20 Hz.

The experiment was run in three phases. In the first and second phases, characteristics of the suspension for fixed values of high and low damping values (valve closed and valve open) were determined. In the third phase the response of the on-off semi-active suspension was evaluated.

In the test setup the two linear bearings used for guidance unfortunately introduced Coulomb type friction. This friction acts as a "skyhook" damper (Figure 1.4). As was seen in chapter 4, skyhook damping is especially effective in lowering the resonance peak. Further, the oil seals in the suspension unit itself gives some Coulomb friction. This causes the unit to lock-up until the inertia force exceeds the friction force [6].

Type 6 semi-active system (relative velocity based On-Off) proposes to combine the good low frequency performance of a highly damped passive system and the good high frequency performance of a lightly damped system. Thus the high and low damping response of the system are evaluated first. Then, based on these, the switching

level of relative velocity is determined and the semi-active scheme is tested.

5.3.1 Passive, High Damping

The performance of the passive suspension unit was evaluated for the case of high damping. The high value of damping is the damping when the solenoid is not energized. Three input amplitude levels were used, namely, 12.7 mm (0.5 in) 19.1 mm (0.75 in), and 25.4 mm (1.0 inch). Since the system is nonlinear, the performance does vary with different input levels.

Figure 5.7 shows the transmissibility for the 3 excitation levels. It is noted that in this case the damping is very high - indeed. At 25.4 mm (1.0 inch) excitation, one could only go upto 2.8 Hz. It was felt that beyond this frequency the forces generated would damage the suspension itself. At 19.1 mm (0.75 inch) and 12.7 mm (0.5 inch) excitations, runs were made upto 3.5 Hz, and 5.0 Hz respectively. The fact that the system is very highly damped can be noticed from the transmissibility at 5 Hz for 12.7 mm (0.5 inch) excitation. This value of 0.61 corresponds to a damping ratio of 1.40 for a linear system (Eqn 1.4).

5.3.2 Passive, Low Damping

The low damping case is obtained when the valve is open (solenoid energized). Once again the transmissibilties are determined for three levels of excitation amplitudes. The results are shown in Figure 5.8. Because of the Coulomb friction

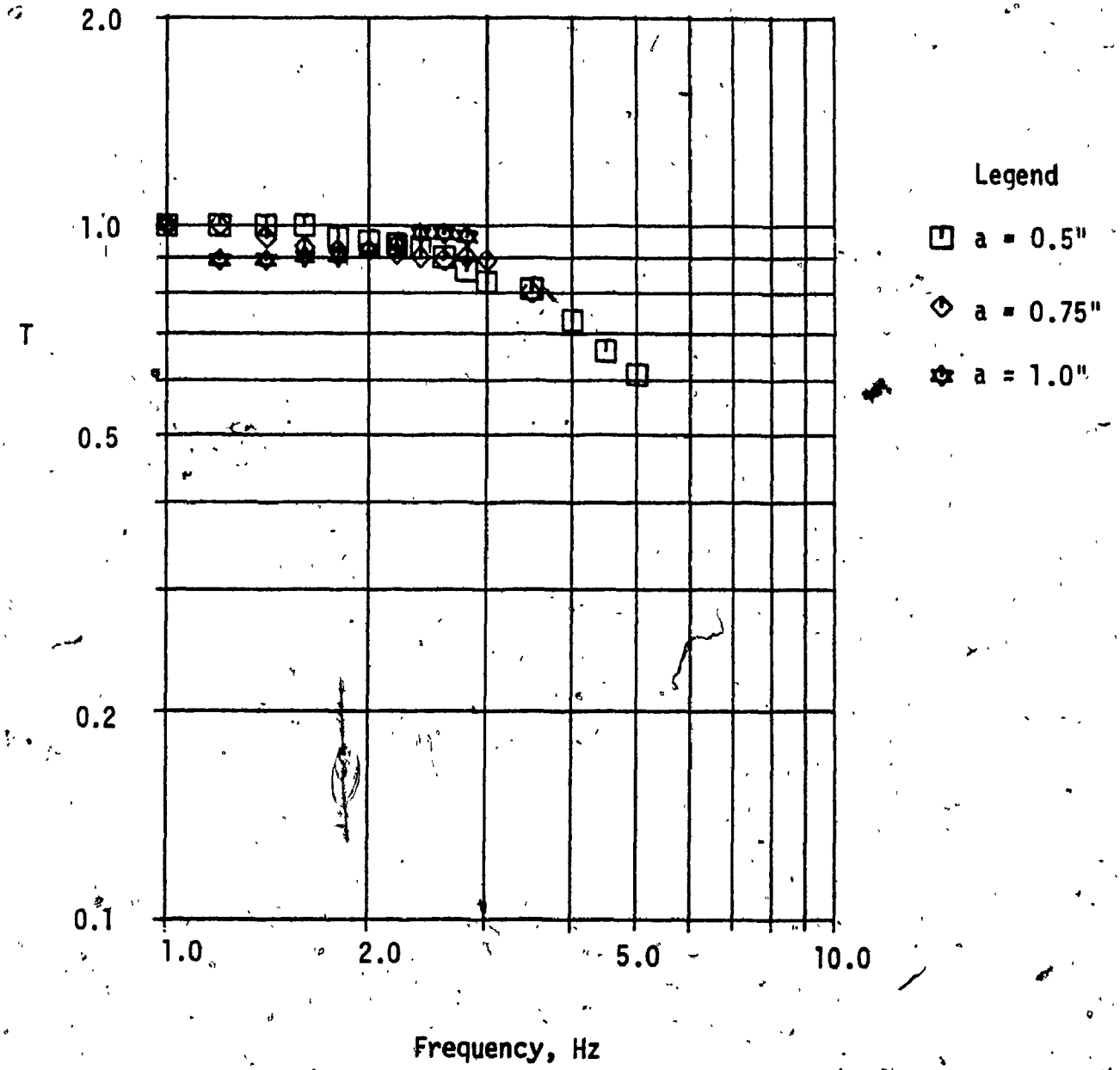

Fig. 5.7: Transmissibility of Passive System with High Damping for 3 Excitation Levels

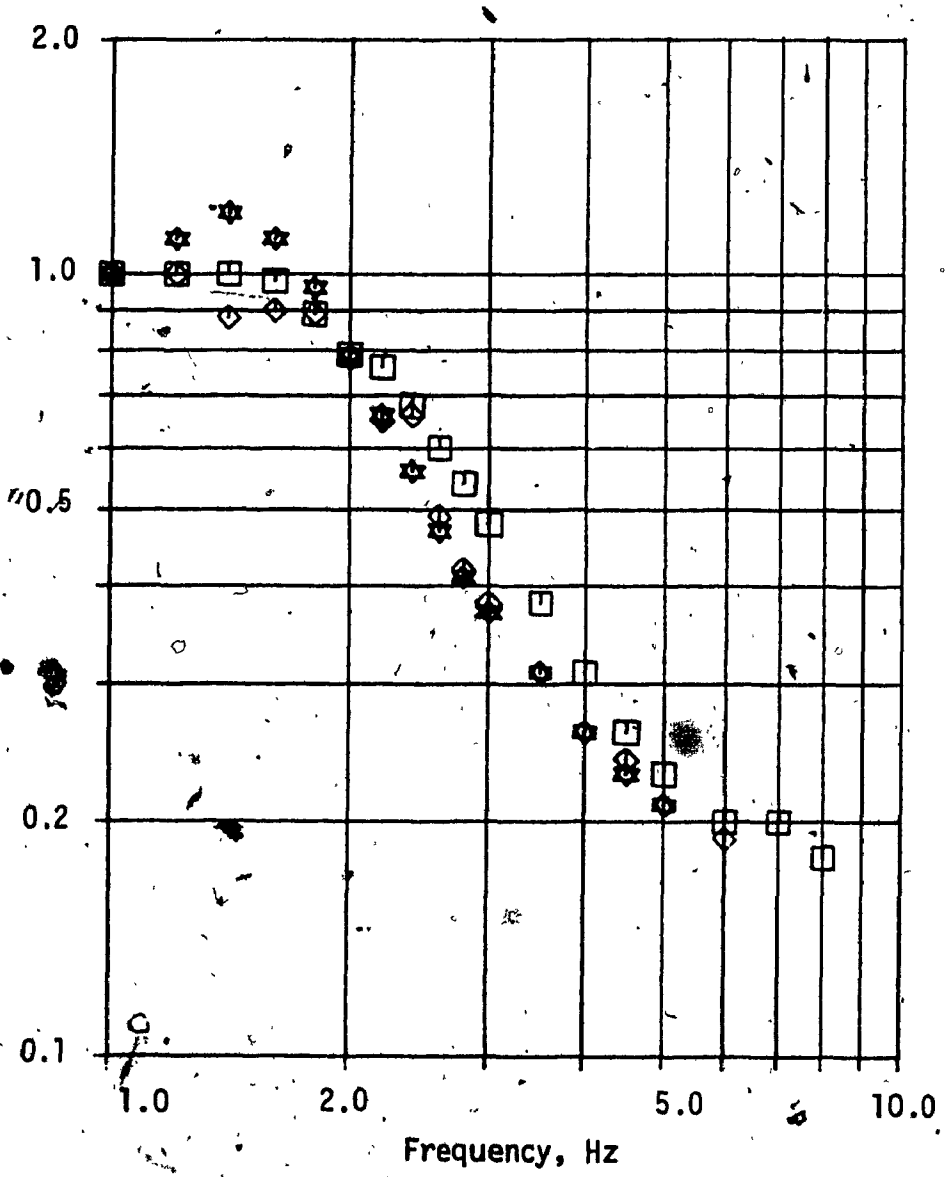

Fig. 5.8: Transmissibilty of Passive System with Low Damping for 3 Excitation Levels

discussed earlier, and relatively high amount of damping, a resonance peak is observed only for the case of excitation amplitude of 25.4 mm (1.0 inch). For this case, at 5 Hz, the transmissibility of 0.21 corresponds to a damping ratio of 0.37 for a linear system.

5.3.3 On-Off Semi-Active Damping

For the high damping case, the amplitude of the relative velocity was seen to be monotonically increasing with frequency. Therefore, the scheme of On-Off damping based on relative velocity is feasible. The objective is to produce a system having high damping at low frequencies and low damping at high frequencies. However, because of the hardware limitations, the difference in performance between high and low damping cases at low frequencies was discernible only for excitation amplitude of 25.4 mm (1.0 inch). In this case, the transmissibilty curves cross over at 1.8 Hz. Therefore the peak value of the relative velocity for the highly damped system corresponding to this frequency is set as the switching velocity, V_s, on the control circuit.

Figure 5.9 shows the response of the semi-active system for 25.4 mm (1.0 inch) exctitation amplitude, together with the response of passive systems. It shows that the semi-active system performs even better than theoretically predicted. Upto 1.8 Hz, the solenoid did not operate because the relative velocity never exceeded the preset value on the control circuit. For 2.0 Hz and 2.2 Hz, the solenoid operates in on-off mode. Above this frequency the solenoid

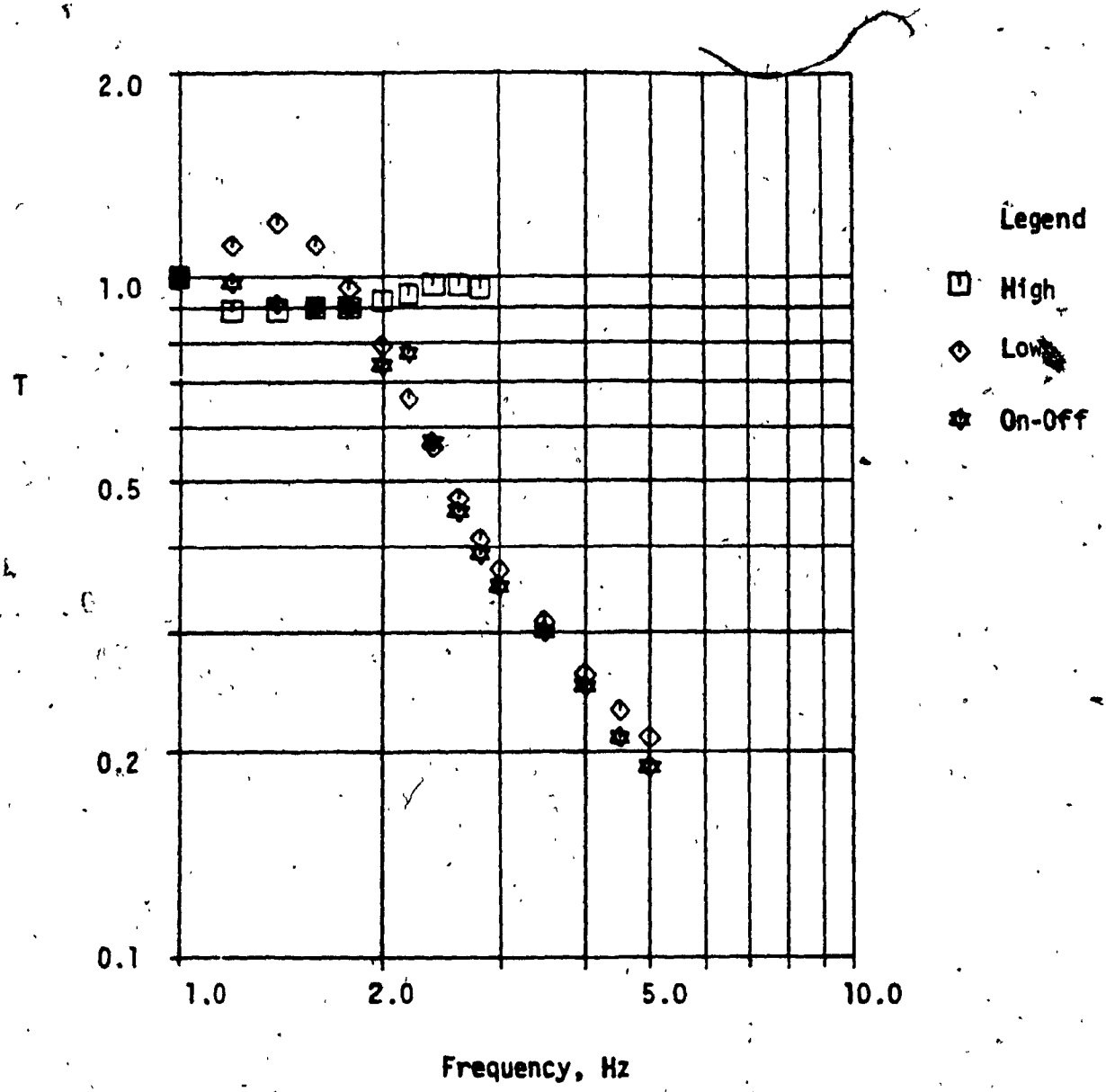

Fig. 5.9: Transmissibility with High, Low and On-Off Damping at a = 2.54 cm(1.0")

remains continually open, giving low damping. Thus the semi-active system transmissibility closely follows the low damping transmissibility at high frequencies.

In the analytical studies carried out earlier, the time constant of the solenoid was not considered. The results showed that the high frequency isolation of the semi-active system is slighty worse than that of a lightly damped passive system. However, the experimental results show the two systems have identical transmissibilities. This improvement was caused by the time delay of the solenoid.

The solenoid selected is capable of operating upto 20 Hz. The reason why it did not switch at frequencies above 2.4 Hz is because, at these frequencies, the off-cycle period was too short. This in turn is due to the fact that the relative velocities had very high amplitudes. Therefore, although the control circuit did switch the voltage supply to the solenoid, it remained energized. Figures 5.10 shows, for various frequencies, the relative velocity signal from the LVT and the voltage at the base of the power transistor that operates the solenoid. When the latter is high (+12v) the solenoid is to be off and when low (0v) on. At 2.4 Hz, the off-cycle is only about 0.3 seconds and the solenoid did not respond.

Since any suspension will have to operate under various excitation levels, one must study how the semi-active system responds for other amplitudes. Therefore transmissibilities were also determined for input amplitudes of 12.7 mm (0.5 inch) and 19.1 mm

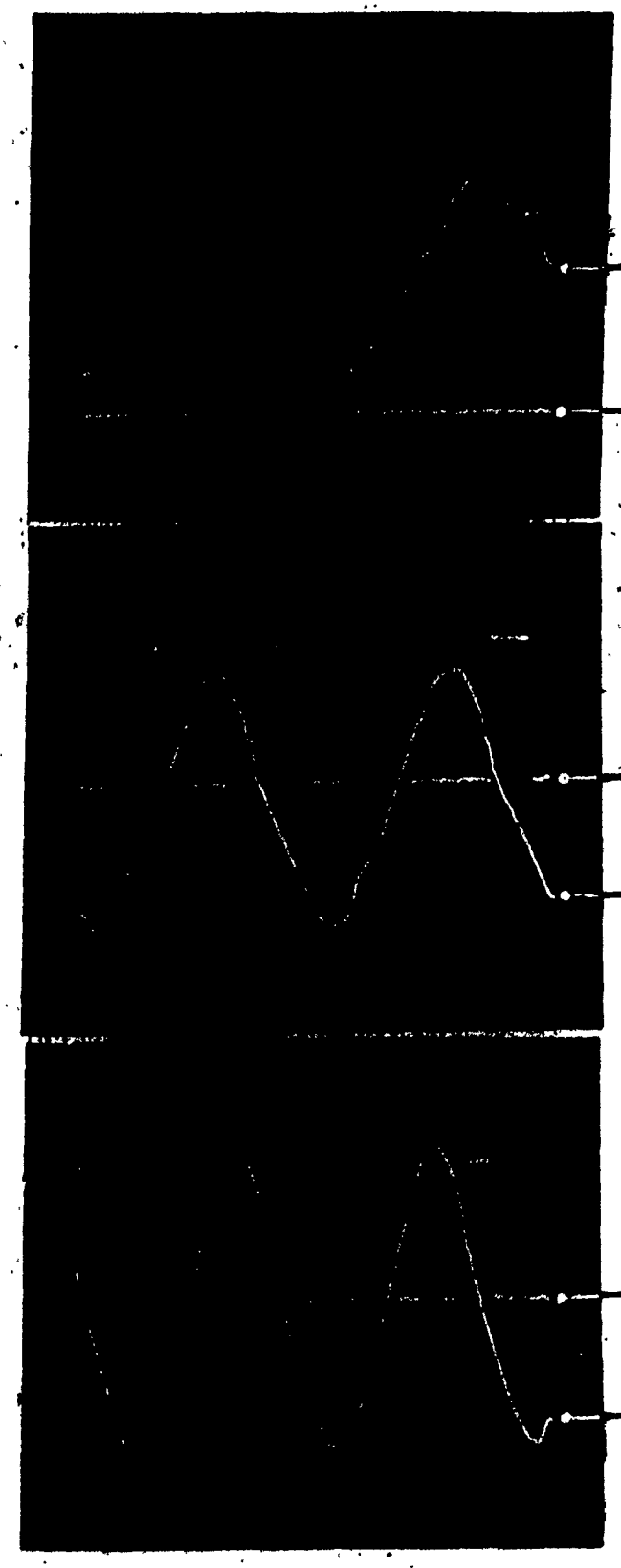

Fig. 5.10: Solenoid Control Signal at 3 Frequencies

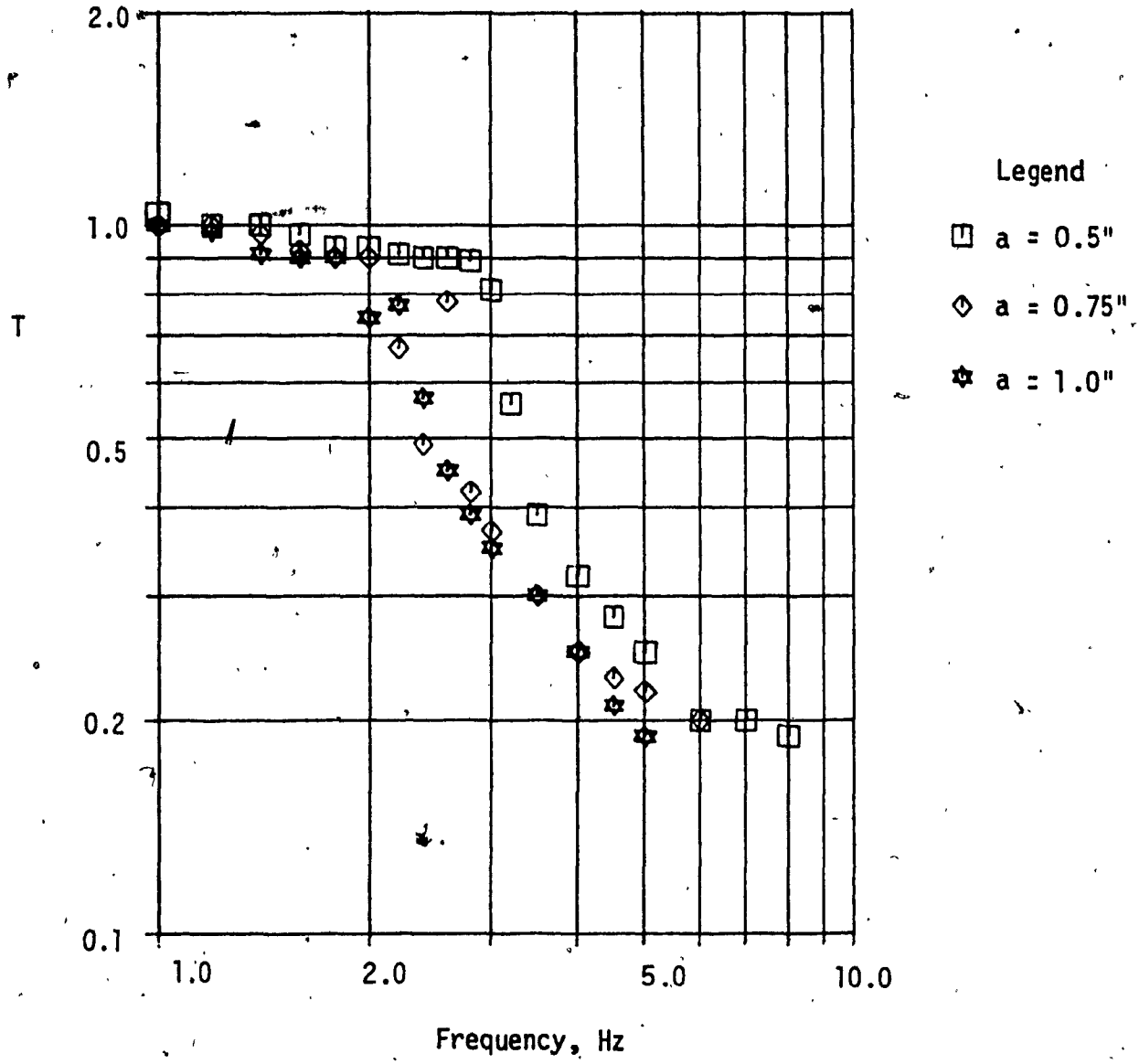

Fig. 5.11: Transmissibility with On-Off Damping at 3 Excitation Levels

(0.75 inch), while keeping the switching velocity the same as before. Figure 5.11 shows these plotted together with the one for a = 25.4 mm (1 inch). Once again the results are as expected. As the amplitude level is decreased, the transmissibility curve breaks off from the high damping one at a later frequency.

5.4 CONCLUSION

Experimental results for the Type 6 semi-active system have fully verified the analytical predictions. This system is shown to be superior to the passive ones. The high frequency response of the experimental setup was even better than expected because of the dynamics of the solenoid.

CHAPTER 6

CONCLUSIONS AND RECOMMENDATIONS FOR FUTURE WORK

6.1 HIGHLIGHTS OF THE PRESENT WORK

In this thesis, the vibration isolation characteristics of six types of semi-active suspension schemes have been presented. All the schemes are analysed with the same basic parameters and the results are compared on the basis of peak and RMS acceleration transmissibilities. The merits and demerits of each type of system is presented in comparison with passive and active isolators and with each other.

The major contribution of this research is the introduction of two new semi-active vibration isolator schemes and the investigation of these in relation to the performance of other semi-active isolators. The continuous control semi-active schemes referred to as Type 3 system is an original contribution. The results of the present investigation show that the vibration isolation characteristics of this scheme is superior to that of a fully active system. Moreover, the control scheme is based on directly measurable quantities and has practical potential for vehicle suspensions. The formulation of Type 6 system employing on-off damping for vibration isolation is also an original contribution. This scheme has been presented earlier by other researchers for shock isolation. In the present study, a systematic theoretical basis has been presented for its use in vibration isolation. The results from theoretical and

experimental studies have demonstrated the effectiveness of this scheme.

Another highlight of this study is the examination of the stability of the various semi-active schemes. The on-off control schemes were checked for the possibility of unstable switching leading to chatter. A unified basis for investigating the lock-up condition for the continuous control schemes was also established.

6.2 CONCLUSIONS

The conclusions from computer simualtion and experimental investigation have been detailed in tne relevant chapters. Therefore only an overall summary is presented in this section.

Theoretical and experimental results for Type 1 system and variations of Type 2 and Type 5 systems, and theoretical results for a variation of Type 4 system have been reported earlier by other investigators. In the present investigation two new schemes are also introduced and a total of six schemes are studied in detail for thier vibration isolation characteristics. The transmissibilities of the various semi-active suspension concepts are presented in terms of RMS acceleration.

Of the three semi-active schemes proposed by earlier investigators, namely, Type 1, Type 2 and Type 4 systems, only the first is seen to have a viable control scheme. However, even in this case it is noted that the difficulty of obtaining accurate absolute velocity measurements in vehicle applications will severly limit the

usefulness of the control scheme. It was shown that the differential equations describing Type 2 system may not have solutions. The implementation of this on-off control scheme will lead to chatter of the on-off control valve leading to performance degradation. Type 4 system exhibits drift at high frequencies. It was shown that even if the drift is disregarded, the acceleration isolation is not any better than what could be achieved through passive means.

Of the three new semi-active schemes proposed in this thesis, Type 5 system can be implemented passively using Coulomb friction. Type 5 and its on-off counterpart, Type 6 systems can avoid resonance peaks and provide good high frequency isolation when the excitation amplitude is within a narrow band. Unlike the Type 5 system, Type 6 system will return to static position after any transients. Furthermore, in the Type 6 system when large amplitude inputs are encountered, the resonance peak is limited by the lower value of damping ratio (resonance amplification of 5 for $\zeta_2 = 0.1$).

Type 3 system has the same condition function as the Type 4 system. This depends on relative displacement and relative velocity and can be implemented even in vehicle applications. The computer simulation results have shown that the high frequency vibration isolation of this novel system can be better than that of an active system, when the damper gain, α, is 1.3. There is a small degradation in the performance at low frequencies due to the discontinuities in the damper force. Considering the overall performance, Type 3 system can be said to be superior to all the other 5 Types of semi-active suspensions studied.

6.3 RECOMMENDATIONS FOR FUTURE WORK

Future work based on the present investigation falls into two categories namely, analytical and experimental. Recommendations for analytical work may be summerized as follows:

1) Analysis of the various semi-active schemes under transient and random inputs.

2) Improvement of the mathematical model to include suspension effects such as seal friction, velocity-squared damping and effect of entrapped air column.

3) Inclusion of a realistic model of the dynamics of the fluid flow control valve and its effect on the suspension performance. As has been noted in Chapter 4, the analysis of Type 2 system cannot be carried out independent of the valve dynamics because of the expected "chatter" phenomenon. A model that includes the valve dynamics may suggest a modified control strategy, whereby the unstable switching may be avoided.

4) Application of semi-active control in multi-degree-of-freedom systems. Some studies have been reported for Type 1 system. The work may be extended for other schemes presented in this thesis.

Experimental studies are important because the analytical work invariably contains approximations and idealizations. Future experimental work may include:

1) Validation of the results predicted for Type 3 and Type 4 systems. In the case of Type 3 systems, if its predicted vibration isolation characteristics are shown to be realizable in practice, it will prove to be a major contribution. For Type 4 system, the experiment may determine how severe the problem of drift may be, and whether it will give any improvement over passive isolators.

2) Study of the effects of valve dynamics. If a programmable controller is built for the modulation of damper force, it will be very easy to study the effect of various controller parameters on the suspension performance. This may lead to innovative concepts or improvements which would not have been possible through analytical means.

REFERENCES

1. Thomson, W.T., Theory of Vibration with Application, Prentice Hall Inc., Englewood Cliffs, N.J., 1972.

2. Crede, C.E., and Ruzicka, J.E., "Theory of Vibration Isolation", in: Shock and Vibration Handbook, C.M. Harris and C.E. Crede, Eds., McGraw-Hill Book Co., 1976, pp 30.1-30.57.

3. Ruzicka, J.E., and Derby, T.F., Influence of Damping in Vibration Isolation, The Shock and Vibration Information Center, Washington, D.C., 1971.

4. Ruzicka, J.E., and Derby, T.F., "Vibration Isolation with Nonlinear Damping", Transactions of the ASME, Journal of Engineering for Industry, May 1971, pp 627-635.

5. Segel, L. and Lang, H.H., "The Mechanics of Automotive Hydraulic Dampers at High Stroking Frequencies", Vehicle System Dynamics, 10(2-3), Sept 1981, pp 82-85.

6. van Vliet, M., "Computer Aided Analysis and Design of Off-Road Motorcycle Suspensions", Ph.D. Thesis, Concordia University, Montreal, 1983.

7. Sutton, H.B., "The Potential for Active Suspension Systems", Automotive Engineer, 4(2), April-May 1979, pp 21-24.

8. Bender, E.K., "Optimum Linear Preview Control With Application to Vehicle Suspension", Transactions of the ASME, Journal of Basic Engineering, 90(2), June 1968, pp 213-221.

9. Karnopp, D.C., "Active and Passive Isolation of Random Vibration", in: Isolation of Mechanical Vibration, Impact and Noise, J.C. Snowdon, Ed., ASME, New York, 1973, pp 64-86.

10. Karnopp, D.C., "Are Active Suspensions Really Necessary?", ASME Paper No. 78-WA/DE-12, 1978.

11. Karnopp, D.C., "Active Damping in Road Vehicle Suspension Systems", Vehicle System Dynamics, 12(6), Dec 1983, pp 291-316.

12. Sevin, E., and Pilkey, W.D., Optimum Shock and Vibration Isolation, The Shock and Vibration Information Center, Washington, D.C., 1971.

13. Margolis, D.L., "The Response of Active and Semi-Active Suspensions to Realistic Feedback Signals", Vehicle System Dynamics, 11(5-6), Dec 1982, pp 267-282.

14. Cavanaugh, R.D., "Air Suspension and Servo-Controlled Isolation System", in: Shock and Vibration Handbook, C.M. Harris and C.E. Crede, Eds., McGraw-Hill Book Co., 1976, pp 33.1-33.26.

15. Schubert, D.W., and Ruzicka, J.E. "Theoretical and Experimental Investigation of Electrohydraulic Vibration Isolation Systems", Transactions of the ASME, Journal of Engineering for Industry, 91(1), pp 981-990.

16. Guntur, R.R., and Sankar, S., "Fail-Safe Vibration Control Using Active Force Generators", Transactions of the ASME, Journal of Vibration, Acoustics, Stress, and Reliability in Design, 105(3), July 1983, pp 361-369.

17. Bender, E.K., "Some Fundamental Limitations of Active and passive Vehicle Suspension Systems", Transactions of the SAE, 77(4), 1968, pp 2910-2915.

18. Sachs, H.K., "An Adaptive Control for Vehicle Suspensions", Vehicle System Dynamics, 12(2-3), Sept 1981, pp 201-206.

19. Goodall, R.M., and Kortüm, W., "Active Controls in Ground Transporation -A Review of the State-of-the-Art and Future Potential", Vehicle System Dynamics, 12(4-5), Aug 1983, pp 225-257.

20. Crosby, M.J., and Karnopp, D.C., "The Active Damper -A New Concept for Shock and Vibration Control", The Shock and Vibration Bulletin, 43(4), June 1973, pp 119-133.

21. Karnopp, D.C., Crosby, M.J., and Harwood, R.A., "Vibration Control Using Semi-Active Force Generators", Transactions of the ASME, Journal of Engineering for Industry, 96(2), May 1974, pp 619-626.

22. Margolis, D.L., Tylee, J.L., and Hrovat, D., "Heave Mode Dynamics of Tracked ACV with Semi-Active Airbag Secondary Suspension", Transactions of the ASME, Journal of Dynamic Systems Measurement and Control, 97(4), Dec 1975, pp 399-407.

23. Margolis, D.L., "Semi-Active Suspensions for Military Ground Vehicles Under Off-Road Conditions", Presented at the 52nd Symposium on Shock and Vibration, New Orleans, Oct 1981.

24. Margolis, D.L., "Semi-Active Heave and Pitch Control for Ground Vehicles", Vehicle System Dynamics, 11(1), Feb 1982, pp 31-42.

25. Margolis, D.L., "Semi-Active Control of Wheel Hop in Ground Vehicles", Vehicle System Dynamics, 12(6), Dec 1983, pp 317-330.

26. Kim, K., "Ride Simulation of Passive Active and Semi-Active Seat Suspensions for Off-Road Vehicles", Ph.D. Thesis, University of Illinois at Urbana-Champaign, 1981.

27. Allan, R.R., and Karnopp, D.C., "Semi-Active Control of Ground Vehicle Structure Dynamics", AIAA Paper No. 75-821, Presented at the 16th Structural Dynamics and Material Conference, Denver, Colorado, May 1975.

28. Karnopp, D.C., and Allan, R.R., "Semi-Active Control of Multimode Vibratory Systems Using ILSM Concept", Transactions of the ASME, Journal of Engineering for Industry, Aug 1976, pp 914-918.

29. Hrovat, D., Barak, P., and Rabins, M., "Semi-Active Versus Passive or Active Tuned, Mass Dampers for Structural Control", ASCE Journal of Engineering Mechanics, 109(3), June 1983, pp 691-705.

30. Roley, D.G., "Tractor Cab Suspension Performance Modeling", Ph.D. Thesis, University of California, Davis, California, June 1975.

31. Roley, D.G., "Performance Characteristics of Cab Suspension Models", Presented at the 1975 Winter Meeting of Americal Society of Agricultural Engineers, Paper No. 75-1517, Dec 1975.

32. Krasnicki, E.J., "Comparison of Analytical and Experimental Results of Semi-Active Vibration Isolator", The Shock and Vibration Bulletin, 50(4), Sept 1980, pp 69-76.

33. Krasnicki, E.J., "The Expermental Performance of an ON-OFF Active Damper", The Shock and Vibration Bulletin, 51(1), May 1981, pp 125-131.

34. Hrovat, D., and Margolis, D.L., "An Experimental Comparison between Semi-Active and Passive Suspensions for Air-Cushion Vehicles", International Journal of Vehicle Design, 2(3), Aug 1981, pp 308-321.

35. Boonchanta, P., "Comparison of Active Passive and Semi-Active Suspensions for Ground Vehicles", Ph.D. Thesis, University of California, Davis, California, 1982.

36. Rakheja, S., "Computer Aided Dynamic Analysis and Optimal Design of Suspension Systems for Off-Road Tractors", Ph.D. Thesis, Concordia University, Montreal, 1983.

37. Snowdon, J.C., "Isolation from Mechanical Shock with a Mounting System Having Nonlinear Dual-Phase Damping", The Shock and Vibration Bulletin, 41(2), Dec 1970, pp 21-45.

38. Guntur, R.R., and Sankar, S., "Performance of Shock Mounts Employing Differnt Kinds of Dual-Phase Damping", Journal of Sound and Vibration 84(2), 1982, pp 253-267.

39. Hundal, M.S., "Impact Absorber with Two-Stage Variable Area Orifice Hydraulic Damper", Journal of Sound and Vibration 50(2), 1977, pp 195-202.

40. Mercer, C.A., and Rees, P.L., "An Optimum Shock Isolator", Journal of Sound and Vibration 18(4), 1971, pp 511-520.

41. Caton, A.T., and Holmes, R., "Design and Performance of a Coulomb Shock Isolator", Journal of Mechanical Engineering Science, 15(4), 1973, pp 285-294.

42. Levitan, E.S., "Forced Oscillations of a Spring-Mass System having Combined Coulomb and Viscous Damping", The Journal of the Acoustical Society of America, 32(10), 1960, pp 1265-1269.

43. Schlesinger, A., "Vibration Isolation in the Presence of Coulomb Friction", Journal of Sound and Vibration 63(2), 1979, pp 213-224.

44. Hundal, M.S., "Response of a Base Excited System with Coulomb and Viscous Friction", Journal of Sound and Vibration 64(3), 1979, pp 371-378.

45. Marui, E., and Kato, S., "Forced Excitation of a Base-Excited Single-Degree-of-Freedom System with Coulomb Friction", Transactions of the ASME, Journal of Dynamic Systems Measurement and Control, 106(4), Dec 1984, pp 280-285.

46. Parnes, R., "Response of an Oscillator to a Ground Motion with Coulomb Friction Slippage", Journal of Sound and Vibration 94(2), 1984, pp 469-482.

47. van Vliet, M., and Sankar, S. "Computer Aided Analysis and Experimental Verification of a Motorcycle Suspension", Transactions of the ASME, Journal of Vibration, Acoustics, Stress, and Reliability is Design, 105(1), Jan 1983, pp 120-132.

48. Haines, G.H., "Landing Gear Shock Absorber Development to Improve Aircarft Operating Performance on Rough and Damaged Runways", AGARD Conference Proceedings No. 326, 1981, pp 16.1-16.19.

49. Bandstra, J.P., "Comparison of Equivalent Viscous Damping in Discrete and Continuous Vibrating Systems", ASME Paper No. 81-DET-89, Presented at the 8th ASME Design Engineering Conference, Hartford, Connecticut, Sept 1981.

50. van Vliet, M., Rakheja, S., and Sankar, S., "An Efficient Algorithm for the Simulation of Nonlinear Vehicle Subsystems", Proceedings of the ASME International Conference on Computers in Mechanical Engineering, Las Vegas, Aug 1984.

51. Burden, R.L., Faires, J.D., Reynolds, A.C., Numerical Analysis, Prindle, Weber and Schmidt, Boston, 1981.

52. Carver, M.B., "Efficient Integration Over Discontinuities in Ordinary Differential Equation Simulations", Mathematics and Computers in Simualtion, XX, 1978, pp 190-196.

53. Borthwick, W.K.D., "The Numerical Solution of Discontinuous Structural Systems", Proceedings of the 2nd International Conference on Recent Advances in Structural Dynamics, University of Southampton, England, April 1984, Vol. 1, pp 307-316.

54. Hindmarsh, A., "EPISODE: An Efficient Package for the Intergration of Systems of Ordinary Differential Equations", UCID-30112, Rev. 1, Lawrence Livermore Labortory, University of California, Livermore, California, 1977.

55. Ellison, D., "Efficient Automatic Intergration of Ordinary Differential Equations with Discontinuities", Mathematics and Computers in Simulation, XXIII, 1981, pp 12-20.

56. Li, Bo-Hu, Yang, W.H., and Ye, Xin-An, "An Effective Method for a System of Ordinary Differential Equations with Right Hand Side Containing Discontinuities", Proceedings of the 10th IMACS World Congress, Concordia University, Montreal, Aug 1982, Vol. 1, pp 6-9.

57. Doedel, E.J., "AUTO: A Subroutine Package for the Bifurcation Analysis of Ordinary Differential Equations", Concordia University, Sept 1984.

58. Doedel, E.J., "Continuation Techniques in the Study of Chemical Reaction Schemes", to Appear in the Proceedings of Special Year in Energy Mathematics, University of Wyoming, K.I. Gross, Ed., SIAM Publication.

59. Keller, H.B., "Numerical Solution of Bifurcation and Nonlinear Eigenvalue Problems", in: Applicantions of Bifurcation Theory, P. H. Robinowitz, Ed., Academic Press, 1977, pp 359-385

60. Crandall, S.H., and Mark, W.D., Random Vibration in Mechanical Systems, Academic Press, New York, 1971.